

NORTHWESTERN UNIVERSITY

Design and Synthesis of Small Molecules, Polyamines, and N-Acylated Polyamines that Affect
Biological Systems

A DISSERTATION

SUBMITTED TO THE GRADUATE SCHOOL IN PARTIAL FULFILLMENT OF THE
REQUIREMENTS

for the degree

DOCTOR OF PHILOSOPHY

Field of Chemistry

By

Jaclyn Ann Iera

EVANSTON, ILLINOIS

December 2008

ABSTRACT

Design and Synthesis of Small Molecules, Polyamines, and N-Acylated Polyamines that Affect Biological Systems

Jaclyn A. Iera

The focus of this thesis is the design of non-natural molecules for use in biological applications. Chapter one details a strategy to use small molecules to reactivate mutated p53, an oncoprotein that is prevalent in several types of cancer, back to its wild-type function. Wild-type p53 has the ability to induce cell death upon DNA damage, thus mutant p53 reactivation could lead to novel cancer therapeutics. By simplifying the scaffold of PRIMA-1, a bicyclic small molecule reported to reactivate p53, we synthesized serine and diaminopropionic acid derived small molecules to examine their affect on mutant p53. Several of these molecules were found to halt the cell growth of R175H and D281G p53 mutant strains.

The second chapter examines inhibition of HIV-1 transcription by the complexation of TAR RNA with a polyamine trimer (YYY) consisting of three tyrosine residues. The solid-phase synthesis of the polyamine was optimized with the use of a new resin linker, Fmoc- β -homoalanine, which increased yield and purity. NMR studies confirmed the binding of YYY specifically and with moderate affinity to the bulge region of TAR RNA, the area critical for inhibition of transcription.

Lastly, chapter three describes the synthesis of a functionally dense N-acylated polyamine scaffold to inhibit protein-protein interactions. Our multivalent platform can display side chains for molecular recognition at a density double that of natural peptides. Two parallel combinatorial libraries of these molecules were synthesized and screened for protein binding using quantum dot fluorescent technology. This strategy yielded a molecule that binds to the

HIV-1 Vpr protein with a K_D of approximately 25 μM , and partially reversed Vpr expression in podocytes.

ACKNOWLEDGEMENTS

When I first started graduate school, I was unaware of the challenges before me. There are many whom without their support, I could not have succeeded. First, I would like to thank Dr. Dan Appella for his guidance over the past five years. Dan, you allowed me much freedom with my projects and ideas, but did not allow me to get off track. Your input when I hit a sticking point was always valuable. I would also like to thank my committee members, Professors Scheidt and Uhlenbeck, for your advice and contributions over the years. You always offered insightful suggestions.

Much of this work would not have been accomplished without my labmates, who were there through the thick and thin. Mike and Graham, you two taught me everything I know about lab work. I appreciate your patience instructing me as an inexperienced first-year. Mark, Jon, and Ethan, you sure made the move to the NIH and building the lab far more entertaining than I ever could have imagined! Mark, it was a joy working with you and I will always remember your infectious laughter. Ethan, it has been a pleasure getting to know you and a delight having someone else in the lab that enjoys rocking out to Poison. Jon, my idea man, what would I do without you? You were and continue to always be there to bounce ideas off of, commiserate with, and celebrate with and I look forward to many more long conversations with you in the future. Tanya, you are an absolute dear and I enjoyed having another female in the lab. Ning, Qun, Chris, and Deyun, it was an honor to work with all of you and learn from you and I wish all of you the best.

I also owe much gratitude to my friends and family. Megan, Tracy, and Emily, you three are the best friends a girl could ask for and I will always appreciate you cheering me on throughout the years. Brent, you have been an unwavering tower of support for the past ten plus

years and for that I am eternally grateful. Mom, Dad, and Rob, you are just a superb family! Not only have you supported all of my decisions throughout the years, but you always made sure I remembered to laugh and find the humor in everything.

Lastly, I would like to thank two of the best teachers I have ever had: my 6th grade science teacher Mr. Biere and my 11th grade organic chemistry teacher Mr. Wienand. Mr. Biere was instrumental in igniting my love of science and Mr. Wienand introduced me to the fascinating subject of organic chemistry. They were a true inspiration to me.

DEDICATION

This thesis is dedicated to all the women in science.

TABLE OF CONTENTS

ABSTRACT	2
ACKNOWLEDGEMENTS	3
DEDICATION	5
LIST OF FIGURES	10
LIST OF SCHEMES	14
LIST OF TABLES	16
Chapter 1. Design and Synthesis of Serine and Diaminopropionic Acid Small Molecules that Reactivate Mutant p53	
1.1 Introduction.....	18
1.2 p53 Structure and Mutations.....	19
1.3 Small Molecule Reactivators.....	22
1.4 <i>Para</i> -Substituted Derivatives.....	24
1.5 ELISA Development.....	31
1.6 Intercalation Studies.....	33
1.7 Diaminopropionic Derivatives.....	35
1.8 Summary.....	38
1.9 Experimental Procedures.....	38
1.9.1 Synthesis of Serine-Derived Molecules.....	40
1.9.2 ELISA.....	47
1.9.3 DNA Melting Studies.....	48
1.9.4 Synthesis of Diaminopropionic Backbone.....	48
1.9.5 Solid-phase synthesis.....	53

	8
1.9.6 Select ¹ H-NMRs.....	56
References: Chapter 1.....	152
Chapter 2. Synthetic Optimization and Biological Studies of YYY Polyamine that Binds to HIV-1 TAR RNA	
2.1 Introduction.....	62
2.2 TAR RNA and HIV-1 Transcription.....	63
2.3 Inhibitors of HIV-1 Transcription.....	63
2.3.1 HIV-1 Transcription Inhibitors Targeting TAR.....	65
2.4 Polyamines.....	68
2.4.1 Polyamine Synthesis.....	68
2.5 Linker Studies.....	70
2.6 NMR Study of YYY and TAR.....	74
2.7 Cell Permeability and Anti-Viral Activity.....	75
2.8 Future Directions.....	78
2.9 Summary.....	79
2.10 Experimental Procedures.....	79
2.10.1 ¹ H-NMRs.....	85
References: Chapter 2.....	156
Chapter 3. Design and Synthesis of N-Acylated Polyamine (NAPA) Libraries to Screen for Protein Binding	
3.1 Introduction.....	88
3.2 Protein-Protein Interactions.....	88
3.3 N-Acyl Polyamine Design and Synthesis.....	92
3.4 1 st Generation Library.....	98

	9
3.4.1 Synthetic Optimization.....	99
3.4.2 Library Design.....	103
3.4.3 Library Screen.....	106
3.4.4 Myostatin.....	107
3.4.5 Anthrax Lethal Factor.....	110
3.4.6 HIV Integrase.....	113
3.5 2 nd Generation Library.....	115
3.5.1 Library Design.....	115
3.5.2 HIV-1 Vpr.....	118
3.5.3 MDMX.....	123
3.5.4 FKBP52.....	126
3.6 Future Work.....	127
3.7 Summary.....	128
3.8 Experimental Procedures.....	129
3.8.1 General Synthesis of Weinreb Amides.....	130
3.8.2 General Synthesis of Aldehydes.....	133
3.8.3 Solid-Phase Synthesis of N-Acylated Polyamines.....	135
3.8.4 Library Synthesis.....	138
3.8.5 Library Screen.....	140
3.8.6 Biacore Binding Assay.....	141
3.8.7 Isothermal Titration Calorimetry.....	141
3.8.8 ¹ H-NMRs.....	142
References: Chapter 3.....	162

LIST OF FIGURES

Chapter 1. Design and Synthesis of Serine and Diaminopropionic Acid Small Molecules that Reactivate Mutant p53

Figure I-1. Schematic representation of the p53 pathways in a cell.....	19
Figure I-2. Mutation Frequencies.....	21
Figure I-3. p53 bound to DNA.....	22
Figure I-4. Small molecule reactivators.....	23
Figure I-5. Original serine-derived small molecule reactivator.....	24
Figure I-6. Cell results for PRIMA-1.....	27
Figure I-7. Cell results for H-Ser(OAc) phenyl ketone.....	27
Figure I-8. Cell results for H-Ser(OAc) <i>p</i> -methoxyphenyl ketone.....	28
Figure I-9. Cell results for H-Ser(OAc) <i>p</i> -fluorophenyl ketone.....	28
Figure I-10. Cell results for H-Ser(OAc) <i>p</i> -tolyl ketone.....	29
Figure I-11. Epitopes of p53 recognized by various antibodies.....	31
Figure I-12. ELISA setup diagram.....	32
Figure I-13. ELISA results.....	33
Figure I-14. DNA sequences for intercalation studies.....	34
Figure I-15. Dap-derived phenyl ketone.....	35

Chapter 2. Synthetic Optimization and Biological Studies of YYY Polyamine that Binds to HIV-1 TAR RNA

Figure II-1. TAR Structure and mechanism of viral genome elongation.....	63
Figure II-2. Fluoroquinolone HIV transcription inhibitors.....	64
Figure II-3. Ro 24-7429.....	65

	11
Figure II-4. CGP64222.....	65
Figure II-5. D-Amino acid tripeptide and cyclized peptide.....	66
Figure II-6. WM5.....	65
Figure II-7. Neamine derived TAR inhibitors.....	67
Figure II-8. Polyamine backbone and YYY.....	68
Figure II-9. HPLC trace of β -alanine-alanine.....	72
Figure II-10. HPLC trace of β -homoalanine-alanine.....	72
Figure II-11. HPLC trace of β -homophenylalanine-alanine.....	73
Figure II-12. NMR titration results.....	75
Figure II-13. Cell permeability assay.....	77
Figure II-14. Effect of YYY on NL4-3 replication in MT4 cells.....	78

Chapter 3. Design and Synthesis of N-Acylated Polyamine (NAPA) Libraries to Screen for Protein Binding

Figure III-1. Crystal structure of p53 bound to MDM2; the Nutlins and MI-219.....	89
Figure III-2. Terphenyl α -helix mimic.....	90
Figure III-3. Bcl-X _L binding chimeric (α/β)+ α peptide.....	91
Figure III-4. HDM2 binding β^3 -decapeptide.....	92
Figure III-5. Polyamine scaffold.....	92
Figure III-6. Proposed N-acyl polyamine scaffold.....	93
Figure III-7. Scaffold comparison.....	94
Figure III-8. Products from the addition of isobutyryl ketene to a secondary amine.....	95
Figure III-9. NAPA scaffold with 4-nitrophenylacetic acid.....	98

	12
Figure III-10. Desired product achieved with TMOF, 1% AcOH/DMF, and NMP.....	100
Figure III-11. Truncated product achieved with TMOF, 1% AcOH/DMF, and NMP.....	100
Figure III-12. Three different truncated products achieved with TMOF, 1% AcOH/DMF, and NMP.....	101
Figure III-13. Library code example – K2K2K2.....	105
Figure III-14. The 216 compounds of the 1 st generation library.....	105
Figure III-15. Screening colorimetric sandwich assay and Qdot structure.....	106
Figure III-16. Belgian Blue Cattle.....	107
Figure III-17. Two positive hits from the myostatin screen.....	109
Figure III-18. Results from the myostatin cellular assay with H2H2H2.....	109
Figure III-19. Anthrax lethal factor crystal structure and cellular incorporation.....	110
Figure III-20. Two positive hits from the LF screen.....	111
Figure III-21. Initial results from the LF cellular assay.....	112
Figure III-22. Truncated forms of K2Y1H1 synthesized for testing.....	113
Figure III-23. Raltegravir.....	114
Figure III-24. A few wells in the <i>H series</i> controls.....	114
Figure III-25. The 512 compounds in the 2 nd generation library.....	117
Figure III-26. Overlay of 15 NMR structures of Vpr's three α -helices.....	118
Figure III-27. Positive hit from the Vpr screen.....	119
Figure III-28. Results from the Vpr cellular assay with K2K2Y2.....	120
Figure III-29. Doxycycline and RSL-1.....	120
Figure III-30. ITC results for K2K2Y2 and Vpr.....	123
Figure III-31. Surface representations of the binding pockets of MDMX and HDM2.....	124

Figure III-32. Three positive hits from the MDMX screen.....125

Figure III-33. Positive hit from the FKBP52 screen.....127

LIST OF SCHEMES**Chapter 1. Design and Synthesis of Serine and Diaminopropionic Acid Small Molecules that Reactivate Mutant p53**

Scheme I-1. Dissection of PRIMA-1 into a modifiable small molecule scaffold.....	23
Scheme I-2. Synthesis of the serine-derived phenyl ketone analogs.....	25
Scheme I-3. Dap backbone synthesis.....	36
Scheme I-4. Solid phase synthesis of the Dap-derived phenyl ketone.....	37

Chapter 2. Synthetic Optimization and Biological Studies of YYY Polyamine that Binds to HIV-1 TAR RNA

Scheme II-1. Fmoc-amino acid aldehyde synthesis.....	69
Scheme II-2. Linker coupling to Rink resin.....	69
Scheme II-3. Solid-phase synthesis of polyamines.....	70
Scheme II-4. Over-alkylation at the first secondary amine.....	70
Scheme II-5. Derivatization of Rink Amide resin.....	71
Scheme II-6. Self reduction of NaBH(OAc) ₃	74
Scheme II-7. Formation of the piperidine-fluorescein adduct.....	76

Chapter 3. Design and Synthesis of N-Acylated Polyamine (NAPA) Libraries to Screen for Protein Binding

Scheme III-1. Formation of a urea side-chain by the addition of an isocyanate.....	92
Scheme III-2. Synthesis of triureas.....	93
Scheme III-3. Proposed synthesis of amides with ketenes; ketene synthesis.....	95
Scheme III-4. Synthesis of a ketene from a mixed anhydride.....	96
Scheme III-5. Attempted formation of hydrocinnamoyl amide side-chain.....	96

	15
Scheme III-6. Solid-phase synthesis of N-acylated polyamines.....	98
Scheme III-7. Optimized NAPA synthesis for filter plates.....	103

LIST OF TABLES**Chapter 1. Design and Synthesis of Serine and Diaminopropionic Acid Small Molecules that Reactivate Mutant p53****Table I-1.** Summary of the cell study results.....30**Table I-2.** DNA melting temperatures.....34**Chapter 3. Design and Synthesis of N-Acylated Polyamine (NAPA) Libraries to Screen for Protein Binding****Table III-1.** Conditions tested for filter plate synthesis optimization.....99**Table III-2.** 1st generation library code.....104**Table III-3.** 2nd generation library code.....116**Table III-4.** Assay setup for interactions between chemical additives in the cell studies.....121

Chapter 1

Design and Synthesis of Serine and Diaminopropionic Acid Small Molecules that Reactivate Mutant p53

1.1 Introduction

In 1979, a 53-kDa protein was isolated based on its binding to the large T antigen, a tumor-associated protein, from the sarcoma-associated virus SV40.¹⁻³ It was another ten years before this protein was recognized as a tumor suppressor. The p53 protein, which is encoded by the TP53 gene, is a transcription factor that is involved in cell-cycle regulation, apoptosis, and DNA repair and p53 is often referred to as the “Guardian of the Genome.”⁴⁻⁷

Since the p53 protein is responsible for activating a number of pathways that may destroy the cell, such as apoptosis or cell cycle arrest, its cellular levels must be regulated in all healthy cells. For instance, murine double mutant-2 (MDM2) protein binds to p53 causing the degradation of p53 via an ubiquitination pathway.^{8, 9} As seen in MDM2 knockout mice,¹⁰ too much p53 in a cell is lethal and small molecules that interrupt this p53-MDM2 interaction are aggressively being researched as a potential cancer therapeutic.¹¹⁻¹⁶ Upon DNA damage, however, p53 is phosphorylated and unable to bind to MDM2 resulting in an increase of p53 levels in the cell and the signaling of various p53 pathways to repair or obliterate the cell (Figure I-1).

While p53 is largely responsible for preventing the uncontrolled proliferation of cancer cells, it is also one of the most frequently mutated proteins. Over half of all human cancers have a mutated form of the p53 protein resulting in a loss of function.¹⁷ The “reactivation” of mutant p53 to wild-type functionality is therefore a prevalent area of research. A small molecule that could act in this regard would be the ideal solution.

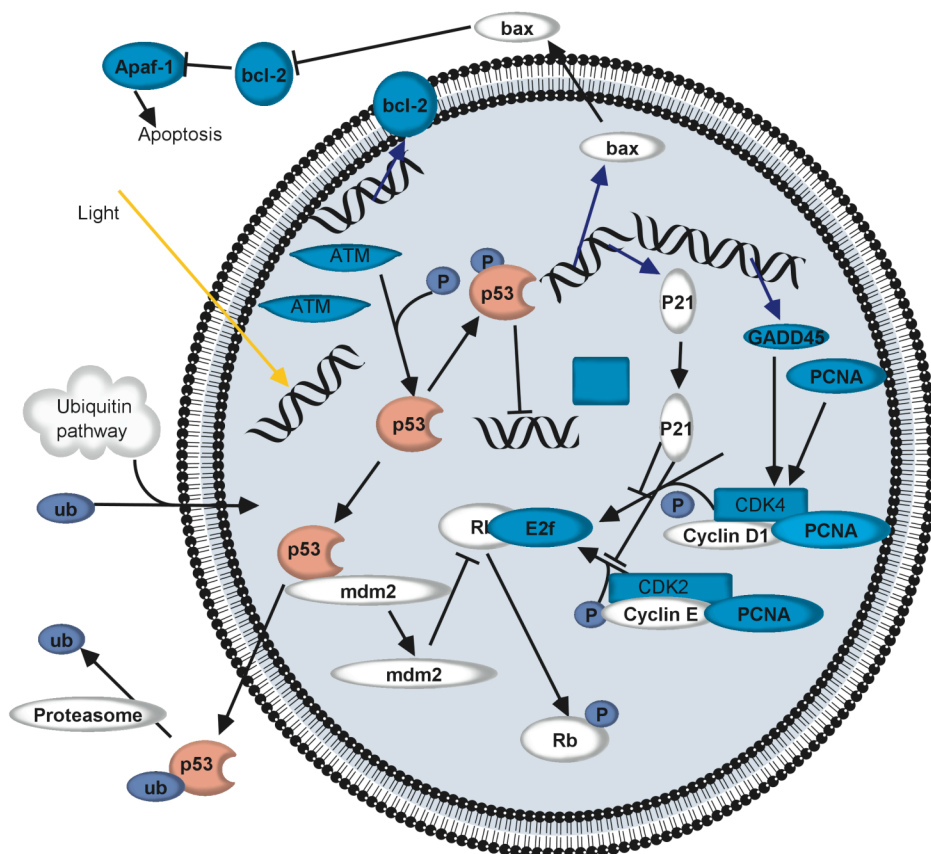


Figure I-1: Schematic representation of the p53 pathways in a cell

1.2 p53 Structure and Mutations

p53 is a 393 amino acid protein that exists as a tetramer (a dimer of dimers) and contains four domains: the N-terminal domain, the DNA binding domain (DBD), the tetramerization domain, and the C-terminal or regulatory domain. Interestingly, while crystal and NMR structures of each of the domains exist independently,^{18, 19} no crystal structure of the p53 protein in its entirety has been captured due to its extreme flexibility. Only recently has the structure of full-length p53 been captured by the use of cryoelectron microscopy.²⁰

The N-terminal domain (amino acids 1-42) of p53 contains the transcriptional portion of p53 as well as a proline-rich SH3 region (amino acids 60-97). As its name states, the tetramerization domain (amino acids 323-356) is where p53 oligomerization occurs, and the C-terminal domain (amino acids 360-393) is believed to regulate the binding of p53 to DNA,

although its precise role and mechanism remain unclear. The DBD (amino acids 102-292) composes most of the p53 protein, and the DBD is where the majority of mutations occur.

Consisting of nearly 200 amino acids, the DNA-binding domain is crucial for the sequence specific DNA binding of the full-length p53 protein. The DBD is one of the most stable regions of the protein and is highly resistant to proteolytic degradation. Additionally, it binds to the specific base pair motif 5'-PuPuPuC(A/T)(T/A)GPyPyPy-3', where "Pu" is a purine and "Py" is one of the pyrimidines.²¹ Two copies of the motif, separated by 0-13 base pairs, are required for the binding of the full-length p53 tetramer. In 1994, Pavletich and co-workers first reported the crystal structure of the DBD, which consists of a β sandwich scaffold, two large loops, and a loop-helix-loop motif.¹⁸ The two large loops are held together with a zinc atom and interact with the minor groove of DNA while the loop-helix-loop motif interacts with the major groove.

Although the DBD exhibits stability, it is also the most commonly mutated portion of p53; over 90% of all p53 mutations occur within the DNA binding domain (Figure I-2).²² The p53 mutations that occur are one of two types: contact mutations or structural mutations. A contact mutation takes place at one of the amino acid residues that is in direct contact with DNA, but the overall structure of p53 remains in its native configuration. Structural mutations, however, happen at residues that are responsible for protein stabilization and result in a change of conformation.

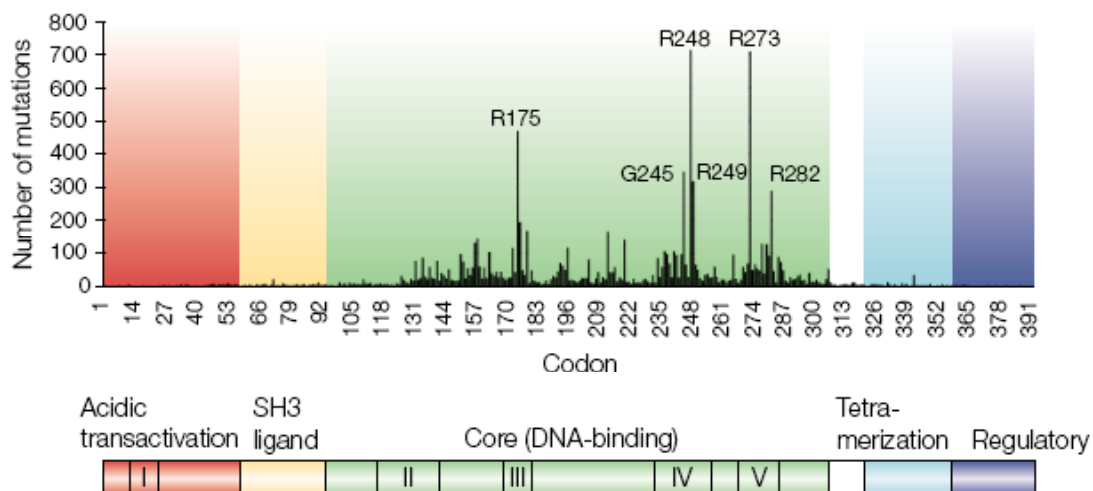


Figure I-2: Graph displaying mutation frequencies at each amino acid residue of p53; the majority of mutations occur in the DNA binding domain (green section).²²

Of the 393 amino acids that make up the p53 protein, six amino acids known as the “hot spots”, are mutated more frequently than all of the other residues. These residues are R282, R273, R248, R249, R175, and G245 and are highlighted in red and green in Figure I-3.²³ The two mutations in red, R273 and R249 are contact mutations and the remaining four hot spots are structural mutations.

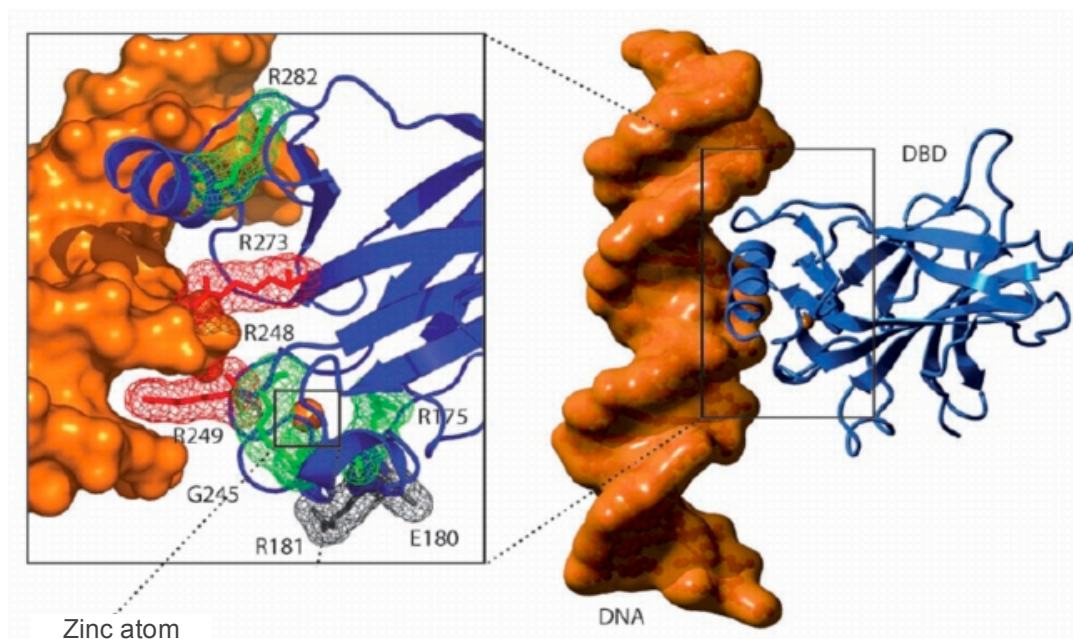


Figure I-3: p53 bound to the major and minor grooves of DNA; six hot spots are highlighted in red and green (red = contact mutations).²³

1.3 Small Molecule Reactivators

Due to the prevalence of p53 mutations in a variety of cancers, much research has been dedicated to finding a therapy for “reactivating” mutant p53 back to its wild-type functionality. While some success has been found with small proteins,^{24, 25} the ideal accomplishment would be to find a small molecule that restores p53 functionality.

Through various screens of large chemical libraries, several molecules appeared with a promising ability to reactivate p53: ellipticine,²⁶ CP-31398,²⁷ PRIMA-1 (*p53* reactivation and induction of massive apoptosis)²⁸, and MIRA-1 (*mutant p53-dependent induction of rapid apoptosis*)²⁹ (Figure I-4).

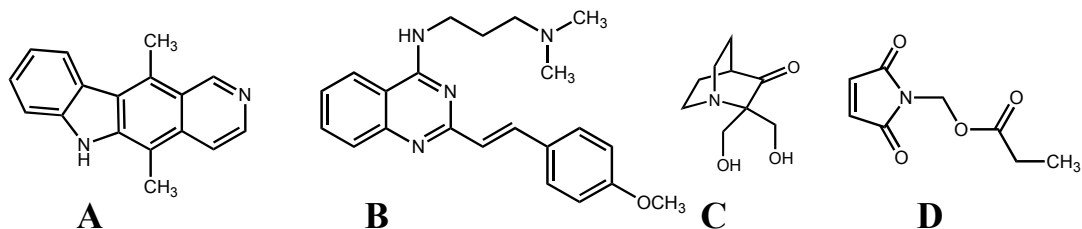
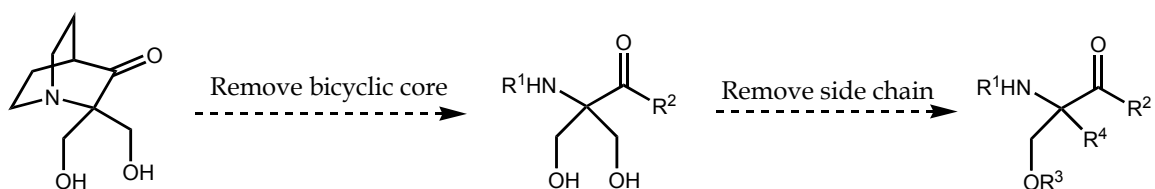


Figure I-4: Small molecules initially found to reactivate p53: A) Ellipticine B) CP-31398 C) PRIMA-1 D) MIRA-1

However, several inherent problems exist with these molecules: ellipticine and CP-31398 are DNA intercalators, PRIMA-1 is somewhat unstable, the number of modifiable positions is very limited, and the molecules are synthetically challenging.

Work previously done in our lab by Dr. Michael Myers started by dissecting PRIMA-1 into a small molecule that would be stable and readily modified synthetically. The design involved removing the bicyclic core, but keeping the amine, carbonyl, and one or two side chains intact (Scheme I-1).



Scheme I-1: Dissection of PRIMA-1 into a modifiable small molecule scaffold.

The original library of small molecules demonstrated that three main features were important for activity: the amine must be a free amine, the side chain(s) must be acetylated, and the carbonyl moiety must be a phenyl ketone. These necessary features produce a small molecule derived from serine (Figure I-5). Surprisingly, stereochemistry had no effect on the activity of the molecules.

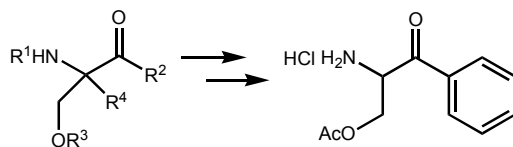


Figure I-5: Original serine-derived small molecule reactivator

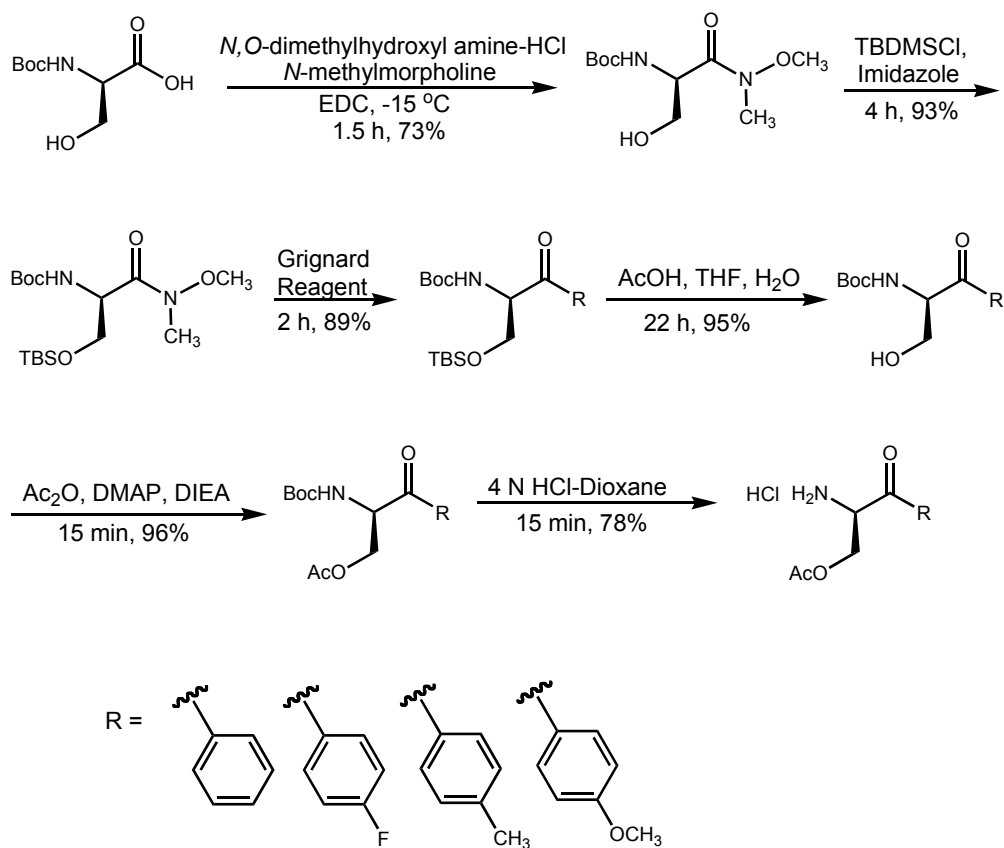
Substituents on the amine resulted in toxicity and when the side chains were free hydroxyl groups, there was no activity. Of particular interest was the absence of activity when the carbonyl group was a methyl ester, amide, or ethyl ketone. The requirement of a phenyl ketone led to the thought that the electronics around the carbonyl were of great importance, and these electronics could be modified easily with varying substituents on the phenyl ring.³⁰

1.4 *Para*-substituted derivatives

With the initial SAR results in hand, we sought to explore the electronics around the phenyl ketone by placing either an electron-withdrawing group or an electron-donating group on the *para*-position of the phenyl ring. The original phenyl ring was installed into the molecule by using a Grignard reaction and by using a variety of commercially available Grignard reagents, we were able to place a fluorine, a methoxy group, and a methyl group in the *para*-position without altering the synthesis.

To synthesize the target molecules, Boc-Ser-OH was first converted to a Weinreb amide, which was accomplished with a slightly different amide bond coupling procedure. *N,O*-dimethylhydroxylamine was added to Boc-Ser-OH first and the flask was then charged with EDC in five equal portions over a 30-minute time span. Weinreb amide formation was followed by protection of the hydroxyl side-chain with *tert*-butyldimethylsilyl chloride (TBDMSCl) and imidazole. After protection of the hydroxyl group, the appropriate Grignard reagent was added

to the Weinreb amide to form the phenyl ketone. At this point, the TBDMS protecting groups must be removed and typically a fluorine source, such as tetrabutylammonium fluoride (TBAF), is used for this procedure. Unfortunately, TBAF deprotection led to racemization, but deprotection occurred without racemization when using acetic acid for 22 hours as an alternative. Once the TBDMS group was removed, the hydroxyl side chain was acylated with acetic anhydride and catalytic DMAP and followed by Boc-deprotection with 4 N HCl-dioxane (Scheme I-2).



Scheme I-2: Synthesis of the serine-derived phenyl ketone analogs

Upon completion of the series of analogs, they were sent to Dr. Gerard Zambetti at St. Jude Children's Research Hospital, for cellular assays. The molecules, along with PRIMA-1

were screened against Saos-2-osteosarcoma cells that were either null for p53 (wild-type cells) or contained a p53 mutation: R175H, R273H, or D281G. The results pictured (Figures I-6 – I-10) are also summarized in Table I-1. PRIMA-1, the molecule on which our design was based, demonstrated some toxicity towards the cell line, while our original phenyl ketone molecule displayed activity towards the R175H and D281G mutants. As we predicted, the different *para*-substitutions affected the activity of the molecules. The *p*-methoxyphenyl ketone exhibited no activity towards any of the mutants while the *p*-fluorophenyl ketone displayed non-specific toxicity. The two opposing electronic effects on the ketone moiety, electron-donating and electron-withdrawing, did indeed produce opposite results on the activity of the molecule. Lastly, the *p*-tolyl molecule had an activity similar to that of our original phenyl ketone with activity towards the R175H and D281G mutants. This result was particularly interesting because the tolerance of a methyl group indicates other substitutions and extensions of the molecule that could be useful for other cellular studies may be possible. It is also interesting to note that out of the three mutant strain lines, none of the molecules tested exhibited any activity towards the R273H mutant.

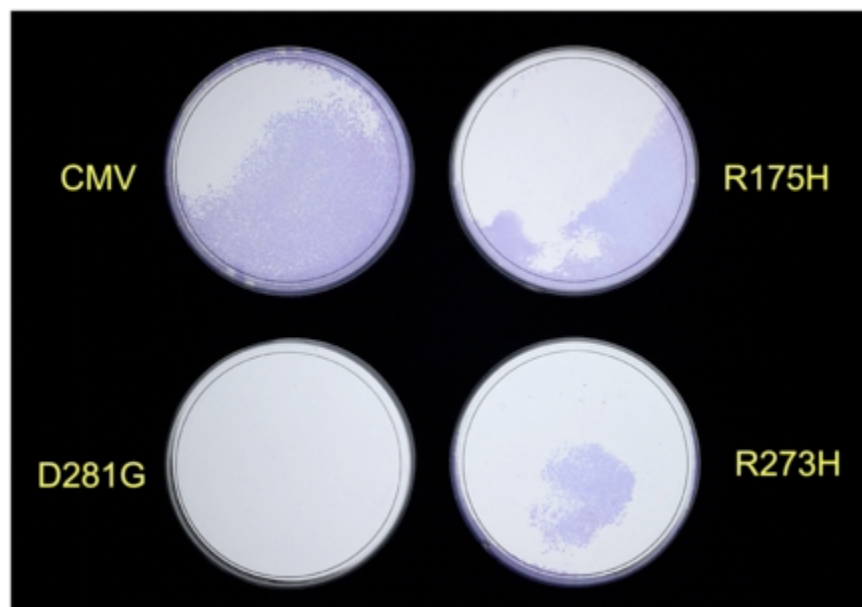


Figure I-6: Cell results for PRIMA-1 at 75 μM , where CMV represents p53 null cells. Dark blue areas are living cells and light blue areas are where cell death has occurred.

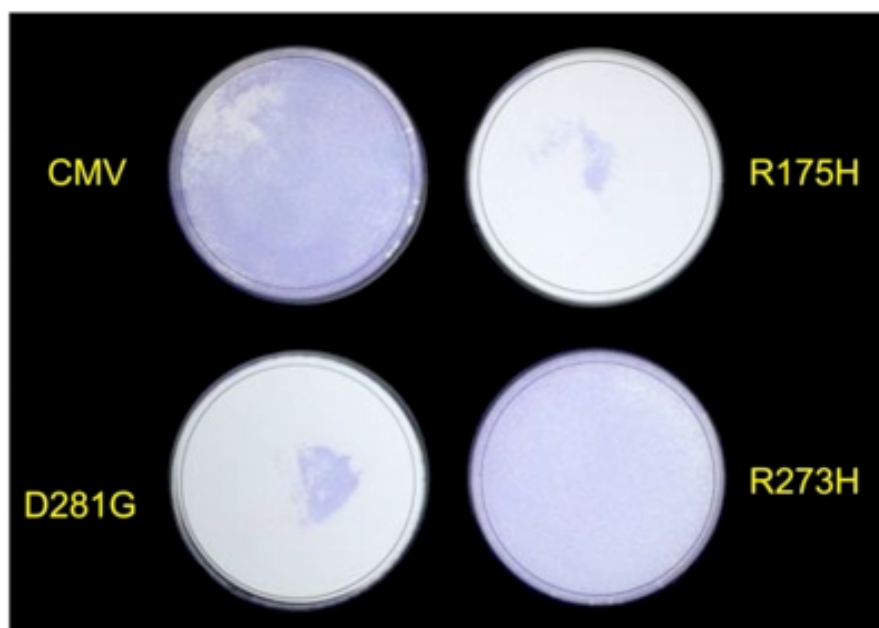


Figure I-7: Cell results for the original hit, H-Ser(OAc)-phenyl ketone, at 50 μM where CMV represents p53 null cells. Dark blue areas are living cells and light blue areas are where cell death has occurred.

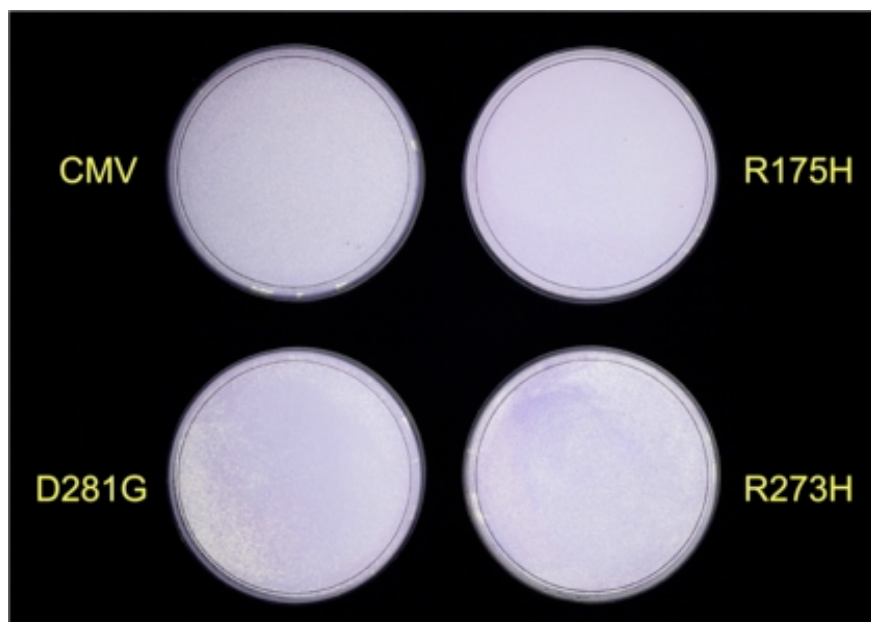


Figure I-8: Cell results for the *p*-methoxy analog, H-Ser(OAc)-*p*-methoxyphenyl ketone, at 100 μ M, where CMV represents p53 null cells. Dark blue areas are living cells and light blue areas are where cell death has occurred.

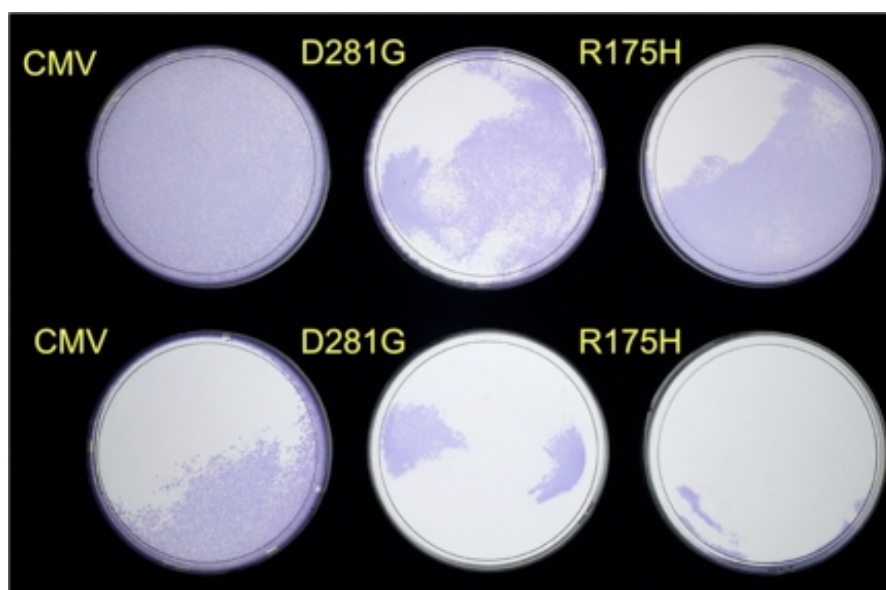


Figure I-9: Cell results for the *p*-fluoro analog, H-Ser(OAc)-*p*-fluorophenyl ketone, at 75 μ M (top row) and 100 μ M (bottom row), where CMV represents p53 null cells. Dark blue areas are living cells and light blue areas are where cell death has occurred.

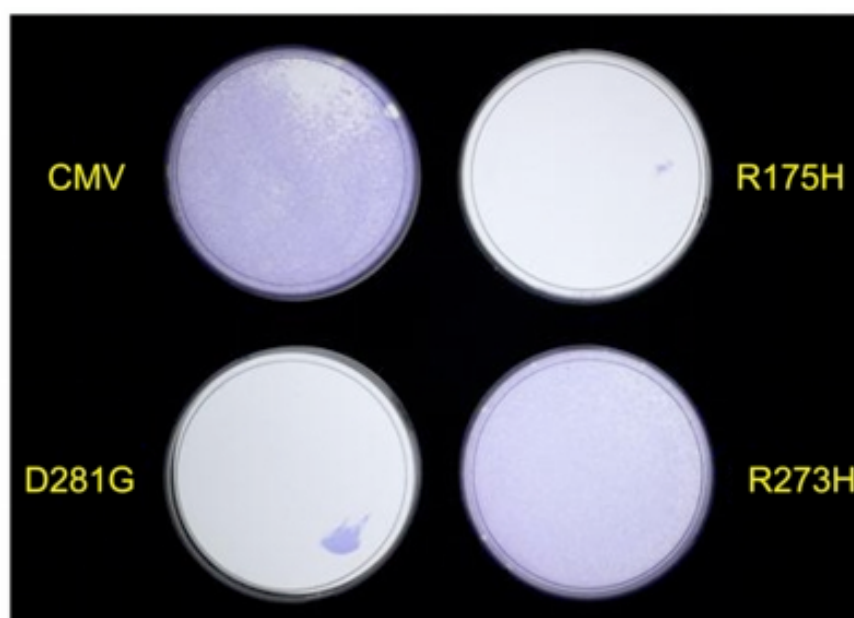


Figure I-10: Cell results for the *p*-methyl analog, H-Ser(OAc)-*p*-tolyl ketone at 100 μ M, where CMV represents p53 null cells. Dark blue areas are living cells and light blue areas are where cell death has occurred.

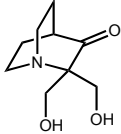
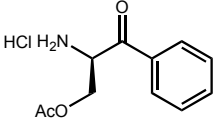
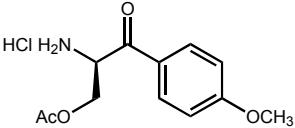
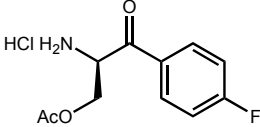
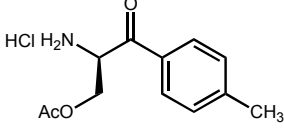
Molecule	Results
	Some toxicity (75 μ M)
	Active (R175H, D281G – 50 μ M)
	Not Active (100 μ M)
	Non-specific toxicity (75-100 μ M)
	Active (R175H, D281G – 100 μ M)

Table I-1: Summary of the cell study results

While the initial results were promising, there were a few limitations with the assay to consider. The molecules designed and synthesized were tested against one cell line and three p53 mutations. Thus, we only have a small subset of data for the molecules, especially considering the vast number of p53 mutations that exist. In addition, there was a small window

between the concentrations at which the molecules exhibited efficacy and toxicity and the results were not dose dependent. Finally, no *in vitro* studies have been performed to study the activity of the phenyl ketone series of molecules. An *in vitro* study would provide more detailed information about the molecules and whether or not they are interacting directly with p53.

1.5 ELISA Development

In an effort to develop an *in vitro* assay, we ventured to design an enzyme-linked immunosorbent assay (ELISA) that could detect whether or not wild-type p53 was present. We based our design on the ELISA used by Peng and co-workers,³¹ who used a similar method to study ellipticine for reactivation of p53. The sandwich assay is based on the principle that mutant p53 with a denatured configuration exposes an epitope of the protein that is recognized by monoclonal antibody 240 (PAb240). PAb240 is unable to recognize the wild-type conformation of p53, which is recognized by monoclonal antibody 1620 (PAb1620) (Figure I-11).³² We proposed that we could detect whether or not our molecules were restoring wild-type conformation based on the selectivity of the antibodies.

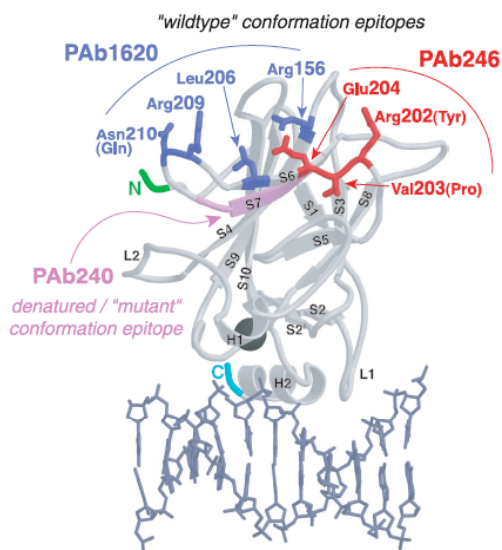


Figure I-11: Epitopes of p53 recognized by various antibodies

To test our strategy, we set up an ELISA with four layers: a monoclonal p53 antibody (mouse), purified p53 protein or cell extracts, a polyclonal reporter antibody (rabbit), and a secondary antibody (anti-rabbit) covalently linked to horseradish peroxidase (HRP). The HRP reacts with an Amplex Red/ H_2O_2 solution to produce the fluorescent resorufin (Figure I-12).

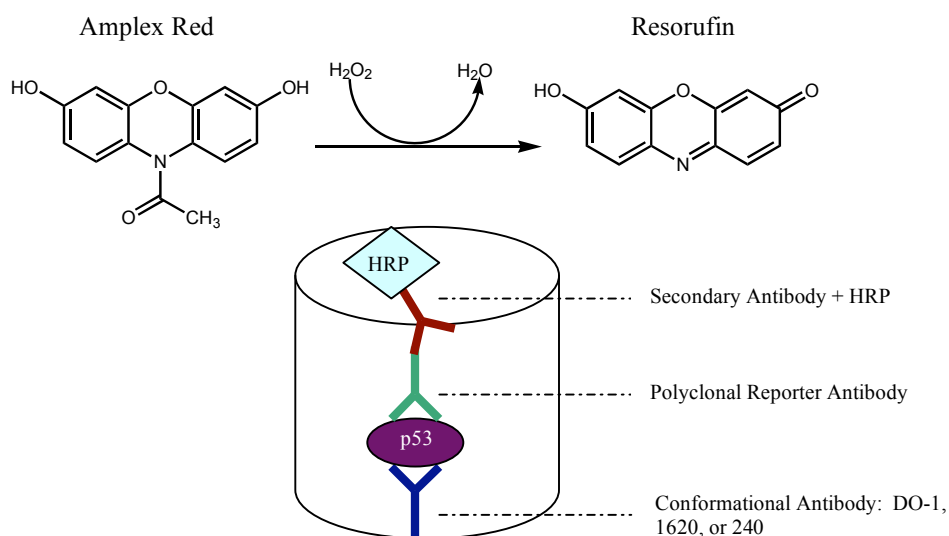


Figure I-12: ELISA setup diagram

The DO-1 antibody, which binds to both wild-type and denatured p53, was used as a control. Our initial studies involved denaturing wild-type p53 with heating at 43 °C for various lengths of time and examining the change in fluorescent signal based on the antibody used. The control wells with DO-1 worked as anticipated; the signal remained strong and was consistent since DO-1 binds both forms of p53. However, neither an increase in signal for PAb240 nor a decrease in signal for PAb1620 was found, despite numerous attempts (Figure I-13).

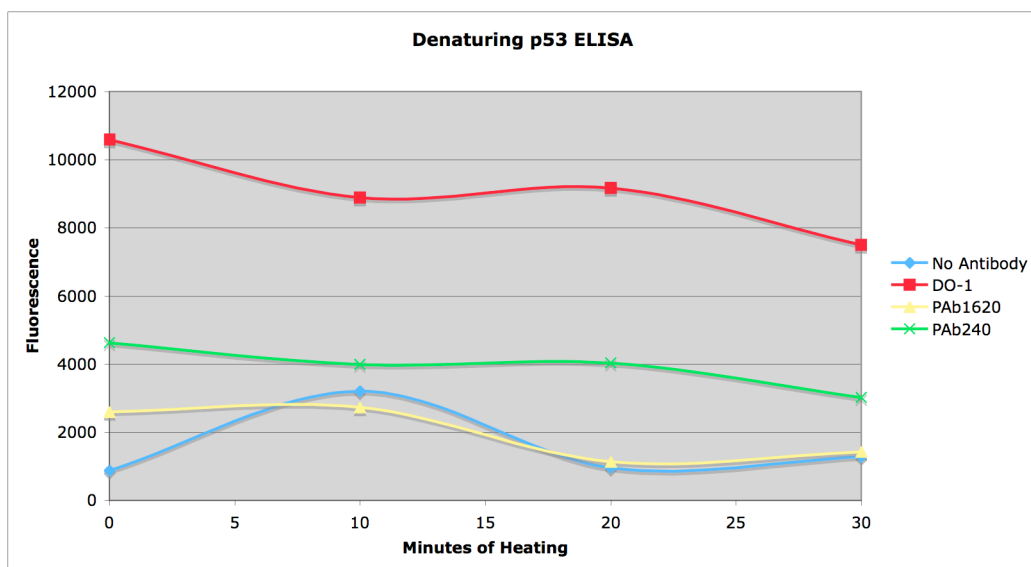


Figure I-13: ELISA results

The signals for PAb240 and PAb1620 also had a low intensity approaching the signal when no antibody is present. Full-length p53 protein is a difficult protein to work with due to low intrinsic thermodynamic stability and aggregation tendencies³³ leading to many compromised assays. We surmise that even though we took the greatest care when working with p53, the ELISA was affected by the unstable nature of p53. Additional tests, including trials with cell extracts of R175H mutant p53 did not fare much better. At this juncture, further design and optimization was exceeding our expertise so we instead focused on various other avenues of the project.

1.6 Intercalation Studies

Molecules that intercalate DNA are typically aromatic and planar. Due to the presence of the phenyl ring in our series of molecules, it was possible that these molecules were intercalating with DNA, just like ellipticine and CP-31398, and causing some of the toxicity they demonstrated. To test this theory, a series of melting studies were run on the phenyl ketone.

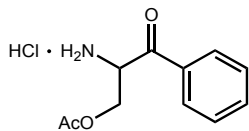
Two different lengths of complimentary DNA each containing the p53 binding sequence (5'-PuPuPuC(A/T)(T/A)GPyPyPy-3') were used, a 12mer and a 20mer (Figure I-14).



Figure I-14: DNA sequences used for intercalation studies.

Using ethidium bromide (EtBr), a known DNA intercalator, as a standard, a series of solutions were made and tested against the two DNA sequences. As seen in Table I-2, increased concentrations of EtBr raised the melting temperature (T_m) indicating intercalation, while the phenyl ketone molecule had no effect. We could therefore conclude that any inherent toxicity of our molecules was not due to DNA intercalation.

		12mer DNA	20mer DNA
		$T_m(^{\circ}\text{C})$	$T_m(^{\circ}\text{C})$
DNA Only		49.5	64.5
EtBr	r = 0.2	49.8	65.8
	r = 0.4	51.6	69.4
	r = 0.6	52.4	69.0
	r = 0.8	52.9	70.9
	r = 1.0	54.8	69.8
	r = 1.3	54.7	72.3
	r = 1.6	57.5	74.2
	10.8 mM (r = 0.3)	48.7	63.8
	25 mM (r = 0.7)	48.5	63.2
	50 mM (r = 1.4)	50.1	64.4



- $r = [\text{EtBr}]/[\text{base pairs}]$
- DNA concentration = 3 μM

Table I-2: DNA melting temperatures with increasing concentrations of either EtBr or the phenyl ketone.

1.7 Diaminopropionic Acid Derivatives

In the initial p53 reactivating small molecules there is an acylated hydroxyl side chain. This acetate has a great propensity to eliminate, rendering the molecule slightly unstable. Our collaborators at the National Cancer Institute (NCI), Dr. Ettore Appella and co-workers, synthesized the phenyl ketone molecule starting from diaminopropionic acid (Dap) instead of serine to produce an N-acylated side chain (Figure I-15). The replacement of the ester with the amide not only made a more stable molecule, but also had a slight increase in activity.

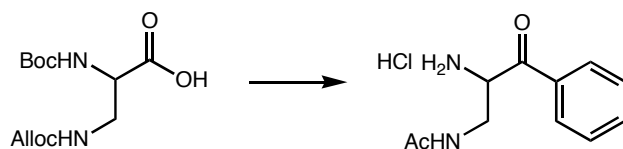
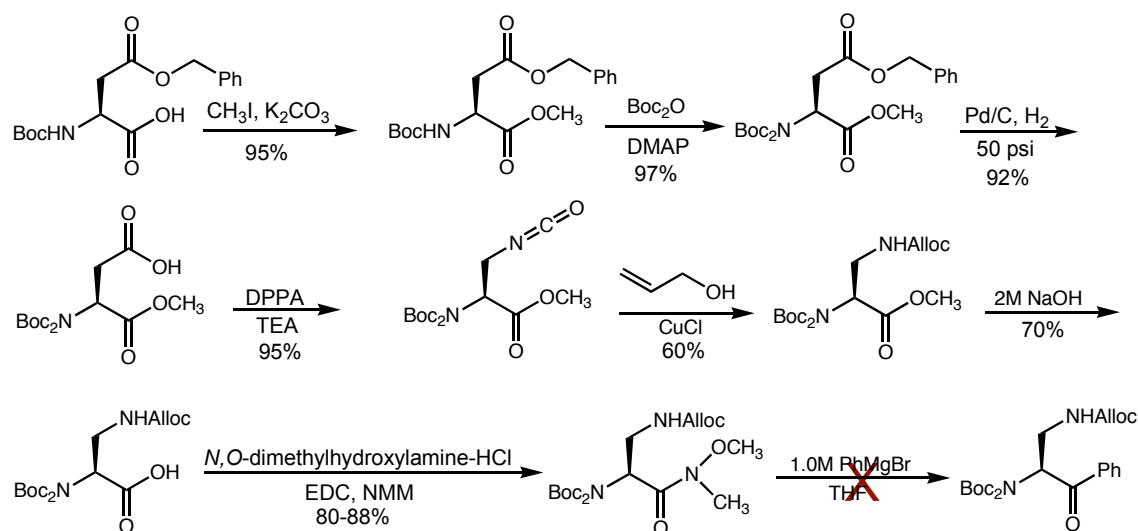


Figure I-15: Phenyl ketone derived from Boc-Dap(Alloc)-OH.

One problem, however, is that the appropriate Dap starting material is much more expensive than serine, costing approximately \$700 for 5 grams. To circumvent this hindrance, the Dap backbone was synthesized from aspartic acid modifying chemistry formally developed in our lab (Scheme I-3).³⁴

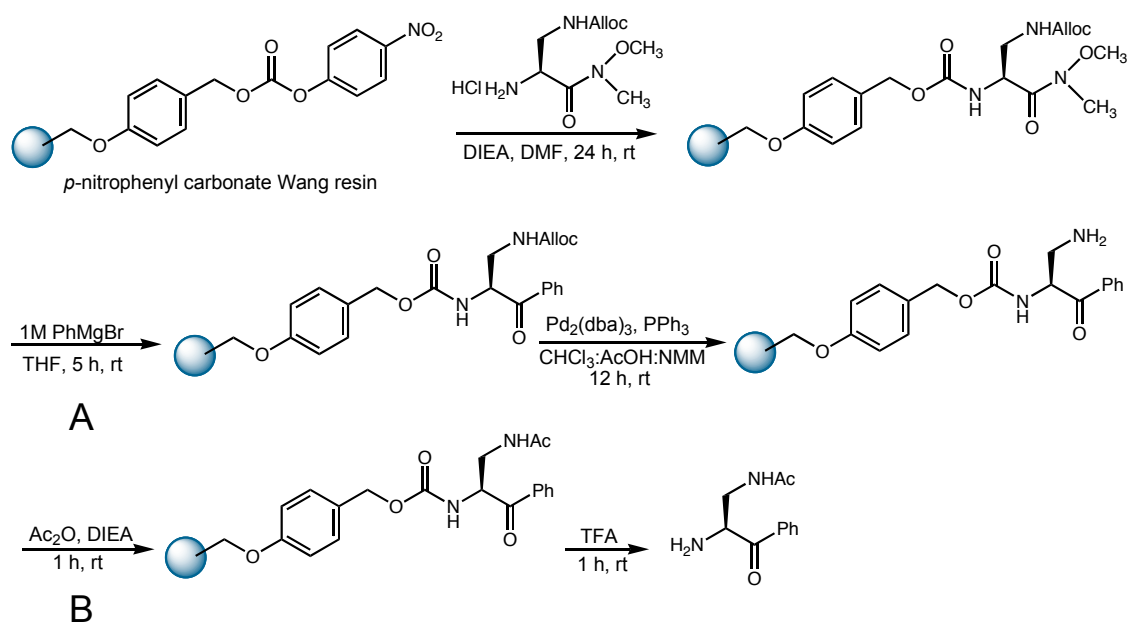


Scheme I-3: Dap backbone synthesis starting from Boc-Asp(OBzl)-OH.

Starting from Boc-Asp(OBzl)-OH, the free carboxylic acid was first protected as the methyl ester followed by the addition of a second Boc group on the amine. This double Boc-protection of the amine is necessary later in the synthesis when an isocyanate is formed. Without the second Boc group, the amine remains capable of reacting with the isocyanate to form a 5-membered cyclic urea. Upon completion of all the necessary protecting groups, the benzyl ester on the α -side chain was hydrogenated to reveal the free acid. To install the isocyanate, the acid was first converted to a mixed anhydride with ethyl chloroformate followed by reaction with NaN_3 and refluxing to form the isocyanate via a Curtius rearrangement. This procedure, however, was lengthy and low yielding. We found that the isocyanate could be formed in under an hour by refluxing the acid with diphenylphosphoryl azide (DPPA).³⁵ The isocyanate was obtained with high yield and purity and then trapped by allyl alcohol and CuCl to afford an alloc-protected amine. Once the orthogonally protected Dap backbone was in place, the methyl ester was saponified and the free acid was converted into a Weinreb amide.

At this juncture of the synthesis, a Grignard reaction was attempted but it was unsuccessful. A large number of by-products were produced that made purification of the desired molecule difficult. As an alternative, the Dap Weinreb amide was Boc-protected and placed on *p*-nitrophenyl carbonate Wang resin. Once on the solid-support, we were able to proceed with the Grignard reaction. After the Grignard, the β -amine was alloc-protected with a combination of $\text{Pd}_2(\text{dba})_3$ and PPh_3 . The β -amine was then acylated with Ac_2O and the final molecule was cleaved from the resin with trifluoroacetic acid. The product was precipitated out of ether and purified by HPLC to produce the Dap derivative.

Performing the remainder of the synthesis on solid-phase is advantageous not only because of the reduced amount of purification, but also because of the capacity to easily functionalize the molecule at two of the synthetic steps. The Grignard addition and the acylation of the amine allow for the placement of different chemical entities, including addition of amino acids to the amine to make a small library of molecules (Scheme I-4).



Scheme I-4: Solid phase synthesis of the Dap-derived phenyl ketone. A and B represent the steps of the synthesis where a wide variety of functionality can be introduced.

1.8 Summary

Based on an initial hit derived from PRIMA-1, we synthesized several phenyl ketone analogs of serine that appeared to have an effect on specific mutations of p53. Our lab proved that the molecule's electronics influence these results as well as verified that any toxicity was not a result of DNA intercalation. We were not able, however, to design a successful *in vitro* assay for our molecules because of the complicated nature of p53. A version of the serine-derived phenyl ketone was also synthesized starting from diaminopropionic acid, which provided a more stable molecule. Due to the costs, though, of the starting material, Dap(Alloc)-OH-HCl was synthesized starting from a derivative of aspartic acid.

With the synthesis of the Dap backbone complete, our group handed the project over to the lab of Dr. Ettore Appella and co-workers, who were better suited to study the biology. The chemistry designed is reproducible, having been repeated by various chemists and is being utilized to make many small molecules. Appella and co-workers have a number of cellular assays set up and are actively pursuing small molecules that have a positive affect on cells containing p53 mutants.

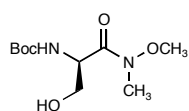
1.9 Experimental Procedures

General Methods. All reactions were performed in oven dry glassware under a positive pressure of nitrogen unless otherwise noted. Dichloromethane (DCM), acetonitrile, tetrahydrofuran (THF), and ether were all purified by passing solvent through a column of activated alumina on a solvent purification system built by Glass Contour prior to use. Dimethylformamide (DMF) was first passed through activated alumina and was additionally purified with an isocyanate scavenger column prior to use. All other solvents were purchased from Sigma-Aldrich and used without further purification. Proton nuclear magnetic resonances

(¹H-NMR) were recorded in deuterated solvents on a Mercury 400 (400 MHz), a Varian Inova 500 (500 MHz), or a Gemini 300 (300 MHz) spectrometer. Chemical shifts are reported in parts per million (ppm, δ) relative to tetramethylsilane (δ 0.00). If tetramethylsilane was not present in the deuterated solvent, the residual protio solvent is referenced (CDCl₃, δ 7.27; D₂O, δ 4.80; DMSO-d₆, δ 2.50). Proton-decoupled (¹³C-NMR) spectra were recorded on a Mercury 400 (100 MHz), a Varian Inova 500 (125 MHz), or a Gemini 300 (75 MHz) spectrometer and are reported in ppm using the solvent as an internal standard (CDCl₃, δ 77.23; DMSO, δ 39.52). Electrospray mass spectra (ESI-MS) were obtained using an Agilent 6100 series Quadrupole LC-MS. All amino acid starting materials, Boc₂O, and EDC were purchased from Advanced ChemTech and used without further purification, and the *p*-nitrophenyl carbonate Wang resin was purchased from Novabiochem. DNA was purchased from IDT, p53 was purchased from ProteinOne, and the antibodies were purchased from AbCam. Unless otherwise noted, all other commercially available reagents and solvents were purchased from Aldrich and used without further purification.

Abbreviations: (DCM), dichloromethane; (DMF), dimethylformamide; (THF), tetrahydrofuran; (Ac₂O), acetic anhydride; (Boc₂O), di-*tert*-butyl diacarbonate; (DIEA), *N,N*-diisopropylethylamine; (DMAP), 4-(dimethylamino)pyridine; (EDC), 1-ethyl-3-(3-dimethylaminopropyl)-carbodiimide; (HOBt), 1-hydroxybenzotriazole; (TEA), triethylamine. (TBDMSCl), *tert*-butyldimethylsilyl chloride; (DPPA), diphenylphosphoryl azide; (NEM), *N*-Ethyl morpholine.

1.9.1 Synthesis of Serine-Derived Molecules



Boc-Ser-Weinreb: Boc-Ser-OH (5.0 g, 24.4 mmol) was added to a 250 mL

RBF followed by DCM (90 mL) and cooled to -15 °C via an ice/salt water bath.

Next, *N,O*-dimethylhydroxyl amine-HCl (2.5 g, 25.6 mmol) and *N*-methyilmorpholine (2.8 mL,

25.6 mmol) were added to the reaction flask. EDC (4.9 g, 25.6 mmol) was then added to the

reaction flask in 5 equal portions over the first 30 min. After completely charged with EDC, the

reaction was allowed to stir an additional 1 h at -15 °C. The reaction was quenched with ice cold

1% HCl (25 mL) and transferred to a separatory funnel with DCM (100 mL). The mixture was

washed with 1% HCl (3 x 30 mL), sat. NaHCO₃ (2 x 30 mL), and sat. NaCl (1 x 30 mL). The

organic layer was separated and dried over Na₂SO₄. The solution was concentrated on a rotary

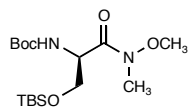
evaporator and dried under vacuum to give 4.4 g (73%) as a white solid. ¹H-NMR (500 MHz,

CDCl₃): δ 5.66 (br d, *J* = 6.0 Hz, 1H, carbamate-NH), 4.81 (br s, 1H, Boc-NH-CH), 3.82 (m, 2H,

CH-CH₂), 3.79 (s, 3H, N-OCH₃), 3.24 (s, 3H, N-CH₃), 2.86 (br s, 1H, CH₂-OH), 1.45 (s, 9H, *t*-

butyl-CH₃); ¹³C-NMR (125 MHz, CDCl₃): δ 171.1, 156.1, 80.2, 63.9, 61.8, 52.6, 32.3, 28.5;

ESI-MS *m/z* = 249.



Boc-Ser(OTBS)-Weinreb: Boc-Ser-Weinreb (4.4 g, 17.5 mmol) was added to

a 100 mL RBF followed by DMF (35 mL) and cooled to 0 °C via an ice bath.

Next, TBDMSCl (2.9 g, 19.3 mmol) and imidazole (2.4 g, 35.1 mmol) were added to the

reaction flask. The solution was stirred at 0 °C for 1 h and then allowed to warm to rt, stirring an

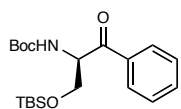
additional 2 h. The reaction solution was transferred to a 500 mL separatory funnel with EtOAc

(150 mL). The mixture was washed with 1% HCl (3 x 40 mL), sat. NaHCO₃ (1 x 40 mL), and

sat. NaCl (2 x 40 mL). The organic layer was separated and dried over Na₂SO₄. The solution

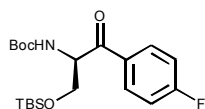
was concentrated on a rotary evaporator and dried under vacuum to give 5.9 g (93 %) as a colorless oil. **¹H-NMR** (500 MHz, CDCl₃): δ 5.34 (br d, *J* = 8.5 Hz, 1H, carbamate-NH), 4.73 (br s, 1H, Boc-NH-CH), 3.83 (m, 1H, CH-CH₂), 3.77 (m, 1H, CH-CH₂), 3.73 (s, 3H, N-OCH₃), 3.19 (s, 3H, N-CH₃), 1.41 (s, 9H, Boc-*t*-butyl-CH₃), 0.84 (s, 9H, Si-*t*-butyl-CH₃), 0.00 (s, 6H, Si-(CH₃)₂); **¹³C-NMR** (125 MHz, CDCl₃): δ 170.9, 155.5, 79.7, 63.6, 61.6, 52.6, 32.3, 28.5, 25.9, 18.4, -5.4; **ESI-MS** *m/z* = 363.

General Procedure for Grignard Reaction: Boc-Ser(OTBS)-Weinreb (6.0 mmol) was added to a 250 mL RBF followed by THF (60 mL). The mixture was cooled to 0 °C via an ice bath and a Grignard reagent in THF (18.0 mmol) was added over 8 min. The reaction stirred for 1.0 h at 0 °C and the ice bath was removed. The reaction stirred for an additional 1.0 h at rt and was again cooled to 0 °C via an ice bath. Next, the reaction was quenched by addition of 1.0 M HCl (55 mL). The solution was transferred to a separatory funnel with additional 1.0 M HCl (40 mL) and extracted with EtOAc (3 x 100 mL). The organic layers were washed with sat. NaCl (1 x 50 mL) and dried over Na₂SO₄. The solution was then concentrated on a rotary evaporator and dried under vacuum to give crude material. The residue was purified by flash column chromatography (10% EtOAc/Hexanes) to give a colorless oil.



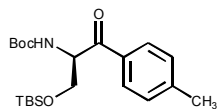
Boc-Ser(OTBS)-Phenyl ketone: Prepared using a 1.0 M solution of PhMgBr in THF. (89%) **¹H-NMR** (500 MHz, CDCl₃): δ 7.97 (d, *J* = 7.0 Hz, 2H, Ph-H), 7.61 (t, *J* = 7.0 Hz, 1H, Ph-H), 7.50 (t, *J* = 7.0 Hz, 2H, Ph-H), 5.73 (d, *J* = 7.5 Hz, 1H, carbamate-NH), 5.35 (m, 1H, Boc-NH-CH), 3.97 (dq, *J* = 9.5, 2.5 Hz, 2H, CH-CH₂), 1.50 (s, 9H, Boc-*t*-butyl-CH₃), 0.79 (s, 9H, Si-*t*-butyl-CH₃), -0.07 (s, 3H, Si-CH₃), -0.12 (s, 3H, Si-CH₃); **¹³C-NMR**

(125 MHz, CDCl₃): δ 197.9, 155.5, 135.6, 133.5, 128.8, 128.7, 79.9, 64.5, 57.4, 28.5, 25.8, 18.2, -5.6, -5.7; **ESI-MS** m/z = 380.



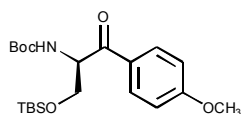
Boc-Ser(OTBS)-*p*-Fluorophenyl ketone: Prepared using a 1.0 M solution of

4-fluorophenyl magnesium bromide. (66%) **¹H-NMR** (500 MHz, CDCl₃): δ 8.08 (dd, J = 8.0, 5.5 Hz, 2H, Ph-H), 7.25 (t, J = 8.0 Hz, 2H, Ph-H), 5.72 (d, J = 7.0 Hz, 1H, carbamate-NH), 5.38 (d, 1H, Boc-NH-CH), 4.04 (dd, J = 10.5, 3.5 Hz, 1H, CH-CH₂), 3.98 (dd, J = 10.0, 5.0 Hz, 1H, CH-CH₂) 1.56 (s, 9H, Boc-*t*-butyl-CH₃), 0.85 (s, 9H, Si-*t*-butyl-CH₃), 0.00 (d, 6H, Si-CH₃).



Boc-Ser(OTBS)-*p*-Tolyl ketone: Prepared using a 1.0 M solution of *p*-tolyl

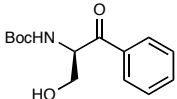
magnesium bromide. (61%) **¹H-NMR** (500 MHz, CDCl₃): δ 7.64 (d, J = 8.0 Hz, 2H, Ph-H), 7.37 (d, J = 8.0 Hz, 2H, Ph-H), 5.79 (d, J = 7.5 Hz, 1H, carbamate-NH), 5.39 (t, J = 4.0 Hz, 1H, Boc-NH-CH), 4.04 (dd, J = 10.5, 3.5 Hz, 1H, CH-CH₂), 4.01 (dd, J = 9.5, 4.5 Hz, 1H, CH-CH₂), 2.50 (s, 3H, Ph-CH₃), 1.55 (s, 9H, Boc-*t*-butyl-CH₃), 0.92 (s, 9H, Si-*t*-butyl-CH₃), 0.00 (d, 6H, Si-CH₃).

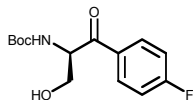


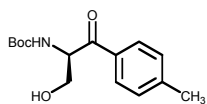
Boc-Ser(OTBS)-*p*-Methoxyphenyl ketone: Prepared using a 0.5 M

solution of 4-methoxyphenyl magnesium bromide. (50%) **¹H-NMR** (500 MHz, CDCl₃): δ 8.04 (d, J = 8.5 Hz, 2H, Ph-H), 7.05 (d, J = 8.5 Hz, 2H, Ph-H), 5.77 (d, J = 7.0 Hz, 1H, carbamate-NH), 5.38 (m, 1H, Boc-NH-CH), 4.02 (m, 2H, CH-CH₂), 3.99 (s, 3H, Ph-OCH₃), 1.55 (s, 9H, Boc-*t*-butyl-CH₃), 0.92 (s, 9H, Si-*t*-butyl-CH₃), 0.00 (d, 6H, Si-CH₃).

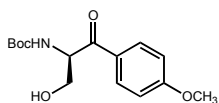
General Procedure for TBS deprotection: Product from General Procedure for Grignard Reaction (4.0 mmol) was added to a 100 mL RBF followed by a 1:1 mixture of THF/H₂O (20 mL). The mixture was stirred and glacial acetic acid (30 mL) was added to the reaction flask. The reaction stirred for 22 h at rt. The reaction was transferred to a 500 mL separatory funnel with sat. NaCl (75 mL) and sat. NaHCO₃ (50 mL). The aqueous layer was extracted with EtOAc (3 x 75 mL) and the combined organic layers were dried over Na₂SO₄. The solution was then concentrated on a rotary evaporator and dried under vacuum to crude material. The residue was purified by flash column chromatography (40% EtOAc/hexanes).

 **Boc-Ser(OH)-Phenyl ketone:** (95%) ¹H-NMR (500 MHz, CDCl₃): δ 8.00 (d, *J* = 7.5 Hz, 2H, Ph-H), 7.62 (t, *J* = 7.5 Hz, 1H, Ph-H), 7.51 (t, *J* = 7.5 Hz, 2H, Ph-H), 5.88 (br s, 1H, carbamate-NH), 5.35 (br s, 1H, Boc-NH-CH), 4.02 (m, 1H, CH-CH₂), 3.86 (m, 1H, CH-CH₂), 2.91 (br s, 1H, CH₂-OH), 1.47 (s, 9H, *t*-butyl-CH₃); ¹³C-NMR (125 MHz, CDCl₃): δ 197.4, 156.3, 134.6, 134.1, 129.0, 128.9, 80.5, 64.7, 58.1, 28.4; **ESI-MS** *m/z* = 288.

 **Boc-Ser(OH)-*p*-Fluorophenyl ketone:** (60%) ¹H-NMR (500 MHz, CDCl₃): δ 8.05 (t, *J* = 6.5 Hz, 2H, Ph-H), 7.17 (t, *J* = 8.5 Hz, 1H, Ph-H), 5.90 (d, *J* = 6.0 Hz, 1H, carbamate-NH), 5.32 (br s, 1H, Boc-NH-CH), 3.98 (dd, *J* = 11.5, 4.0 Hz, 1H, CH-CH₂), 3.87 (dd, *J* = 11.5, 4.5 Hz, 1H, CH-CH₂), 2.90 (br s, 1H, CH₂-OH), 1.45 (s, 9H, *t*-butyl-CH₃).

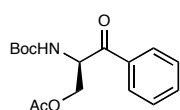


Boc-Ser(OH)-*p*-Tolyl ketone: (61%) $^1\text{H-NMR}$ (500 MHz, CDCl_3): δ 7.60 (d, $J = 8.0$ Hz, 2H, Ph-H), 7.29 (d, $J = 8.0$ Hz, 1H, Ph-H), 5.87 (br s, 1H, carbamate-NH), 5.30 (br s, 1H, Boc-NH-CH), 4.01 (m, 1H, CH-CH₂), 3.84 (m, 1H, CH-CH₂), 2.91 (br s, 1H, CH₂-OH), 2.40 (s, 3H, Ph-CH₃), 1.42 (s, 9H, *t*-butyl-CH₃).

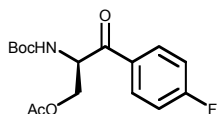


Boc-Ser(OH)-*p*-Methoxyphenyl ketone: (72%) $^1\text{H-NMR}$ (500 MHz, CDCl_3): δ 8.00 (d, $J = 8.5$ Hz, 2H, Ph-H), 6.98 (d, $J = 9.0$ Hz, 1H, Ph-H), 5.88 (br s, 1H, carbamate-NH), 5.30 (br s, 1H, Boc-NH-CH), 4.00 (dd, $J = 8.0$ Hz, 3.0 Hz, 1H, CH-CH₂-AB), 3.89 (s, 3H, Ph-OCH₃), 3.84 (dd, $J = 9.5$ Hz, 4.5 Hz, 1H, CH-CH₂), 2.90 (br s, 1H, CH₂-OH), 1.47 (s, 9H, *t*-butyl-CH₃).

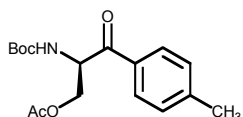
General Procedure for Acylation: Product from General Procedure for TBS deprotection (3.0 mmol) was added to a 100 mL RBF followed by DCM (30 mL). The resulting solution was cooled to 0 °C via an ice bath. Next, acetic anhydride (340 μL , 3.6 mmol), DIEA (630 μL , 3.6 mmol), and DMAP (36 mg, 0.3 mmol) were added to the reaction flask. The reaction solution stirred for 15 min at 0 °C, was quenched with 1% HCl (50 mL), and transferred to a separatory funnel with DCM (100 mL). The resulting organic layer was washed with 1% HCl (2 x 40 mL) and sat. NaCl (2 x 40 mL). The organic layer was dried over Na_2SO_4 , concentrated on a rotary evaporator, and dried under vacuum to give a crude colorless oil. The residue was purified by flash column chromatography (25% EtOAc/hexanes).



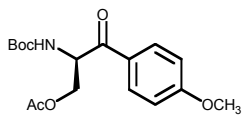
Boc-Ser(OAc)-Phenyl ketone: (96%) $^1\text{H-NMR}$ (500 MHz, CDCl_3): δ 8.02 (d, $J = 7.5$ Hz, 2H, Ph-H), 7.62 (t, $J = 7.5$ Hz, 1H, Ph-H), 7.51 (t, $J = 7.5$ Hz, 2H, Ph-H), 5.66 (d, $J = 8.0$ Hz, 1H, carbamate-NH), 5.59 (m, 1H, Boc-NH-CH), 4.51 (dd, $J = 11.5, 4.0$ Hz, 1H, CH-CH₂), 4.18 (dd, $J = 11.5, 6.0$ Hz, 1H, CH-CH₂), 1.99 (s, 3H, O=C-CH₃), 1.46 (s, 9H, *t*-butyl-CH₃); $^{13}\text{C-NMR}$ (125 MHz, CDCl_3): δ 196.2, 170.9, 155.5, 134.6, 134.3, 129.1, 128.8, 80.3, 64.9, 54.6, 28.5, 20.8; **ESI-MS** $m/z = 330$.



Boc-Ser(OAc)-*p*-Fluorophenyl ketone: (79%) $^1\text{H-NMR}$ (500 MHz, CDCl_3): δ 8.08 (dd, $J = 8.0, 5.5$ Hz, 2H, Ph-H), 7.18 (t, $J = 8.5$ Hz, 1H, Ph-H), 5.63 (d, $J = 8.0$ Hz, 1H, carbamate-NH), 5.54 (m, 1H, Boc-NH-CH), 4.48 (dd, $J = 11.0, 4.0$ Hz, 1H, CH-CH₂), 4.16 (dd, $J = 11.0, 6.0$ Hz, 1H, CH-CH₂), 2.00 (s, 3H, O=C-CH₃), 1.46 (s, 9H, *t*-butyl-CH₃).



Boc-Ser(OAc)-*p*-Tolyl ketone: (85%) $^1\text{H-NMR}$ (500 MHz, CDCl_3): δ 7.92 (d, $J = 7.5$ Hz, 2H, Ph-H), 7.30 (t, $J = 8.0$ Hz, 1H, Ph-H), 5.65 (d, $J = 7.0$ Hz, 1H, carbamate-NH), 5.55 (m, 1H, Boc-NH-CH), 4.50 (dd, $J = 11.5, 4.0$ Hz, 1H, CH-CH₂), 4.16 (dd, $J = 11.0, 5.5$ Hz, 1H, CH-CH₂), 2.41 (s, 3H, Ph-CH₃), 2.00 (s, 3H, O=C-CH₃), 1.42 (s, 9H, *t*-butyl-CH₃).

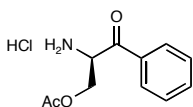


Boc-Ser(OAc)-*p*-Methoxyphenyl ketone: (91%) $^1\text{H-NMR}$ (500 MHz, CDCl_3): δ 8.02 (d, $J = 8.0$ Hz, 2H, Ph-H), 6.98 (t, $J = 8.5$ Hz, 1H, Ph-H),

5.65 (d, $J = 7.0$ Hz, 1H, carbamate-NH), 5.54 (m, 1H, Boc-NH-CH), 4.50 (br d, $J = 8.0$ Hz, 1H, CH-CH₂), 4.12 (dd, $J = 11.0, 6.5$ Hz, 1H, CH-CH₂), 3.89 (s, 3H, Ph-OCH₃), 2.00 (s, 3H, O=C-CH₃), 1.46 (s, 9H, *t*-butyl-CH₃).

General Procedure for Boc-deprotection: Product from General Procedure for acylation (1.0 mmol) was added to a 100 mL RBF followed by a 4.0 N HCl-Dioxane solution (7.5 mL, 30.0 mmol). The solution was stirred for 15 - 60 min and a precipitate formed. Et₂O (50 mL) was added to the reaction flask and the precipitate was filtered with a Buchner funnel. The precipitate was then washed with an additional portion of Et₂O (50 mL) and dried under vacuum.

H-Ser(OAc)-Phenyl ketone: (79%) ¹H-NMR (500 MHz, DMSO): δ 8.94 (s,



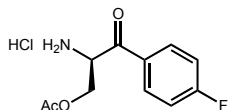
3H, CH-NH₃) 8.09 (d, $J = 7.5$ Hz, 2H, Ph-H), 7.73 (t, $J = 7.5$ Hz, 1H, Ph-H),

7.59 (t, $J = 7.5$ Hz, 2H, Ph-H), 5.47 (s, 1H, ⁺NH₃-CH), 4.60 (AB, $J = 12.5$ Hz,

1H, CH-CH₂), 4.42 (AB, $J = 12.5$ Hz, 1H, CH-CH₂) 1.94 (s, 3H, O=C-CH₃); ¹³C-NMR (125

MHz, DMSO): δ 193.3, 169.9, 134.6, 133.3, 129.1, 128.7, 62.0, 54.3, 20.5; ESI-MS $m/z = 208$.

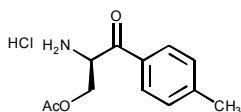
H-Ser(OAc)-*p*-Fluorophenyl ketone: (96%) ¹H-NMR (500 MHz,



DMSO): δ 8.64 (s, 3H, CH-NH₃) 8.18 (dd, $J = 9.5, 6.5$ Hz, 2H, Ph-H), 7.46

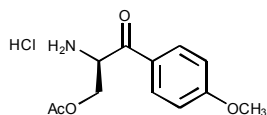
(t, $J = 9.0$ Hz, 2H, Ph-H), 5.45 (s, 1H, ⁺NH₃-CH), 4.53 (dd, $J = 12.5, 3.0$ Hz, 1H, CH-CH₂), 4.38

(dd, $J = 12.5, 4.0$ Hz, 1H, CH-CH₂), 1.96 (s, 3H, O=C-CH₃).



H-Ser(OAc)-*p*-Tolyl ketone: (87%) $^1\text{H-NMR}$ (500 MHz, DMSO)

δ 8.68 (s, 3H, CH-NH₃), 7.97 (d, $J = 8.0$ Hz, 2H, Ph-H), 7.39 (d, $J = 7.5$ Hz, 2H, Ph-H), 5.40 (s, 1H, $^+\text{NH}_3\text{-CH}$), 4.53 (dd, $J = 13.0, 3.5$ Hz, 1H, CH-CH₂), 4.36 (dd, $J = 12.5, 4.5$ Hz, 1H, CH-CH₂), 2.41 (s, 3H, Ph-CH₃), 1.95 (s, 3H, O=C-CH₃).



H-Ser(OAc)-*p*-Methoxy ketone: (94%) $^1\text{H-NMR}$ (500 MHz, DMSO):

δ 8.41 (s, 3H, CH-NH₃), 8.07 (d, $J = 9.0$ Hz, 2H, Ph-H), 7.13 (d, $J = 9.0$ Hz, 2H, Ph-H), 5.37 (s, 1H, $^+\text{NH}_3\text{-CH}$), 4.52 (dd, $J = 12.5, 3.5$ Hz, 1H, CH-CH₂), 4.33 (dd, $J = 12.5, 4.5$ Hz, 1H, CH-CH₂), 3.88 (s, 3H, Ph-OCH₃), 1.95 (s, 3H, O=C-CH₃).

1.9.2 ELISA

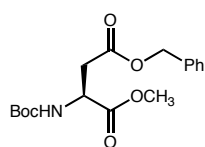
Using half-area black 96-well plates, 120 ng of conformational antibody DO-1, 240, or 1620, in 1X TBS (25 μL) was added to each well. The plate was incubated for 2 hours at rt. The wells were blocked with 1% BSA in 1X TBS (50 μL) overnight at 4 $^\circ\text{C}$, followed by washing with 1X TBST (TBS + 0.05% Tween-20) (3 x 50 μL). 0-25 ng of p53 in 1X p53 binding buffer (25 μL) was added to each well. Binding buffer (BB) consisted of 10X BB, 5X BDG (500 μL 10 mg/mL BSA, 10 μL DTT, and 500 μL glycerol), and water. If necessary, the solution of p53 was heated at 43 $^\circ\text{C}$ for the desired length of time. The plate was then incubated overnight at 4 $^\circ\text{C}$ followed by washing with 1X TBST (3 x 50 μL). A 1:1500 dilution in 1X TBS of the reporter antibody, rabbit anti-p53 polyclonal (25 μL), was added to each well and incubated for 2 hours at 4 $^\circ\text{C}$. After washing with 1X TBST (3 x 50 μL), a 1:1000 dilution in 1X TBS of the secondary antibody, donkey anti-rabbit-HRP polyclonal (25 μL), was added to each well. The plate was

incubated for another 2 hours at 4 °C and washed with 1X TBST (3 x 50 µL). Amplex Red solution (50 µL) was added to each well and the plate was protected from light and incubated for 30 minutes at rt. The plate was read using a fluorescent plate reader at 405 nm.

1.9.3 DNA Melting Studies

The oligonucleotides were dissolved in DEPC treated ultra-pure water and their concentration was determined by UV absorption at 260 nm on an Agilent 8453 UV/Vis spectrometer equipped with an Agilent 89090A peltier temperature controller. The supplier provided extinction coefficients for the DNA sequences. Solutions (300 µL) were prepared with 1X SSPE buffer (10 mM sodium phosphate, 0.1 mM EDTA, and 150 mM NaCl). All DNA concentrations were 3 µM. Base pair concentration ([bp]) was the DNA concentration multiplied by the number of base pairs in the oligonucleotide. The appropriate concentration of intercalator was determined by the base pair concentration. Ethidium bromide dilutions were prepared from a 10 mg/mL stock solution. For the temperature range 80-79 °C, UV absorbance was recorded at 260 nm with an equilibration time of 5 minutes. For the temperature range 79-20 °C, UV absorbance was recorded at 260 nm every 0.5 °C, with an equilibration time of 60 s for each measurement point. A cooling profile was recorded for each complex. The melting temperature (T_m) was determined from the maximum of the first derivative of the cooling.

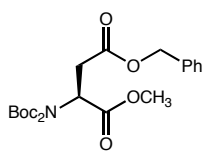
1.9.4 Synthesis of Diaminopropionic Acid Backbone



Boc-Asp(OBn)-OMe: Boc-Asp(OBn)-OH (4.8 g, 14.9 mmol) was dissolved in dry DMF (35 mL) in a 100 mL RBF. Finely ground K_2CO_3 (3.0 g, 22 mmol)

was added to the solution to form a suspension. The mixture was cooled to 0 °C in an ice bath

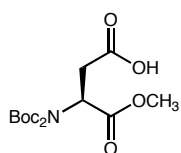
over five minutes. Methyl iodide (2.0 mL, 30 mmol) was then added to the RBF over 30 seconds. The resulting mixture was stirred at 0 °C for 3 hours. A yellow color developed within 20-30 minutes. The ice bath was removed, and H₂O (50 mL) was added, producing a grayish white precipitate. The mixture was extracted with EtOAc (3 x 50 mL). The organic layers were combined and washed with sat. NaHCO₃ (1 x 50 mL) and sat. NaCl (4 x 50 mL). The organic layer (which was yellow) was dried over Na₂SO₄, and passed through a plug of silica, eluting with ethyl acetate. Evaporation under vacuum afforded 2.52 g of a white powder (98%). ¹H-NMR (CDCl₃, 500 MHz): δ 7.34 (m, 5H, Ph-CH), 5.48 (d, *J* = 7.9 Hz, 1H, NH), 5.13 (dd, *J* = 12.3, 17.2 Hz, 2H, CH₂), 4.59 (t, *J* = 3.8 Hz, 1H, NH-CH), 3.70 (s, 3H, CH₃), 3.05 (dd, *J* = 4.0, 16.8 Hz, 1H, HC-H), 2.86 (dd, *J* = 4.5, 13.8 Hz, 1H, H-CH), 1.44 (s, 9H, *t*-butyl-CH₃); ¹³C-NMR (CDCl₃, 125 MHz): δ 171.73, 171.00, 135.62, 128.83, 128.65, 128.54, 80.36, 67.02, 52.89, 50.18, 37.11, 28.51.



Boc₂-Asp(OBn)-OMe: Di-*tert*-butyl dicarbonate (9.2 g, 42.3 mmol) and DMAP (3.44 g, 28.2 mmol) were placed into a dry 100 mL RBF. Boc-

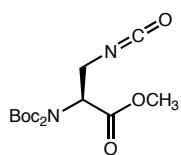
Asp(OBn)-OMe (9.5 g, 28.2 mmol) was added and the solids were dissolved in dry acetonitrile (30 mL). The resulting solution was stirred for 24 hours, during which time the reaction color went from light to dark yellow. Water (50 mL) was added, and the solution became cloudy white. The resulting mixture was extracted with EtOAc (3 x 50 mL). The combined organic layers were washed with 1 M HCl (1 x 50 mL) and saturated NaCl (4 x 50 mL). The combined organic layers were dried over Na₂SO₄ and evaporated under reduced pressure to afford

13.71 g of a viscous red oil (96%). **¹H-NMR** (CDCl₃, 500 MHz): δ 7.34 (m, 5H, Ph-CH), 5.48 (dd, *J* = 6.9, 6.8 Hz, 1H, NCH), 5.13 (dd, *J* = 12.3, 18.1 Hz, 2H, CH₂), 3.70 (s, 3H, CH₃), 3.30 (dd, *J* = 7.3, 16.7 Hz, 1H, HC-H), 2.77 (dd, *J* = 6.4, 16.5 Hz, 1H, H-CH), 1.48 (s, 18H, *t*-butyl-CH₃); **¹³C-NMR** (CDCl₃, 125 MHz): δ 170.75, 170.49, 151.80, 135.96, 128.76, 128.47, 83.79, 66.86, 55.10, 52.73, 36.11, 28.17.



Boc₂-Asp-OMe: Boc₂-Asp(OBn)-OMe (8.82 g, 20.2 mmol) was dissolved in MeOH (70 mL), and the solution was placed into a dry Parr reaction vessel. Palladium on activated carbon (1.76 g, 10% by weight) was added to the solution.

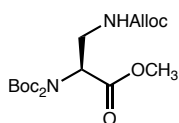
The solution was shaken on a Parr apparatus for 2 hours under an H₂ atmosphere of 50 psi. The Pd/C was filtered off through Celite 545, eluting with MeOH. The MeOH was evaporated under reduced pressure to give 9.02 g of a white powder (89%). **¹H-NMR** (CDCl₃, 500 MHz): δ 5.42 (dd, *J* = 6.6, 6.8 Hz, 1H, N-CH), 3.74 (s, 3H, CH₃), 3.30 (dd, *J* = 7.0, 17.0 Hz, 1H, HC-H), 2.81 (dd, *J* = 6.4, 17.0 Hz, 1H, H-CH), 1.49 (s, 18H, *t*-butyl-CH₃). **¹³C-NMR** (CDCl₃, 125 MHz): δ 176.96, 170.39, 151.76, 83.89, 54.81, 52.81, 35.85, 28.14.



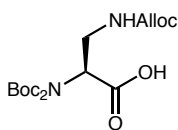
Isocyanate: Boc₂-Asp-OMe (1.70 g, 4.9 mmol) was dissolved in dry toluene in a 100 mL RBF and triethylamine (721 μL, 5.14 mmol) was added. DPPA (1.11 mL, 5.14 mmol) was added dropwise and the solution was refluxed for 45 min.

The reaction was cooled and quenched with sat. NH₄Cl. The aqueous layer was extracted with ether (3 x 25 mL) and the combined organic layers were washed with sat. NaCl and dried over

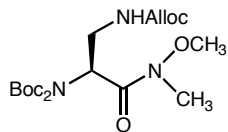
MgSO₄. The solvent was then removed under reduced pressure to afford 1.6 g of a light oil (95 %). **¹H-NMR** (CDCl₃, 500 MHz): δ 5.13 (dd, *J* = 5.5, 9.1 Hz, 1H, NCH), 3.94 (dd, *J* = 4.9, 13.4 Hz, 1H, HC-H), 3.83 (dd, *J* = 9.2, 13.4 Hz, 1H, H-CH), 3.75 (s, 3H, CH₃), 1.52 (s, 18H, *t*-butyl-CH₃). **¹³C-NMR** (CDCl₃, 125 MHz): δ 169.06, 152.09, 128.46, 84.23, 58.23, 52.74, 43.00, 28.16.



Boc₂-Dap(Alloc)-OMe: In a dry 50 mL RBF, CuCl (584 mg, 5.9 mmol) and allyl alcohol (401 μL, 5.9 mmol) were suspended in DMF (5 mL) to afford a yellowish green mixture. A solution of isocyanate (2.0 g, 5.8 mmol) in dry DMF (7 mL) was added. The resulting suspension turned bright green, and was stirred for 1 hour. Water (20 mL) was added to the reaction, and the resulting mixture was extracted with EtOAc (4 x 20 mL). The combined organic layers were then washed with 1 M HCl (20 mL) and saturated NaCl (4 x 20 mL), dried over Na₂SO₄ and evaporated under reduced pressure to afford a brownish red oil. The oil was redissolved in EtOAc (20 mL), and eluted through a silica plug to afford 1.56 g (67%) of a colorless oil. **¹H-NMR** (CDCl₃, 300 MHz): δ 5.90 (m, 1H, CH=CH₂), 5.21 (m, 2H, CH=CH₂), 5.00 (t, 1H, *J* = 6.7 Hz, NCH), 4.56 (d, 2H, *J* = 6.3, CH₂-CH), 3.80 (m, 1H, H-CH), 3.64 (m, 1H, HC-H), 3.74 (s, 3H, OCH₃), 1.50 (s, 18H, *t*-butyl-CH₃); **¹³C-NMR** (75 MHz): δ 170.0, 156.0, 152.0, 132.5, 117.6, 83.6, 65.5, 57.5, 52.0, 41.5, 28.0.

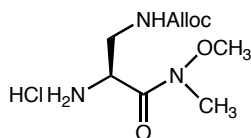


Boc₂-Dap(Alloc)-OH: A solution of Boc₂-Dap(Alloc)-OMe (1.14 g, 2.8 mmol in 10 mL of MeOH) was added to a 100 mL RBF. To the stirring solution, 2 M NaOH (12 mL) was added slowly. The color changed from a light yellow to gold. Precipitate briefly formed when all the NaOH solution had been added. After three minutes, the precipitate had dissipated. The reaction was left for two hours. The solution was concentrated by evaporation under reduced pressure, diluted with water (20 mL) and washed with ethyl ether (3 x 10 mL). The organic layer was washed with 2 M NaOH (2 x 25 mL). The combined aqueous layers were made acidic using 1 M HCl (pH ~3), which resulted in formation of a cloudy white solution. The aqueous mixture was extracted with ethyl acetate (3 x 50 mL). The combined organic layers (yellow) were washed with 1 M HCl (2 x 20 mL), and saturated NaCl (2 x 25 mL). The organic layer was dried over Na₂SO₄ and evaporated under reduced pressure to give a sticky yellow solid (70%). **¹H-NMR** (CDCl₃, 300 MHz): δ 10.53 (s, 1H, COOH), 5.90 (m, 1H, CH=CH₂), 5.26 (m, 2H, CH=CH₂), 5.08 (t, *J* = 6.7 Hz, 1H, NCH), 4.55 (d, *J* = 5.1 Hz, 2H, CH₂-CH), 3.81 (m, 1H, H-CH), 3.68 (m, 1H, HC-H), 1.49 (s, 18H, *t*-butyl-CH₃); **¹³C-NMR** (CDCl₃, 75 MHz): δ 173.5, 156.5, 151.7, 132.7, 117.8, 83.9, 65.8, 57.7, 41.0, 27.9.



Boc₂-Dap(Alloc)-Weinreb: A solution of Boc₂-Dap(Alloc)-OH (1.0 g, 2.6 mmol) in DCM was added to a round bottom flask. *N,O*-dimethylhydroxylamine HCl (351 mg, 3.6 mmol) and *N*-methylmorpholine (396 μL, 3.6 mmol) were added and the reaction stirred at rt. EDC (688 mg, 3.6 mmol) was added to the reaction in 5 equal portions over 30 minutes and the reaction stirred for an additional hour. The reaction was

quenched with 1% HCl (20 mL) and transferred to a separatory funnel with DCM. Organic layers were washed with 1% HCl (3 x 20 mL), sat. NaHCO₃ (2 x 20 mL), and sat. NaCl (1 x 20 mL), dried over anhydrous Na₂SO₄, and concentrated on a rotary evaporator and dried under vacuum to produce a colorless oil (93%). **¹H-NMR** (CDCl₃, 300 MHz): 5.9 (m, 1H, CH=CH₂), 5.24 (m, 2H, CH-CH₂), 5.08 (t, *J* = 6.7 Hz, 1H, NCH), 4.54 (d, *J* = 5.4 Hz, 2 H, CH₂-CH), 3.72 (m, 2H, CH₂), 3.66 (s, 3H, OCH₃), 3.18 (s, 3H, NCH₃), 1.50 (s, 18H, *t*-butyl-CH₃); **¹³C-NMR** (CDCl₃, 75 MHz): δ 171.2, 156.1, 152.0, 132.9, 117.3, 83.2, 65.4, 61.5, 56.1, 41.5, 32.2, 27.8.



Dap(Alloc)-Weinreb-HCl: Boc₂Dap(Alloc)-Weinreb (748 mg, 1.7 mmol)

was added to a RBF and stirred in 4 N HCl-Dioxane (8.5 mL, 34 mmol) for 2-3 hours. The dioxane was evaporated under nitrogen. Ether was added

to the flask to precipitate product, which was filtered and washed with ether. Product was dried under vacuum to produce a sticky white solid (75%). **¹H-NMR** (DMSO, 300 MHz): δ 8.65 (s, 3H, NH₃), 7.47 (br s, 1H, NH), 5.87 (m, 1H, CH=CH₂), 5.21 (dd, *J* = 14.0, 32.0 Hz, 2H, CH=CH₂), 4.45 (d, *J* = 5.0 Hz, 2H, CH₂-CH), 4.25 (s, 1H, NCH), 3.73 (s, 3H, OCH₃), 3.41 (m, 2H, CH₂), 3.14 (s, 3H, NCH₃); **¹³C-NMR** (DMSO, 75 MHz): δ 167.2, 156.2, 133.6, 117.2, 100.3, 64.8, 61.9, 50.3, 32.2.

1.9.5 Solid phase synthesis

Resin functionalization: *Para*-nitrophenylcarbonate Wang resin (410 mg, 0.29 mmol) was swelled in DMF. Dap(Alloc)-Weinreb (100 mg, 0.29 mmol) was stirred in DMF (1 mL) and

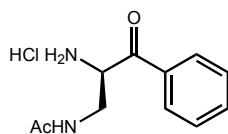
DIEA (100 μ L, 0.58 mmol) was added. The solution was added to the resin and shaken at rt for 24 hours. The resin was filtered and a solution of DCM/MeOH/DIEA (37:2:1) was added to the resin and shaken for 5 min. After filtering, the resin was washed with DCM (3 x 5 mL).

Grignard addition: The resin was solvated in dry THF at 0 °C and 1 M PhMgBr (1.5 mL, 1.5 mmol) was added dropwise and the reaction was shaken at rt for 5 hours. The reaction was filtered and washed with THF (3 x 5 mL), acetone (3 x 5 mL), 0.28 M hydrocinnamic acid in THF (3 x 15 mL), and DCM (3 x 5 mL).

Alloc deprotection: Pd₂(dba)₃ (128 mg, 0.14 mmol) and PPh₃ (183 mg, 0.7 mmol) were added to the resin in a solution of CHCl₃/AcOH/NEM (37:2:1), protected from light, and shaken for 5 hours. The resin was filtered and washed with CHCl₃/AcOH/NEM (3 x 5 mL), CHCl₃ (3 x 5 mL), DMF (3 x 5 mL), and DCM (3 x 5 mL).

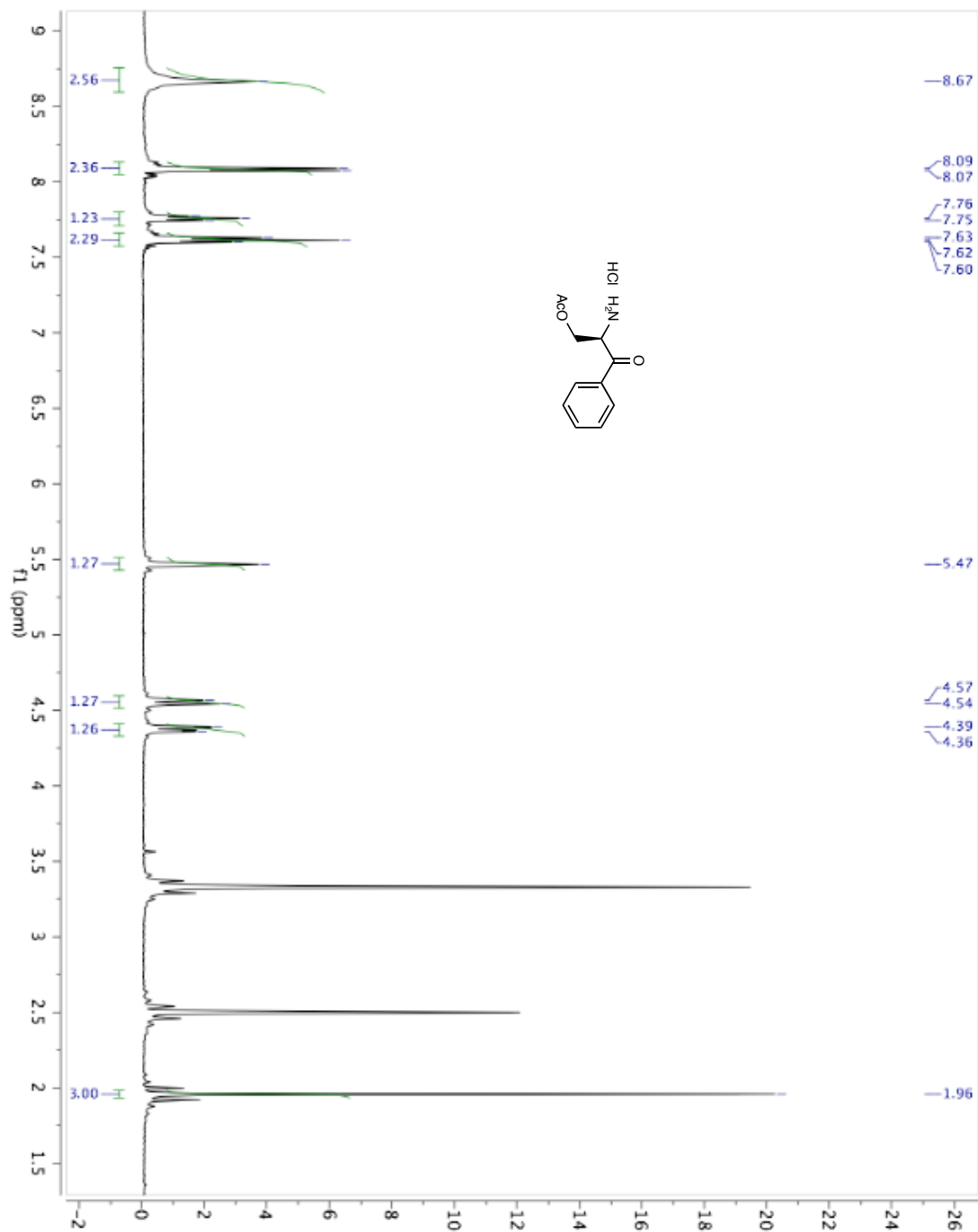
Acylation: Acetic anhydride (80 μ L, 0.84 mmol) and DIEA (146 μ L, 0.84 mmol) were added to the resin in DMF and shaken for 1 hour. The resin was filtered and washed with DMF (3 x 5 mL) and DCM (3 x 5 mL).

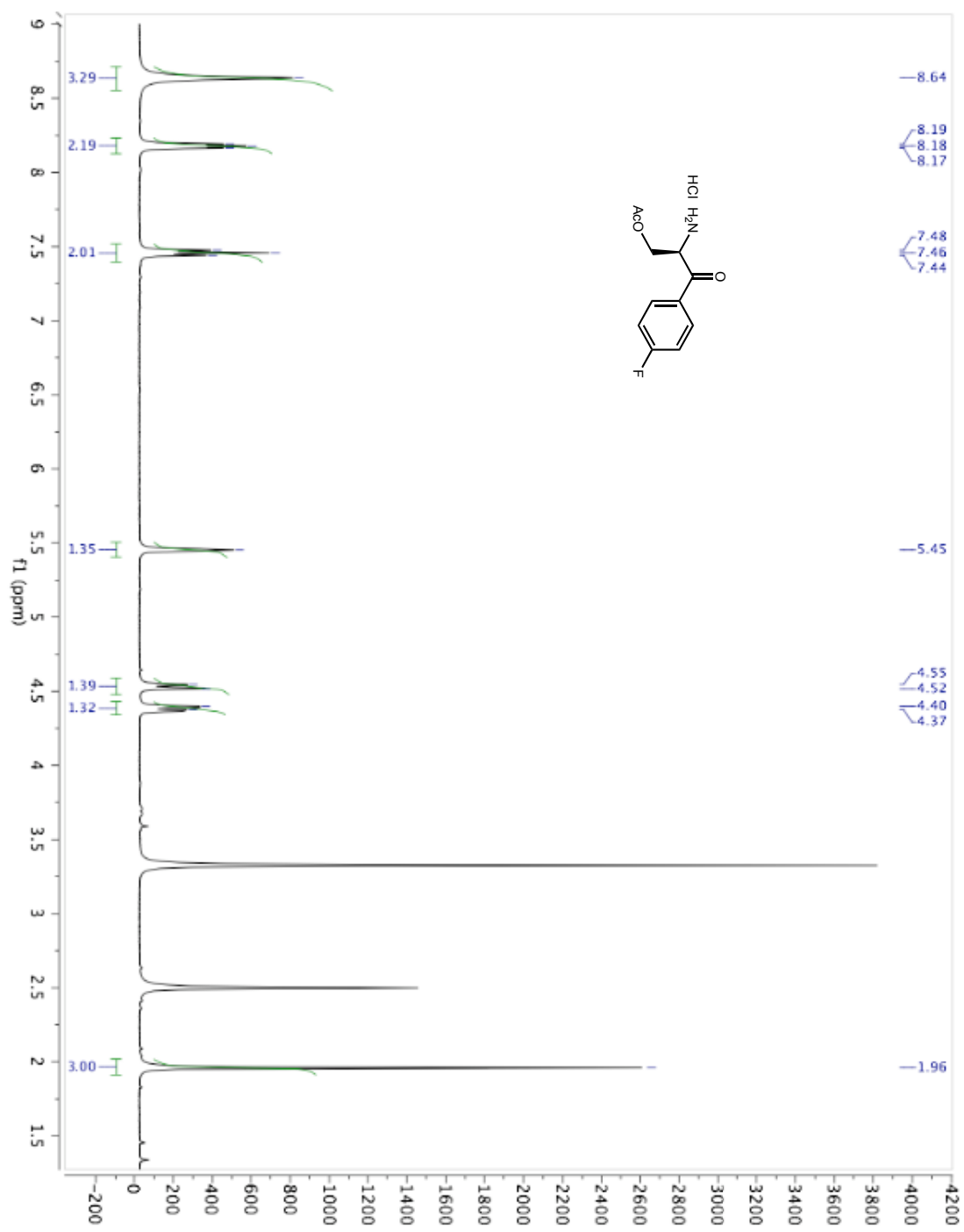
Cleavage: TFA was added to the resin and allowed to shake for 1 hour. After draining the resin and washing with DCM, the solvent was evaporated. Ether was added to the resulting residue to precipitate a white solid. The solid was filtered and washed with ether and purified by HPLC.

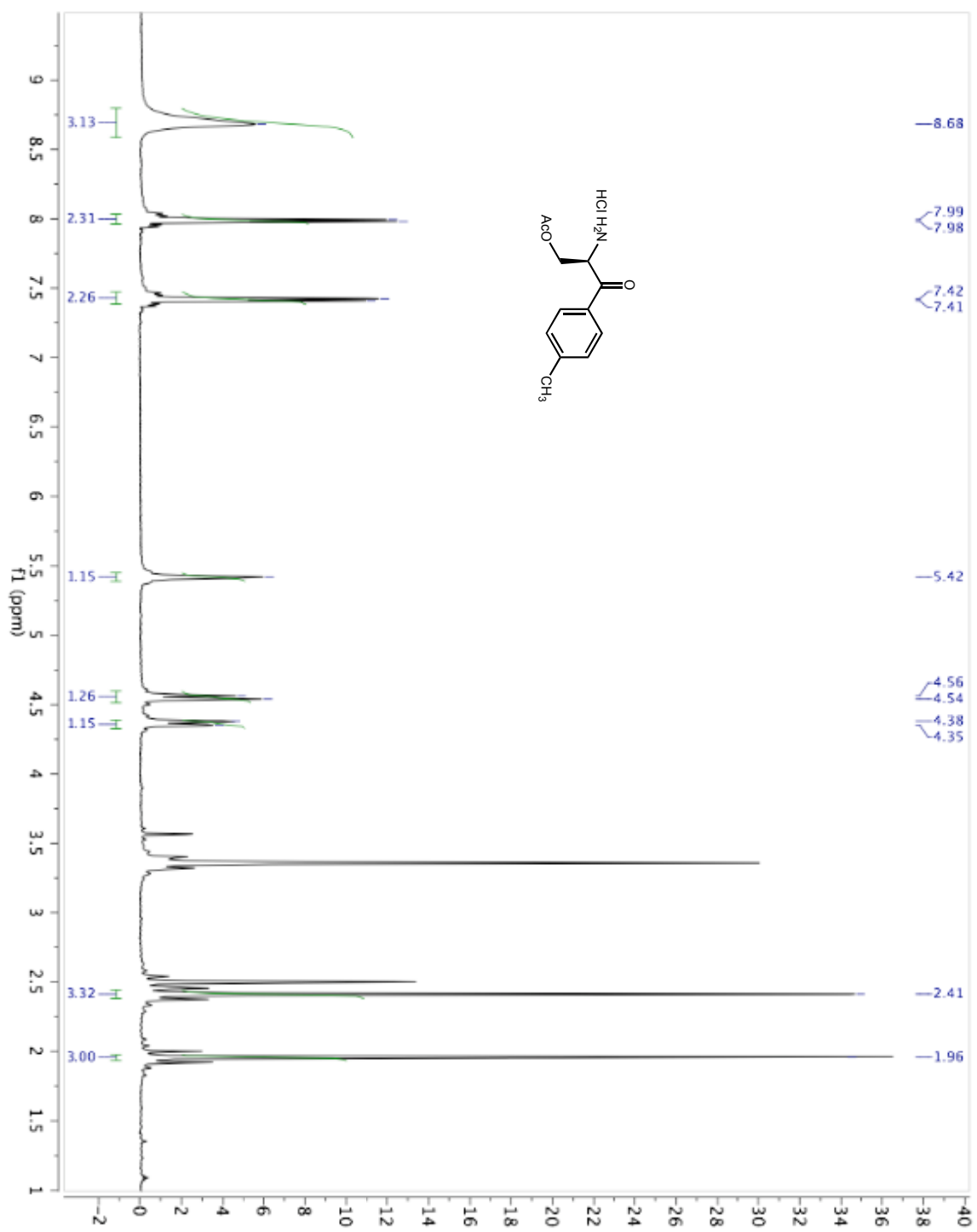


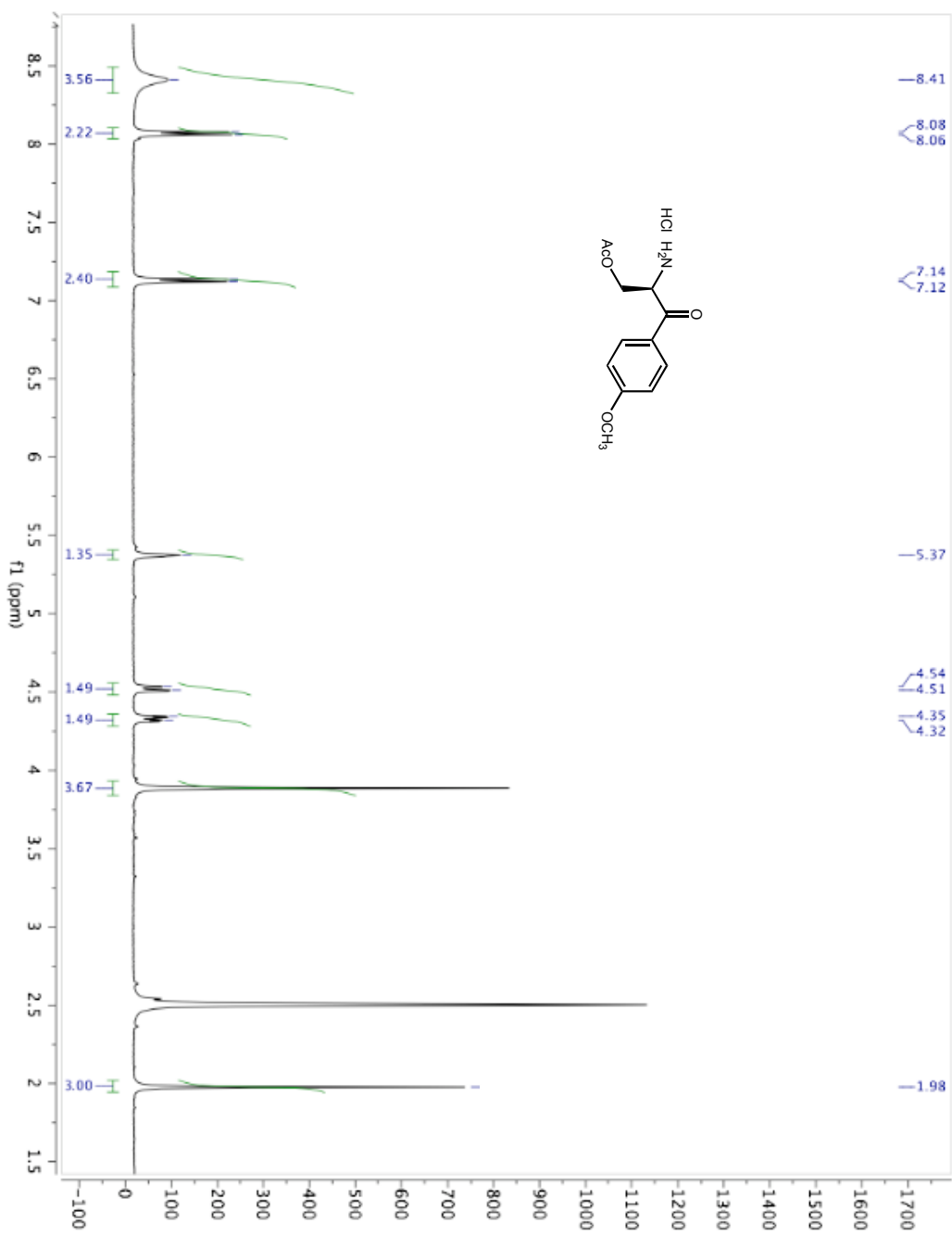
H-Dap-Phenyl ketone. ¹H-NMR (DMSO, 300 MHz): δ 8.48 (s, 3H, NH₃), 8.24 (t, $J = 4.32$ Hz, 1H, NH), 8.08 (d, $J = 7.23$, 2H, Ph-H), 7.75 (t, $J = 4.56$,

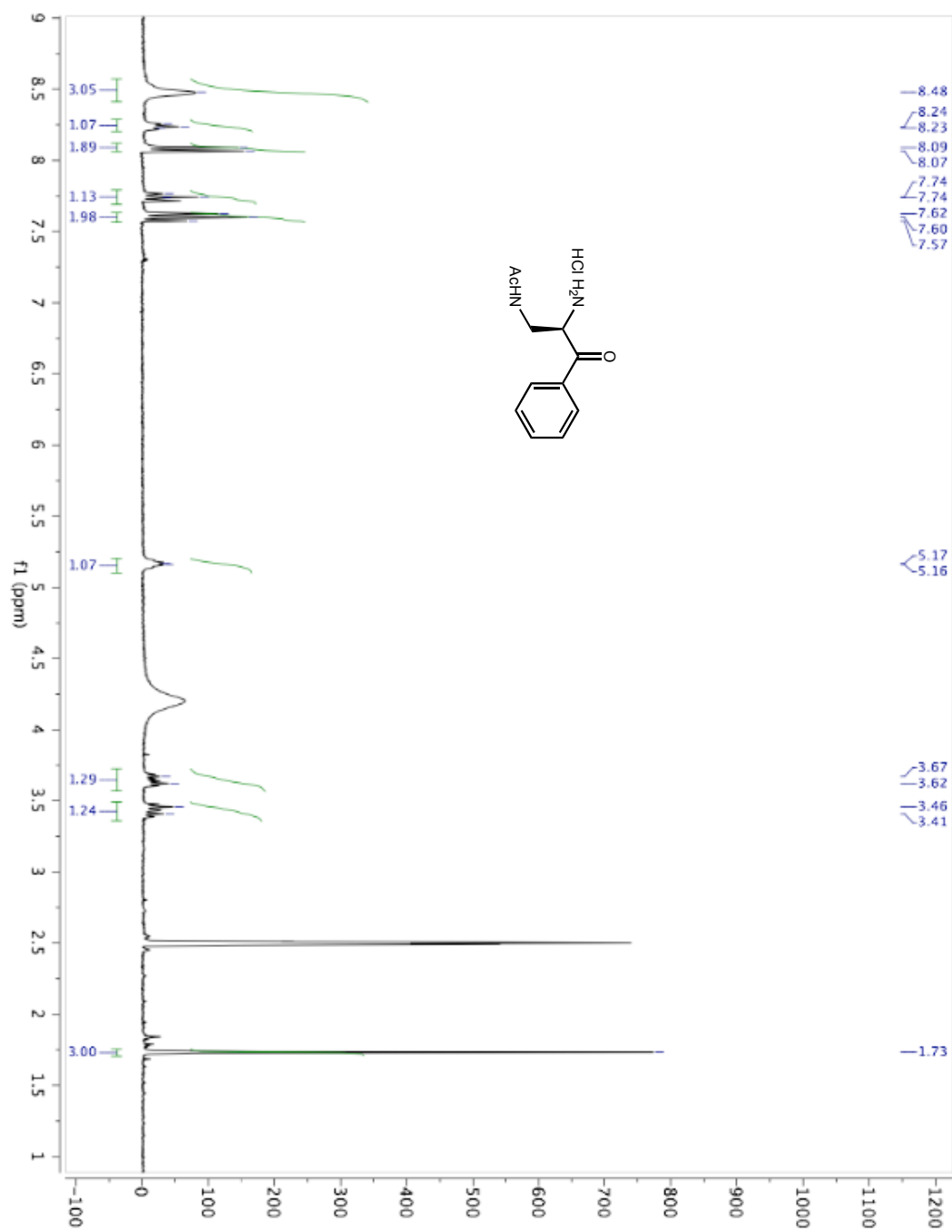
1H, Ph-H), 7.60 (t, $J = 7.59$ Hz, 2H, Ph-H), 5.16 (m, 1H, CH-CH₂), 3.65 (m, 1H, HC-H), 3.43 (m, H-CH), 1.73 (s, 3H, CH₃).

1.9.6 Select ^1H -NMRs









Chapter 2

Synthetic Optimization and Biological Studies of YYY Polyamine that Binds to HIV-1 TAR RNA

2.1 Introduction

The search for viable drug targets is conventionally limited to proteins, most often at a catalytic or binding site. Proteins may contain pockets or cavities as attractive sites for disruption often leaving other biomolecules as overlooked targets. In recent years however, RNA has become a potential drug target.^{1,2} The ability of RNA to fold into complex structures, much like proteins, allows it to act as a biological catalyst, a site for protein binding, a translator of genetic information, and a structural scaffold.³ One RNA of particular interest is the transactivation response element (TAR) of HIV. TAR is a highly conserved region of the HIV-1 mRNA genome that is responsible for binding the HIV transactivator protein Tat, which is necessary for viral replication. The pyrimidine bulge of TAR is explicitly involved in binding Tat and disruption of this process inhibits viral replication. Many efforts have been made towards the discovery of an inhibitor that would bind specifically to the bulge region of TAR. Among these efforts are peptidomimetics, peptides, small molecules, and aminoglycosides.¹⁹⁻³⁵

Our lab previously explored whether side-chain functionalized polyamines could bind specifically and with high affinity to TAR. The polyamines were designed to contain a cationic backbone with various side chains to guide specificity. One of our molecules, YYY, was found via a footprinting assay to bind to the TAR bulge with a K_D of 5 μM . With these promising data, we sought to optimize the synthesis to minimize the amount of branching usually seen at the first amine thus increasing yield and simplifying purification. In addition, we required further studies including NMR and cellular assays to verify our initial binding results.

2.2 TAR RNA and HIV-1 Transcription

All HIV-1 mRNAs begin at the 5' end with the formation of an identical 59-base structure call the Trans-Activation Responsive (TAR) element. TAR forms a stable hairpin and consists of a six-nucleotide loop and a tripyrimidine bulge. This tri-nucleotide bulge (U23, C24, U25) is essential for the high affinity binding of the trans-activator of transcription (Tat) protein.⁴⁻⁶ Tat, one of two regulatory HIV-1 proteins, is necessary for viral replication; the transcription of mRNAs cannot be efficiently lengthened to produce the full-length viral genome in the absence of Tat. The TAR-Tat complex recruits several transcription factors to promote the formation of elongation complexes that lead to the production of full length HIV viral RNA.⁷⁻⁹ (Figure II-1)¹⁰

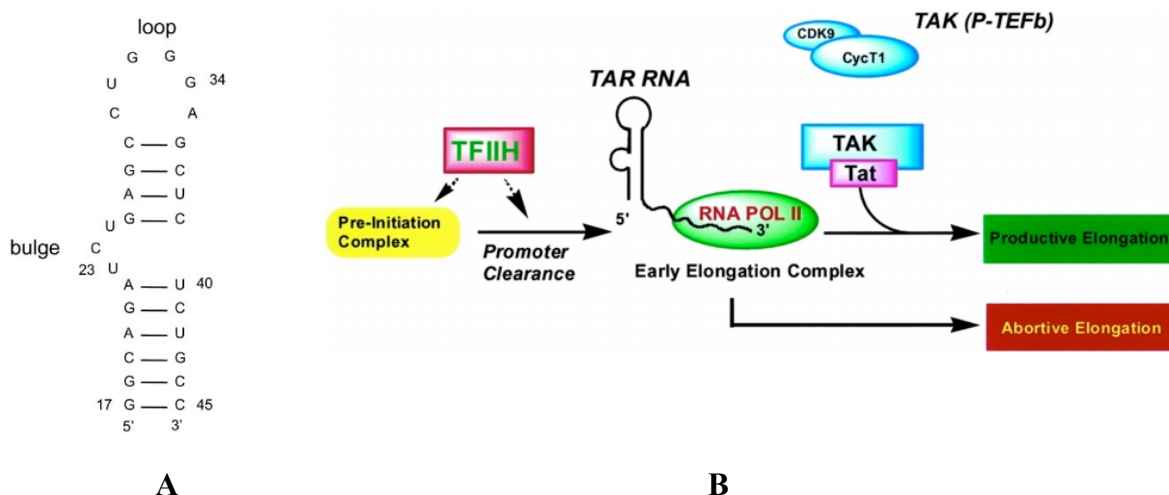


Figure II-1: A) TAR loop/bulge structure B) Mechanism of viral genome elongation¹⁰

2.3 Inhibitors of HIV-1 Transcription

The disruption of the TAR-Tat binding has been shown to inhibit viral replication.^{11, 12} TAR or Tat antagonists would have great potential as HIV-1 therapeutics. However, since a number of co-factors are involved in HIV-1 transcription, hindering any of these co-factors

should also block HIV replication.¹³ Kashanchi and co-workers found that the expression of a cyclin-dependent kinase (cdk) inhibitor, p21/Waf1, was lacking in HIV-1 infected cells and they suggested that ckd's were required for HIV-1 transcription and cdk inhibitors could be possible therapeutic agents. In fact, the cdk inhibitor Roscovitine prevented HIV-1 transcription and induced apoptosis.¹⁴

Okamoto and co-workers reported several fluoroquinolone derivatives that inhibited HIV-1 transcription by targeting one of the cellular factors. The initial structure (K-12) had potent activity against both acutely and chronically infected cells.¹⁵ Additional derivatives (K-38, K-37, and K-42) were also found to target Tat co-factors and possessed improved activity and specificity over K-12 (Figure II-2). Unfortunately, as the activity increased, so did the cellular toxicity prohibiting them from being therapeutic candidates.¹⁶

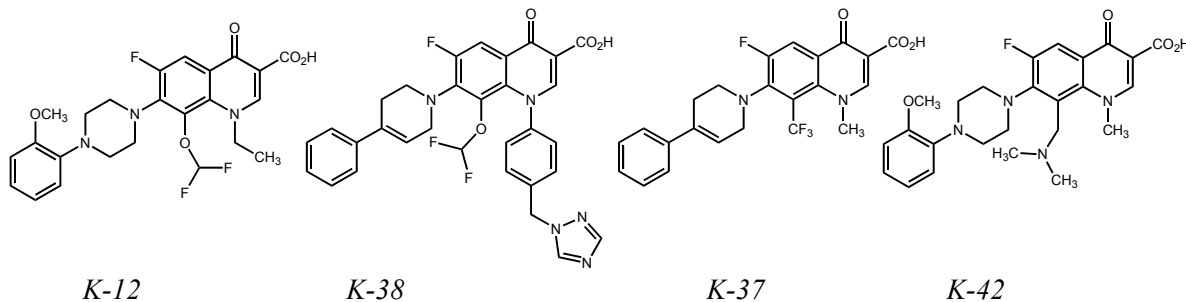


Figure II-2: Fluoroquinolone derivatives that inhibit HIV-1 transcription by targeting Tat co-factors

Workers at Hoffmann-LaRoche discovered a benzodiazepine similar to Valium (Ro 24-7429) that acts as a Tat antagonist. HIV replication was inhibited in both acutely and chronically infected cells. The precise mechanism remains unknown, but no evidence was found of Ro 24-7429 preventing Tat-TAR binding.¹⁷ Ro 24-7429 (Figure II-3) is the only HIV-1 transcription

inhibitor to undergo clinical trials. No evidence of antiviral activity, though, was observed in patients during a 12 week trial.¹⁸

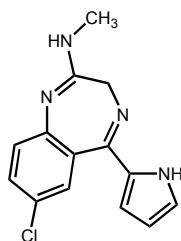


Figure II-3: Ro 24-7429

2.3.1 HIV-1 Transcription Inhibitors Targeting TAR

While many interactions are involved in HIV-1 transcription, the Tat-TAR interaction is unique to HIV-1. Much research has therefore been dedicated to discovering an inhibitor that targets the bulge region of TAR and competes with Tat binding.^{12, 19, 20} Specifically, an arginine-rich region of Tat (YGRKKRRQRRRP) binds the bulge of TAR and many inhibitors try to mimic Tat's cationic properties.

One of the first attempts to inhibit the TAR-Tat interaction was with short peptides similar to Tat.²¹ Due to the insufficient properties of peptides to act as therapeutics, other types of oligomers and small molecules were explored. Researchers at Novartis identified a 9-residue peptoid-peptide hybrid (CGP64222) that inhibited the formation of the TAR-Tat complex with an IC_{50} of 12 nM (Figure II-4).²²

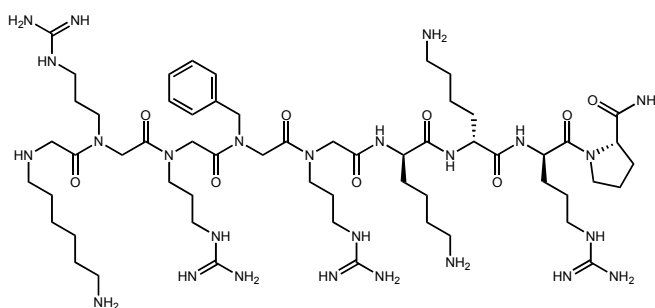


Figure II-4: CGP64222

Another potent inhibitor of the TAR-Tat complex is a D-amino acid containing tripeptide synthesized by Rana and co-workers (Figure II-5A), which has an IC_{50} of 50 nM.²³ To improve pharmacokinetics, the tripeptides were cyclized (Figure II-5B) since cyclic peptides demonstrate improved stability, selectivity, and bioavailability over their linear counterparts. Cyclization, however, fared only slightly better (IC_{50} ~40 nM) than the binding of the tripeptide.²⁴

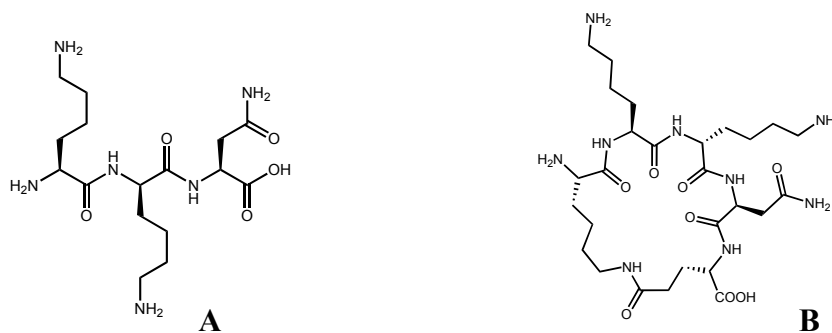


Figure II-5: A) D-amino acid tripeptide B) Cyclized tripeptide

In addition to peptides and peptidomimetics, a limited number of small molecules have been explored as Tat-TAR inhibitors with many possessing the guanidinium moiety of arginine or intercalation properties.²⁵⁻²⁷ One quinolone molecule, derived from Okamoto's fluoroquinolone series, WM5, was found to bind exclusively to the three base bulge region of TAR through chelation of magnesium ions (Figure II-6).^{28, 29}

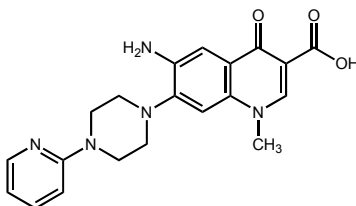


Figure II-6: WM5

A greater effort has focused on aminoglycoside antibiotics that are known to bind to ribosomal RNA.³⁰ Neomycin B (Figure II-7A) in particular binds to TAR RNA, but its toxicity and promiscuity for other nucleic acids make it an undesirable candidate for drug development.^{31, 32} Fortunately the neamine portion of neomycin B, which is much less toxic, is sufficient for RNA binding and derivatives of neamine can be probed for Tat-TAR inhibition. Décout and co-workers synthesized a neamine-peptide nucleic acid (PNA) conjugate that targets TAR RNA (Figure II-7B).³³ Neamine allows for the cellular uptake of the PNA, which results in potent inhibition of viral replication. The Décout lab also synthesized neamine dimers (Figure II-7C) that were found to hinder Tat-TAR binding at submicromolar concentrations and more effectively than either neomycin or neamine alone.³⁴

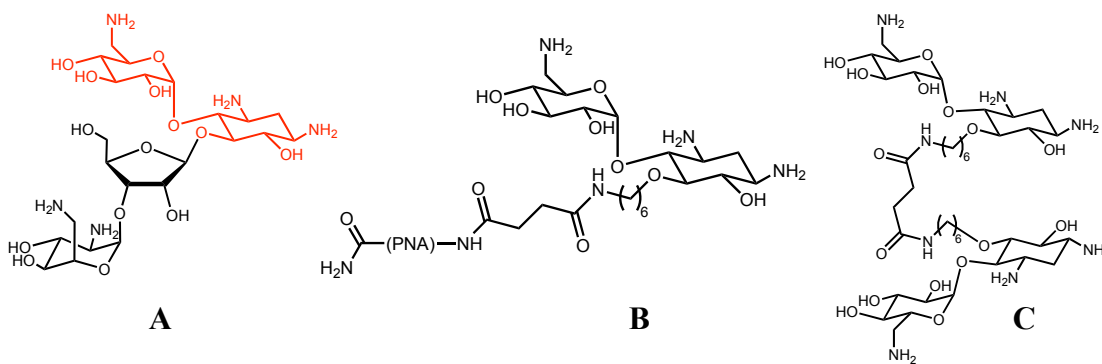


Figure II-7: A) Neomycin B with the neamine portion highlighted in red B) Neamine-PNA conjugates C) Neamine dimers

These examples, as well as other TAR binding molecules^{35, 36} typically possess a dense cationic charge that augments the binding affinity to TAR RNA. All nucleic acids, however, consist of an anionic backbone and the peripheral cationic charge on these molecules will bind to other nucleic acids lessening their specificity for TAR.

2.4 Polyamines

Our lab aimed to devise a molecular scaffold suitable for synthesizing a library of molecules to test for TAR RNA binding and we wanted to design a molecule that would exhibit both high affinity and high selectivity. A polyamine derived from amino acids was proposed with the idea that a cationic amine backbone (Figure II-8A) would enhance the affinity of the molecule while various non-cationic amino acid side-chains would direct the specificity of the molecule. Additionally the polyamine synthesis is suitable for solid-phase chemistry, which is ideal for library syntheses. One polyamine with three tyrosine residues (YYY) was initially identified in our lab to bind to TAR RNA with a K_D of 5 μM (Figure II-8B).³⁷

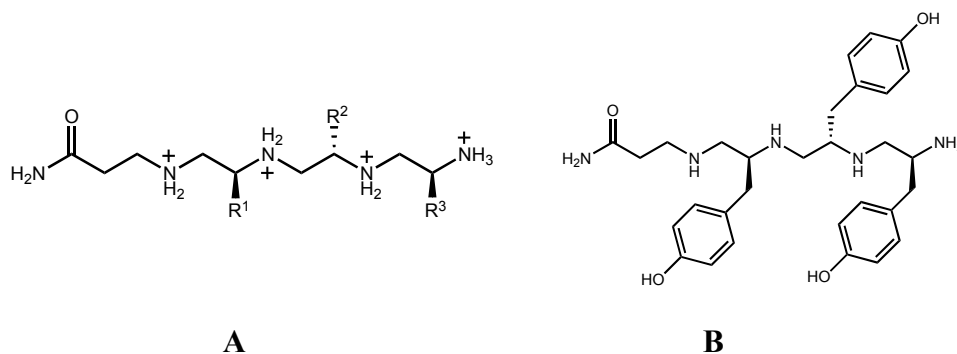
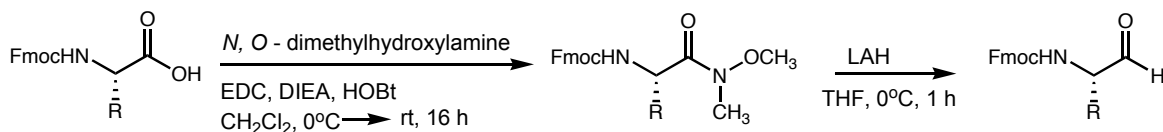


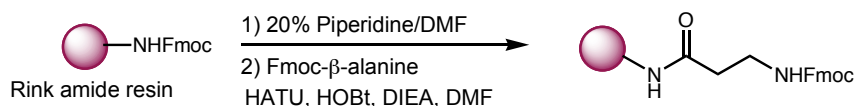
Figure II-8: A) Cationic polyamine backbone B) YYY polyamine

2.4.1 Polyamine Synthesis

The polyamines are synthesized on Rink Amide resin through a series of reductive aminations and using standard Fmoc-chemistry. Initially, Fmoc-amino acids are converted to Weinreb amides followed by reduction to aldehydes using lithium aluminum hydride (LAH)^{38, 39} and the Fmoc-amino aldehydes can be stored in a -20 °C freezer for at least a month with no degradation (Scheme II-1). Fmoc- β -alanine linker is coupled to the Rink Amide resin using a solution of HATU/HOBt/DIEA in DMF (Scheme II-2).

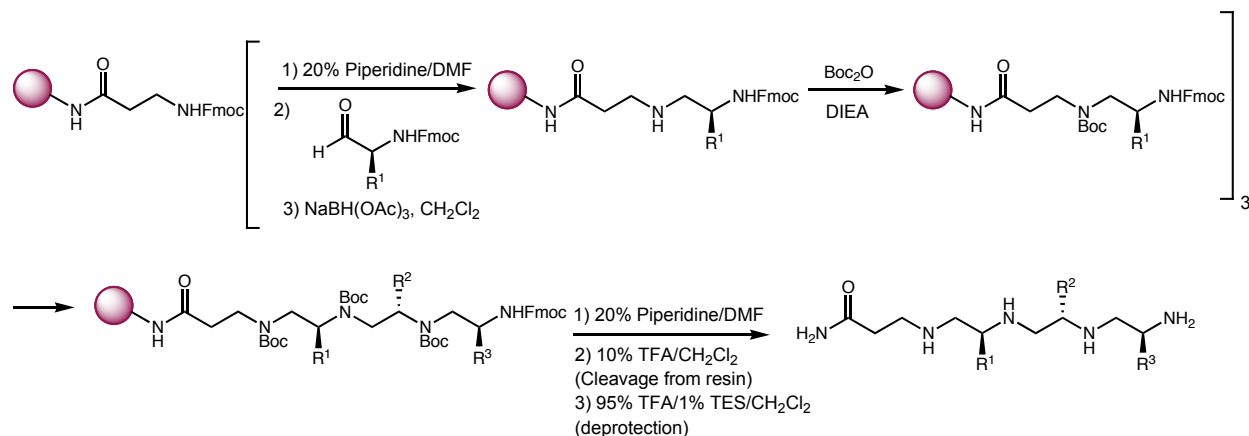


Scheme II-1: Fmoc-amino aldehyde synthesis



Scheme II-2: Linker coupling to Rink resin

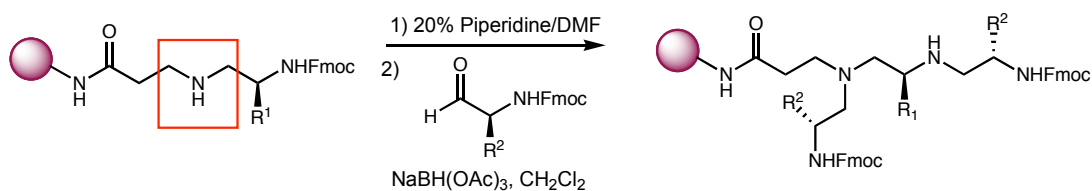
Once the linker is on the resin, the β -alanine is Fmoc-deprotected with 20% piperidine in DMF. An amino aldehyde is added to the resin in dichloromethane and allowed to shake for 10 minutes before it is drained and followed by a solution of $\text{NaBH}(\text{OAc})_3$ in dichloromethane for 45 minutes. After the completion of the reductive amination, the secondary amine is Boc-protected to prevent branching. The series of Fmoc-deprotection, reductive amination, and Boc-protection is repeated two more times to synthesize a polyamine trimer. One final Fmoc-deprotection takes place before the molecule is cleaved from the resin with a 10% TFA/DCM solution and all of the protecting groups are successfully removed with a solution of 95% TFA/1% Triethylsilane/DCM. The final product is precipitated out of ether and purified by HPLC to produce a white solid, which is stored in water at 4 °C or colder (Scheme II-3).



Scheme II-3: Solid phase synthesis of polyamines

2.5 Linker Studies

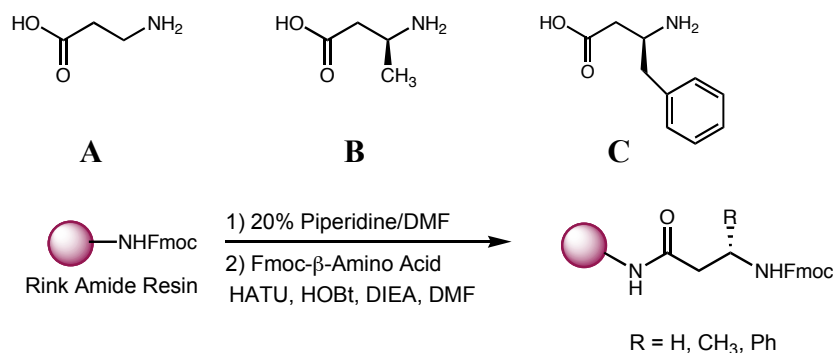
One difficulty with the synthesis was that branching still occurred at the first reductive amination due to over-alkylation (Scheme II-4). Over-alkylation did not appear to be a problem at the subsequent amines, presumably due to the steric bulk the amino acid sidechains provided. We reasoned that introducing some steric hindrance in the linker molecule might circumvent this dilemma. Two other linkers, Fmoc- β -homoalanine and Fmoc- β -homophenylalanine, were tested to see if they would hinder branching.



Scheme II-4: Over-alkylation at the first secondary amine

Three batches of Rink Amide resin were synthesized with each β -amino acid, and the reductive amination was performed with Fmoc-alanine aldehyde (Scheme II-5). Alanine is not a bulky

amino acid and should branch easily; the Fmoc-protecting group was left intact on the alanine to aid HPLC visualization.



Scheme II-5: Derivatization of Rink Amide resin with A) β-alanine, B) β-homoalanine, or C) β-homophenylalanine

When the HPLC of the β-alanine-alanine molecule was run, three distinct peaks were found and each peak was collected and its mass determined (Figure II-9). The first (and major) peak was the desired product and the third peak, which was also strong, contained the branched molecule. The second HPLC peak contained a mass that was 28 units greater than our desired product (M+28 peak). Three peaks were also present in the HPLC trace of the β-homoalanine-alanine molecule (Figure II-10), although both the M+28 and branching peaks were greatly reduced. These two peaks were virtually non-existent in the chromatograph of the β-homophenylalanine-alanine molecule (Figure II-11). As we had hypothesized, introducing some steric bulk into the linker of the molecule did inhibit branching, but we had to determine where the extra 28 mass units were originating.

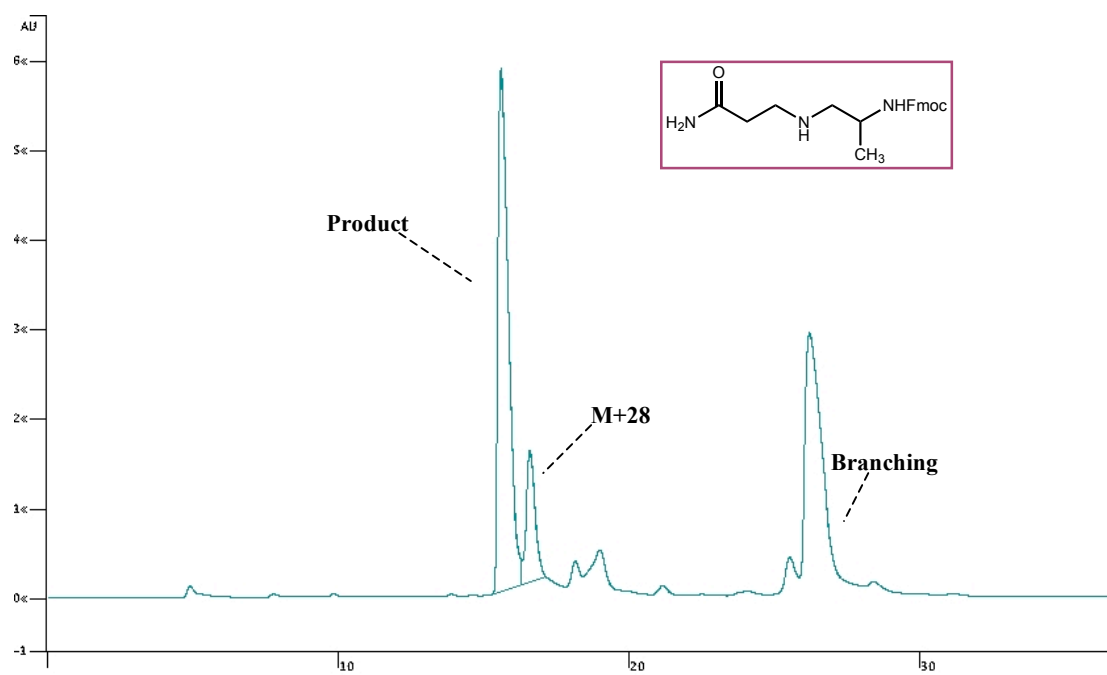


Figure II-9: HPLC trace of β -alanine-alanine

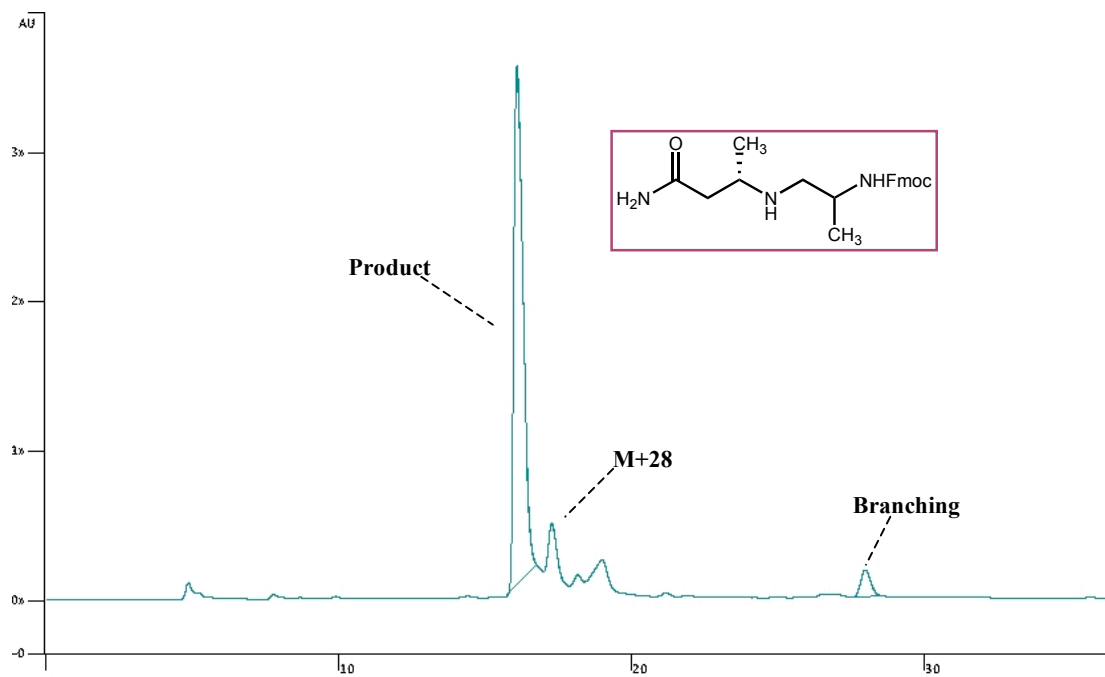


Figure II-10: HPLC trace of β -homoalanine-alanine

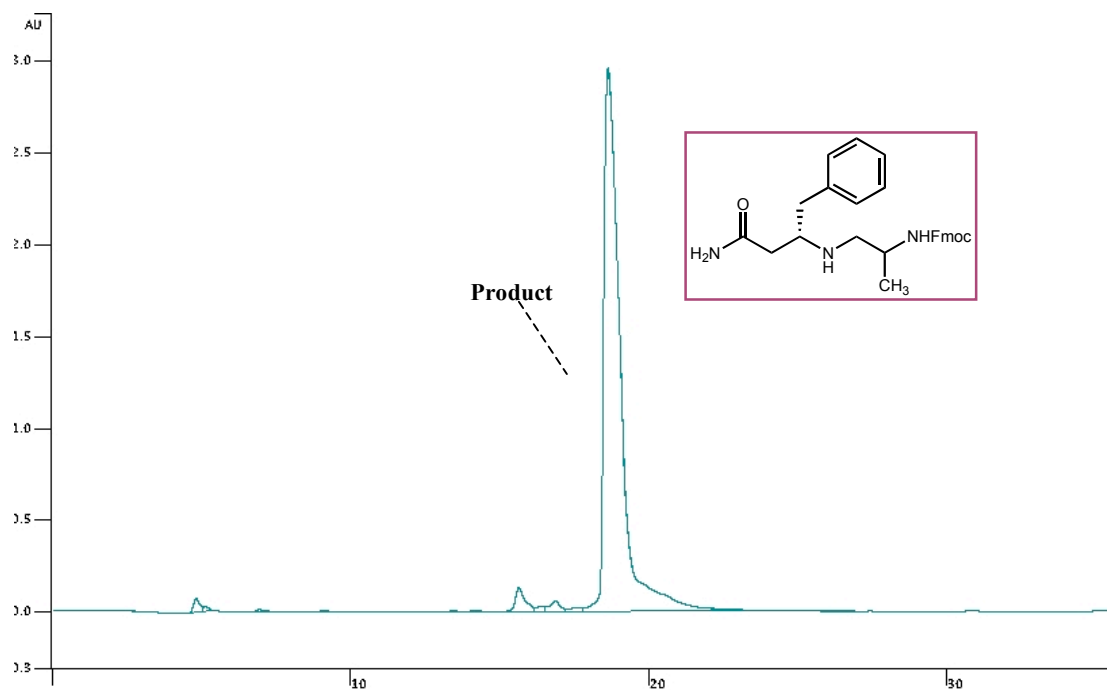
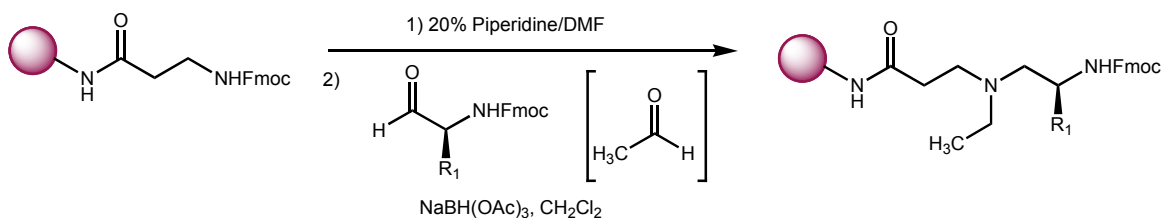


Figure II-11: HPLC trace of β -homophenylalanine-alanine

In the synthesis, sodium triacetoxyborohydride is used as the reducing agent to avoid the toxicity associated with sodium cyanoborohydride. However, sodium triacetoxyborohydride will undergo a self-reduction producing acetaldehyde from the acetate groups.⁴⁰⁻⁴³ We suspect that the M+28 peak is the result of a reductive amination of acetaldehyde with the amine to produce an ethyl group branching from the amine (Scheme II-6).



Scheme II-6: Self reduction of $\text{NaBH}(\text{OAc})_3$

Fortunately the addition of bulkier linkers alleviated this difficulty along with the branching. We proceeded to use Fmoc- β -homoalanine as the linker for future syntheses even though small amounts of branching still occurred. The Fmoc- β -homophenylalanine may have proved to be too bulky thus hindering reductive amination with larger amino acids. In addition, we believed that the addition of a phenyl group may affect the binding affinity of the molecule while a methyl group would be relatively benign.

2.6 NMR Study of YYY and TAR

Footprinting assays afforded our binding data for the polyamines, but we wished to obtain secondary confirmation of the bulge specificity of YYY. In collaboration with the lab of Dr. Pascale Legault at the University of Montreal, we used ^1H NMR spectroscopy to follow the imino protons of TAR RNA and their response to increasing concentrations of YYY. Typically, imino protons only appear in NMR spectra when they are engaged in a hydrogen bonding interaction that hinders proton exchange with the solvent.⁴⁴ We were therefore unable to examine the bulge directly, but instead relied on the four stable base pairs adjacent to the bulge region. The resonances of these four base pairs either shifted or exhibited significant line broadening as the concentration of YYY increased. The imino protons that were not located near the bulge showed no change as YYY was added (Figure II-12). These NMR results confirm that the YYY polyamine is binding to the bulge region of TAR.

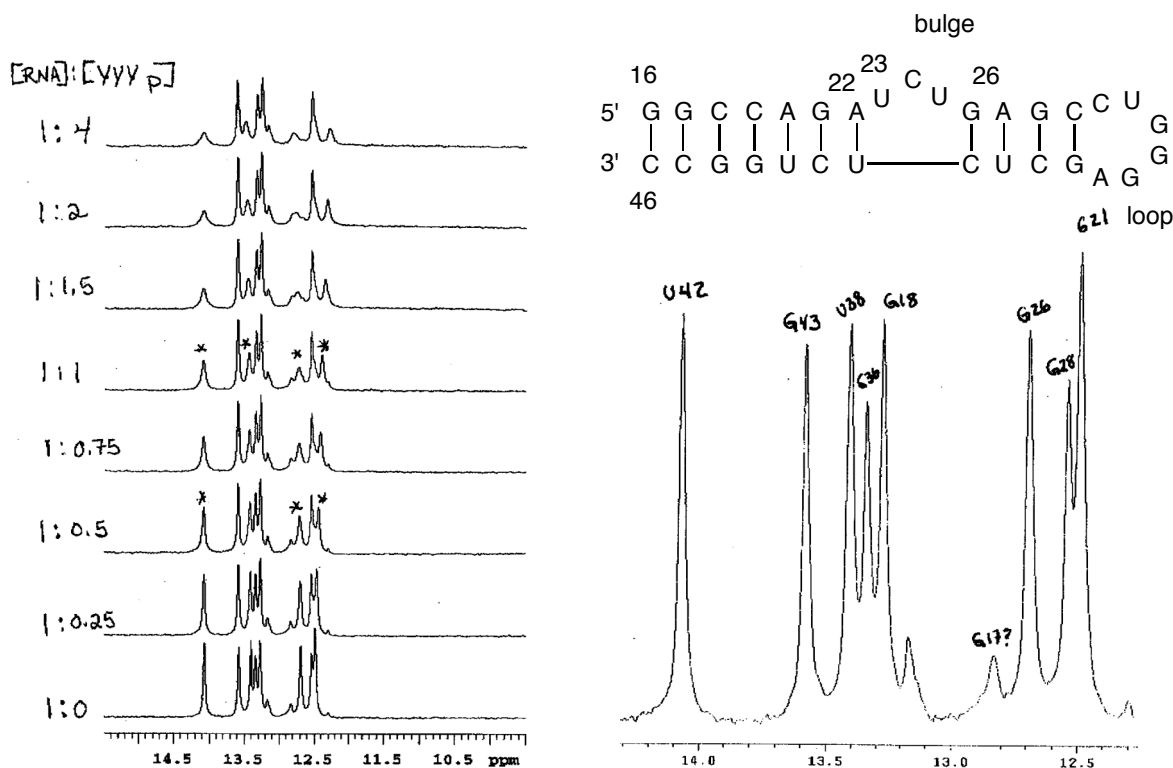
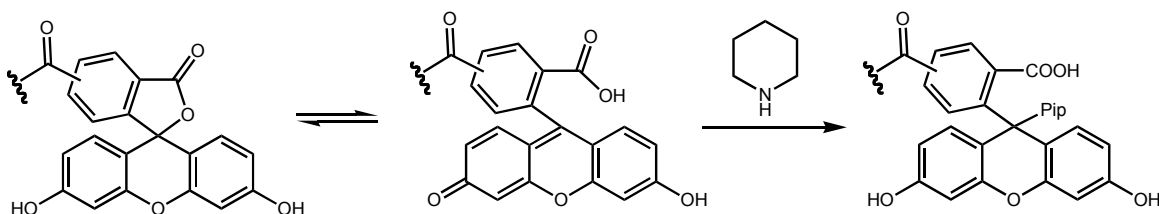


Figure II-12: NMR titration results for YYY ligand with TAR RNA; the imino proton region is expanded.

2.7 Cell Permeability and Anti-viral Activity

We next sought to determine if YYY was cell permeable and could reach the nucleus of the cell. YYY required a fluorescein label, which was easily added onto the molecule while still on the resin. After the final Fmoc-deprotection step, carboxyfluorescein succinimidyl ester (NHS-fluorescein) and DIEA were added to the resin in NMP and shaken for 24 hours while protected from light.^{45, 46} It was imperative that the resin was washed thoroughly before the

addition of NHS-fluorescein. Residual piperidine from the Fmoc-deprotection has the propensity to add to the carboxyfluorescein resulting in a piperidine-fluorescein adduct (Scheme II-7).



Scheme II-7: Formation of the piperidine-fluorescein adduct

All cleavage, deprotection, and purification steps proceeded as usual for polyamines, but the final product (YYY-FI) was stored in DMSO due to low water solubility.

We submitted YYY-FI to Dr. Teh Jeang and co-workers in National Institute of Allergy and Infectious Diseases (NIAID) and the solution of YYY-FI was added to HeLa cells, which were visualized under fluorescence. As seen in Figure II-13, column I depicts the nuclei of the cells stained with dapi, and column II exhibits the differential interference contrast (DIC) of the cells giving them a three-dimensional appearance. The cells in column III fluoresce green due to the presence of fluorescein indicating that YYY-FI did indeed successfully permeate the cells. Column IV consists of overlapping images of I and III.

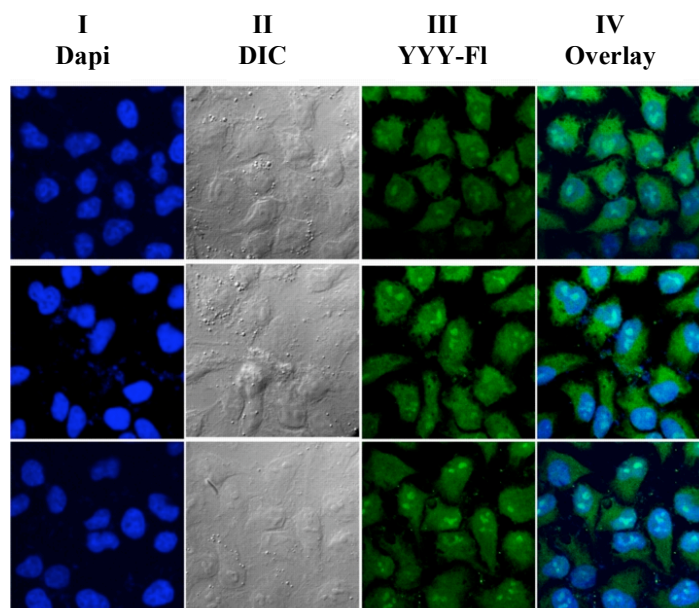


Figure II-13: Cell permeability assay

Lastly, we sought to determine if YYY had anti-viral activity. MT-4 cells are a human T-cell line that have been used extensively in anti-HIV drug development for the past 20 years.⁴⁷⁻⁵⁰ A small molecule is used to treat the MT-4 cells that have been infected with a strain of HIV to establish whether or not the molecule prevents viral replication. In the assay by the Jeang Lab, MT-4 cells were infected with the viral strain NL4-3 and treated with YYY and the initial results looked promising. The reverse transcriptase (RT) counts were extremely low with treatment of YYY compared to the controls indicating reduced viral replication (Figure II-14). Unfortunately, additional studies performed by the Southern Research Institute using a Tat/LTR-reporter gene system described by Jeeninga and co-workers⁵¹ found that YYY had negligible anti-viral activity.

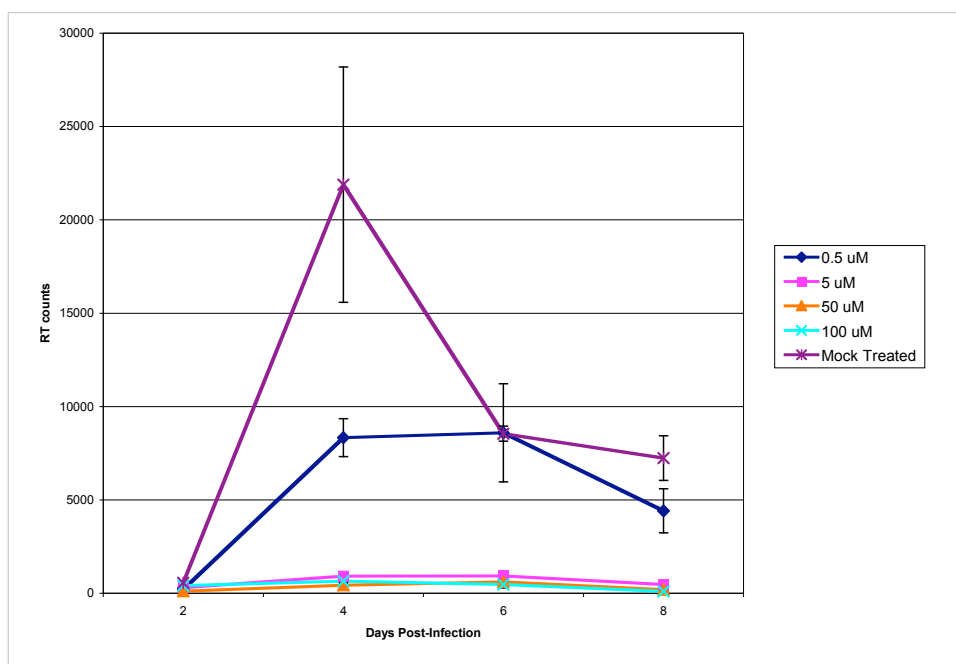


Figure II-14: Effect of YYY on NL4-3 replication in MT4 cells

2.8 Future Directions

Currently we have a promising molecule that binds to the bulge region of TAR RNA. Many questions, however, remain unanswered and should be addressed in future work. We have little information regarding the structure of YYY and YYY-TAR and more NMR work will be required to obtain this information. Additionally, titration experiments to determine the charge states of the amines at physiological pH could prove to be beneficial.

The future of this project also requires discovering a polyamine with a K_D that is much stronger than 5 μM . Only six polyamines were synthesized and tested against RNA, but with the combination of amino acids available a large library of polyamines could be analyzed. Our laboratory is currently set up to synthesize parallel libraries on solid phase and to screen them against TAR RNA as well as other RNAs. The limiting step with this methodology is a simple

method to validate any screen hits. Footprinting with radiolabeled RNA is currently the accepted method for determining RNA binding, but this task is long and laborious. Ideally a secondary assay to validate hits would be developed that was robust but did not involve radioactivity or numerous gels.

2.9 Summary

In our lab, we have designed and synthesized molecules with the intent of developing an inhibitor of the TAR-Tat complex. The polyamine backbone was intended to have a high affinity for RNA due to its positive charge, but non-cationic amino acid side chains would direct the binding and enhance specificity for TAR. YYY was found to have a K_D of 5 μ M and we proceeded to optimize the synthesis as well as perform secondary tests to validate our molecule.

A new linker, Fmoc- β -homoalanine, was introduced into the molecule, which successfully decreased the amount of over-alkylation at the first secondary amine. In addition, Fmoc- β -homoalanine reduced the amount of alkylation caused by the self-reduction of $\text{NaBH}(\text{OAc})_3$ to acetaldehyde. NMR studies confirmed that YYY binds to the bulge region of TAR, and YYY-F1 was found to permeate cell nuclei. No reasonable amount of anti-viral activity, however, was found for YYY.

Overall, we have successfully designed a TAR binding molecule and future work will hopefully improve upon these results and perhaps find a molecule with superior properties to YYY.

2.10 Experimental Procedures

General Methods

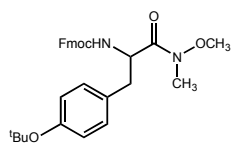
Proton nuclear magnetic resonances ($^1\text{H-NMR}$) were recorded in deuterated solvents on a Gemini 300 (300 MHz) relative to tetramethylsilane (δ 0.00). Proton-decoupled carbon ($^{13}\text{C-}$

NMR) spectra were recorded on a Gemini 300 (75 MHz) and are reported in ppm using the solvent as an internal standard (CDCl_3 , δ 77.23; DMSO, δ 39.52). Electrospray mass spectra (ESI-MS) were obtained using an Agilent 6100 series LC-MS. Tetrahydrofuran (THF) was purified by passing solvent through a column of activated alumina on a Glass Contour Solvent Purification System. Nitrogen was bubbled through dimethylformamide (DMF) for 16 hours prior to use. All solution phase reactions were performed in oven dry glassware under a positive pressure of nitrogen. Silanization of glassware was performed using Sigmacote, in accordance with the manufacturer's instructions. All protected amino acids, Rink resin, and HOBt hydrate were purchased from Advanced ChemTech. HATU was purchased from Applied Biosystems. Kaiser test reagents, Fmoc- β -alanine, Fmoc- β -homoalanine, and Fmoc- β -phenylalanine were purchased from Fluka. NHS-Fluorescein was purchased from Pierce. All other chemicals were purchased from Sigma-Aldrich. All HPLC purification was done via reverse phase on an Agilent 1100 series semi-prep system with UV detection at 254 nm. A Vydac C18 semi-prep column (10 mm x 250 mm) was utilized. The column was kept at room temperature. Solution A was 0.05% TFA in water and solution B was 0.05% TFA in acetonitrile. A typical elution was a gradient of 100% A to 100% B over 40 minutes at a flow rate of 5.0 mL/min.

Abbreviations

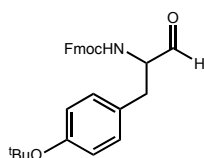
(Fmoc), *N*-(9-fluorenylmethoxycarbonyl); (DIEA), *N*-diisopropylethylamine; (HATU), *O*-(7-Azabenzotriazol-1-yl)-*N,N,N',N'*-tetramethyluronium hexafluorophosphate; (HOBt), 1-hydroxybenzotriazole; (EDC), 1-Ethyl-3-(3-dimethylaminopropyl)carbodiimide hydrochloride; (Boc), *t*-butoxycarbonyl; (DMF), dimethylformamide; (THF), tetrahydrofuran; (DCM), dichloromethane; (NMP), *N*-methylpyrrolidinone; (TFA), trifluoroacetic acid; (TES), triethylsilane

Synthesis of Fmoc-Tyr(*t*Bu)-Weinreb Amide



Fmoc-Tyr-OH (5.0 g, 10.9 mmol) was dissolved in DCM with DIEA (1.9 mL, 10.9 mmol) and the reaction was allowed to cool to 0 °C. Once cool, HOBt hydrate (1.98 g, 13.1 mmol) and EDC (2.5 g, 13.1 mmol) were added to the reaction, which was allowed to stir for 10 minutes at 0 °C. *N,O*-dimethylamine hydrochloride (1.3 g, 13.1 mmol) and second portion of DIEA (2.3 mL, 13.1 mmol) were added to the flask. The mixture was allowed to stir for an hour at 0 °C and then warmed to room temperature and allowed to stir overnight. Upon completion, the reaction was transferred to a separatory funnel with DCM and washed with 1 M HCl (3 x 40 mL), sat. NaHCO₃ (2 x 40 mL), and sat. NaCl (2 x 40 mL). The organic layer was dried over anhydrous Na₂SO₄ and concentrated under vacuum to yield 5.15 g (94%) of Weinreb amide as a white solid. **¹H-NMR** (CDCl₃, 300 MHz): δ 7.73 (d, *J* = 7.41 Hz, 2H, Fmoc aromatic CH), 7.56 (t, *J* = 6.85 Hz, 2H, Fmoc aromatic CH), 7.37 (t, *J* = 7.41 Hz, 2H, Fmoc aromatic CH), 7.28 (t, *J* = 7.41 Hz, 2H, Fmoc aromatic CH), 7.08 (d, *J* = 8.17 Hz, 2H, Tyr aromatic CH), 6.89 (d, *J* = 8.24 Hz, 2H, Tyr aromatic CH), 5.72 (d, *J* = 8.88 Hz, 1H, carbamate NH), 4.99 (m, 1H, CH), 4.29 (m, 2H, Fmoc CH₂), 4.16 (t, *J* = 7.12, 1H, Fmoc CH), 3.60 (s, 3H, -OCH₃), 3.14 (s, 3H, -NCH₃), 3.00 (m, 2H, CH₂), 1.28 (s, 9H, C(CH₃)₃); **¹³C-NMR** (CDCl₃, 75 MHz): δ 172.2, 155.9, 154.3, 144.0, 143.9, 141.3, 131.4, 130.0, 127.8, 127.1, 125.3, 124.2, 120.0, 78.5, 67.1, 61.6, 52.2, 47.2, 38.3, 32.1, 29.1, 28.9; **ESI-MS** *m/z* = 502.6

Synthesis of Fmoc-Tyrosine Aldehyde



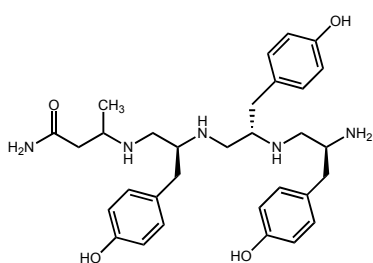
Fmoc-Tyr-Weinreb amide (2.26 g, 4.5 mmol) was dissolved in dry THF and cooled to 0 °C. Lithium aluminum hydride (212 mg, 5.6 mmol) was added slowly to the reaction. The mixture was allowed to stir for 1 hour at 0 °C. The reaction was quenched with 0.1 M NaHSO₄ (2.6 g, 18.9mmol), which was added dropwise. The mixture was allowed to stir an additional 10 minutes at 0 °C before being transferred to a separatory funnel with EtOAc and sat. NaCl. The aqueous layer was extracted with EtOAc and combined organic layers were washed with 1 M HCl (3 x 40 mL), sat. NaHCO₃ (2 x 40 mL), and sat. NaCl (2 x 40 mL). The organic layer was dried over anhydrous Na₂SO₄ and concentrated under vacuum to yield a yellow oil. Re-dissolving the product in ether and removing the solvent under vacuum produced 1.77 g (89%) of aldehyde as a yellow solid. The aldehyde was found to be stable for 1 month if stored at -20 °C. **¹H-NMR** (CDCl₃, 300 MHz): δ 9.59 (s, 1H, CHO), 7.75 (d, *J* = 7.47 Hz, 2H, Fmoc aromatic CH), 7.55 (d, *J* = 7.10, 2H, Fmoc aromatic CH), 7.39 (t, *J* = 7.44, 2H, Fmoc aromatic CH), 7.30 (t, *J* = 7.38 Hz, 2H, Fmoc aromatic CH), 7.00 (d, *J* = 8.03 Hz, 2H, Tyr aromatic CH), 6.89 (d, *J* = 8.30 Hz, 2H, Tyr aromatic CH), 5.36 (d, *J* = 6.88 Hz, 1H, carbamate NH), 4.42 (m, 3H, CH, Fmoc CH₂), 4.19 (t, *J* = 6.68, 1H, Fmoc CH), 3.07 (d, *J* = 6.47, 2H, CH₂), 1.32 (s, 9H, C(CH₃)₃); **¹³C-NMR** (CDCl₃, 75 MHz): δ 198.97, 155.94, 154.60, 143.78, 141.42, 127.85, 127.00, 125.10, 124.41, 124.09, 120.10, 119.92, 100.33, 67.03, 61.24, 47.28, 34.80, 28.92; **ESI-MS** *m/z* = 443.5

Synthesis of Rink Amide Resin Linkers

Rink amide resin (1.0 g, 0.75 mmol) was swelled in a silanized filter vessel with DMF. The Fmoc protecting group was cleaved with 20% piperidine in DMF (5 min., DMF wash, 20

min.). The resin was washed with DMF (3x) and DCM (3x). A red chloranil test indicated the presence of a primary amine. Fmoc-amino acid (2.25 mmol) was dissolved in DMF and added to the resin. HATU (843 mg, 2.25 mmol), HOBT (340 mg, 2.25 mmol), and DIEA (888 μ L, 5.1 mmol) were dissolved in DMF and added to the resin. The mixture was shaken for 1.5 hours. The reagents were drained and the resin was washed with MeOH (1x), DMF (3x), and DCM (3x). A negative chloranil test indicated the absence of free amine. The resin was dried under vacuum and transferred to a silanized vial for storage.

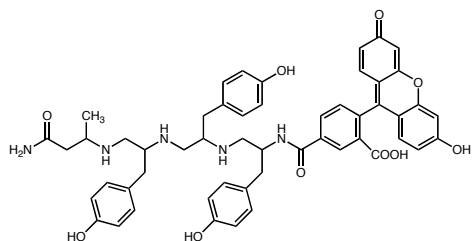
Synthesis of YYY



Fmoc- β -homoalanine resin (500 mg, 0.375 mmol) was swelled in a silanized filter vessel with DMF. The Fmoc group was deprotected with 20% piperidine in DMF (3 x 5 min) and the resin was washed with DMF (3x) and DCM (3x). This method was used for all subsequent Fmoc deprotections. A red chloranil test indicated a primary amine. Fmoc-Tyrosine aldehyde (832 mg, 1.875 mmol) was dissolved in DCM and added to the resin and shaken for 10 min. The aldehyde was drained and the resin washed with DCM (1x). A mixture of NaBH(OAc)₃ (238 mg, 1.125 mmol) in DCM was added to the resin and shaken for 45 min. The solution was drained and the resin was washed with MeOH (1x), DMF (3x), and DCM (3x). A positive chloranil test indicated the presence of a secondary amine. A solution of Boc₂O (818 mg, 3.75 mmol) and DIEA (261 μ L, 1.5 mmol) in DCM was added to the resin and shaken for 2 hours. The solution was drained and the resin was washed with MeOH (1x), DMF (3x), and DCM (3x). A negative chloranil test indicated the absence of any free amine. This procedure, starting with the Fmoc deprotection, was repeated two more times, followed by a

final Fmoc deprotection. The resin was cleaved with 10% TFA in DCM for 10 min. The solution was evaporated under nitrogen and the product was re-dissolved in 95% TFA/1% TES in DCM and stirred for 30 min. to 1 hr. to deprotect the Boc groups. The solution was evaporated under nitrogen. Product was re-dissolved in a minimum amount of DCM, transferred to eppendorf tubes, and precipitated out of cold Et₂O. The mixture was centrifuged and the Et₂O layer was removed. The pellet was dissolved in H₂O and purified via HPLC. **MS-ESI** m/z = 550.3

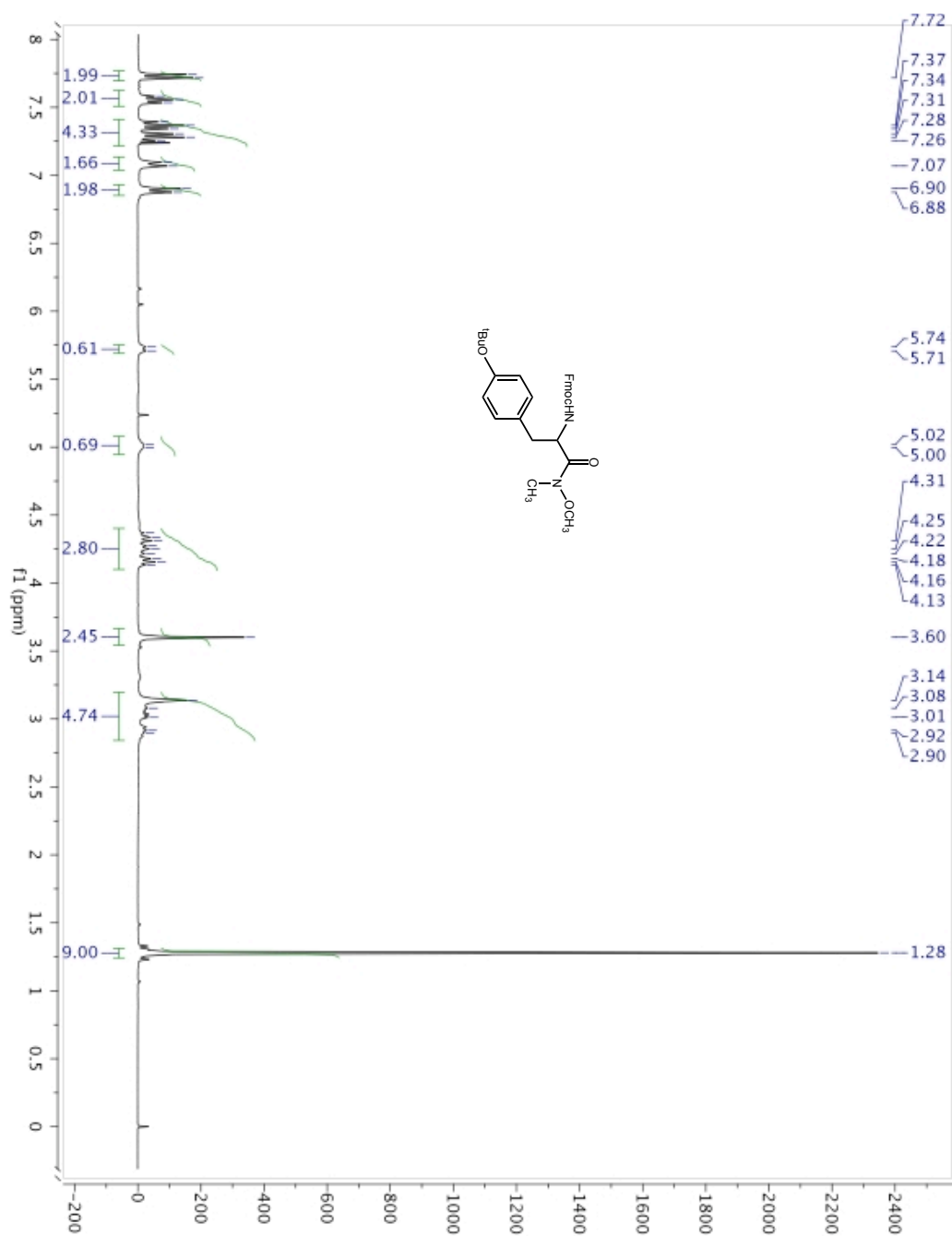
Synthesis of YYY-Fluorescein

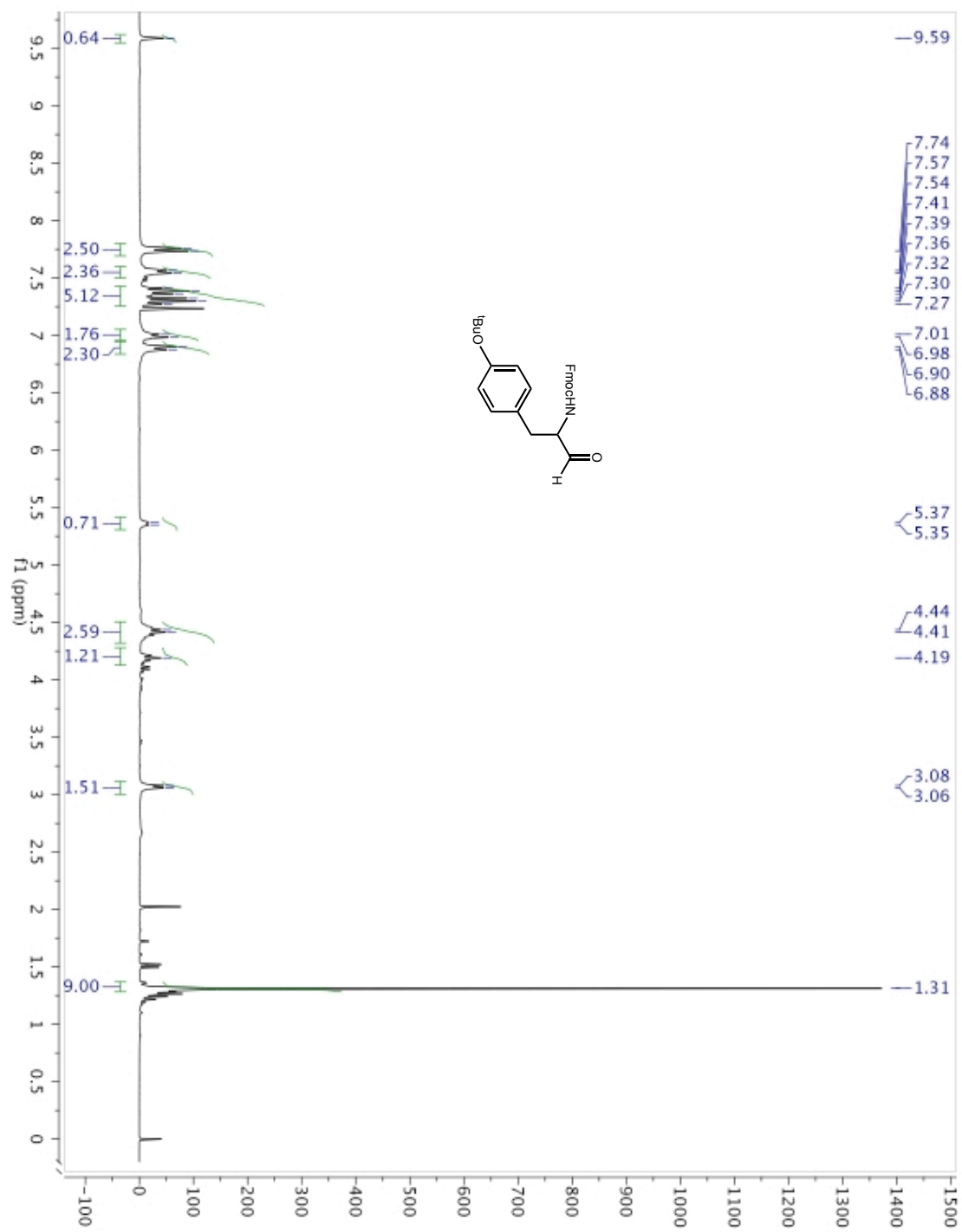


YYY was synthesized using the described procedure (200 mg, 0.15 mmol). After the final Fmoc deprotection, the resin was washed with NMP (6x) and DMF (6x). NHS-fluorescein (78 mg, 0.165 mmol) and DIEA (29 μ L, 0.165 mmol) were added to the resin in NMP and shaken for 24

hours (peptide vessel was wrapped in foil to protect from light). The solution was drained and the resin was washed with NMP (3x), DMF (3x), and DCM (3x). Cleavage and purification procedures proceeded as described for the unlabeled polyamine. **MS-ESI** m/z = 908.0

2.10.1 Select NMRs





Chapter 3

Design and Synthesis of N-Acylated Polyamine (NAPA) Libraries to Screen for Protein Binding

3.1 Introduction

The field of drug discovery is largely based on identifying molecules that bind to specific biomolecules. Designing small molecules that bind to enzyme active sites is the most common strategy in the pharmaceutical industry. Enzymes often possess a well-defined cavity with specific amino acid interactions that accept precise molecular scaffolding. Only recently is the inhibition of protein-protein interactions being explored as a new strategy for drug development. While proteins frequently possess large, flat areas that interact with other proteins and may be difficult to target with a small molecule, there are a number of successful examples where inhibitors of protein-protein interactions have been developed.

Rather than craft a molecule around a specific protein-protein complex, we designed a library of molecules that could be screened for binding to a variety of proteins. Using a polyamine structure previously developed in our lab, we acylated the secondary amines with acid chlorides to synthesize N-acylated polyamines (NAPAs). We synthesized two libraries of NAPAs and screened them for protein binding using quantum dot (Qdot) technology. None of the hits in our 1st generation library of 216 compounds produced molecules with *in vivo* activity. The 2nd generation library of 512 compounds produced a ligand that binds to HIV-1 Vpr protein with a K_D of approximately 25 μ M and partially reverses induced Vpr expression.

3.2 Protein-protein Interactions

Many biochemical pathways, particularly in disease progression, involve numerous interactions between proteins. These interactions are difficult to modulate with small molecules for several reasons: the key interacting sites are often unclear, large interfaces of buried surface are involved in the interactions, the binding regions are often non-contiguous, many interfaces are fairly featureless, few molecules have been identified from random libraries as inhibitors of

protein-protein interactions, and sophisticated binding assays are required.¹ Despite these challenges, inhibition of a number of protein-protein interactions has been achieved.²

One of the most notable protein-protein interactions is p53-MDM2. Murine double mutant 2 (MDM2) is responsible for regulating the cellular levels of the p53 protein, which is responsible for apoptosis and cell cycle arrest.³ Inhibition of this interaction has the potential to halt the progression of some cancers by increasing the p53 levels and causing cell death in tumorigenic cells. The crystal structure of MDM2 exhibits a well-defined hydrophobic cleft where p53 binds as an alpha helix (Figure III-1A).⁴ Three residues, Phe¹⁹, Trp²³, and Leu²⁶, on the p53 helix are key to the interface and often targeted in the design of small-molecule inhibitors. A group from Hoffman-LaRoche discovered a class of imidazolines, the Nutlins, which bind to MDM2 with an IC₅₀ in the sub-micromolar range (Figure III-1B).⁵ Crystal structures illustrate the Nutlins replicate the features of the p53 helix and bind deep in the cleft of MDM2.

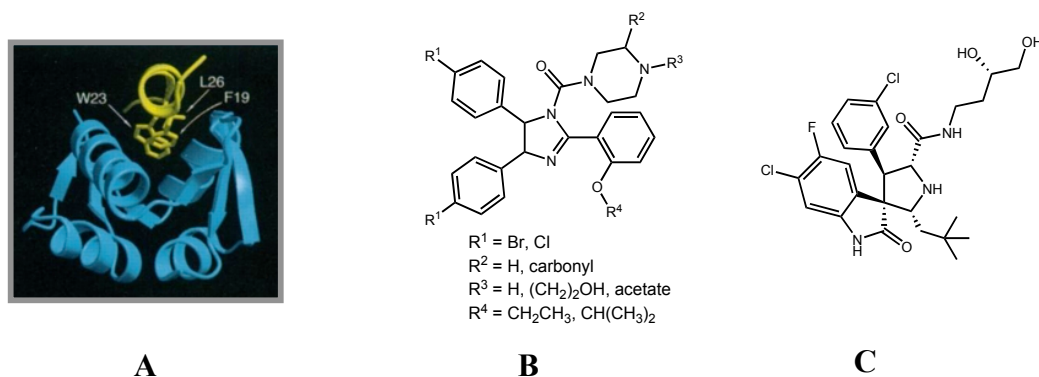


Figure III-1: A) Crystal structure of the p53 helix bound to MDM2 B) General structure of the Nutlins C) MI-219

Recently, another small molecule similar to the Nutlins has been discovered as a potent MDM2-p53 inhibitor. This molecule, MI-219 (Figure III-1C), mimics key p53 residues and binds to MDM2 with a K_i of 5 nM.⁶

Hamilton and co-workers developed a novel terphenyl helical mimetic that they used to target protein-protein interactions, including p53-MDM2 inhibition.⁷ The side chains on the terphenyl structure are designed to spatially mimic the i , $i+4$, and $i+7$ residues on an α -helix (Figure III-2A). One of the terphenyl derivatives (Figure III-2B) was found to bind strongly to human double mutant (HDM2) ($K_i \approx 0.2 \mu\text{M}$) and NMR studies further confirmed the binding of terphenyl to the p53-binding cavity of HDM2.

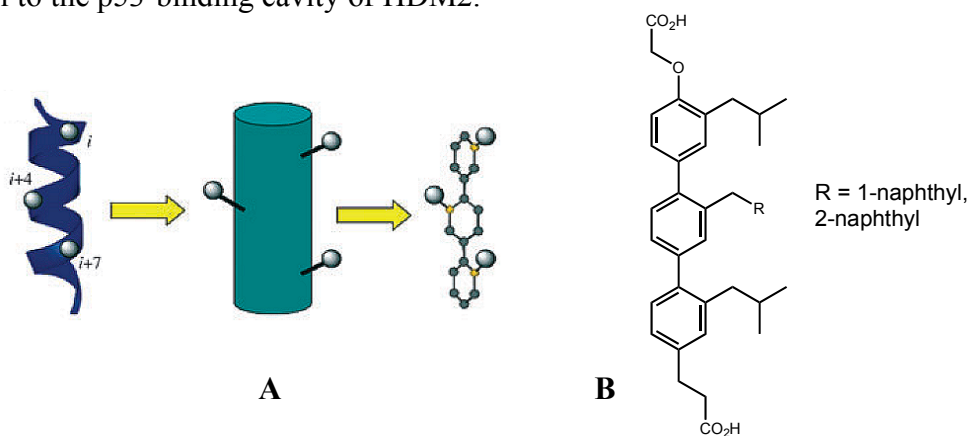


Figure III-2: A) Schematic representation of the terphenyl structure mimicking the spatial orientation of α -helix residues B) Protein binding terphenyl structure

Remarkably, changing the side chain on the middle phenyl ring from 2-naphthylmethylene to 1-naphthylmethylene changes the selectivity of the terphenyl for helix-binding proteins, specifically the anti-apoptotic Bcl-2 and Bcl-X_L proteins.⁸ Overexpression of these proteins blocks the apoptotic pathway often impeding many anti-cancer agents. Several hydrophobic Bak residues, Val⁷⁴, Leu⁷⁸, Ile⁸¹, and Ile⁸⁵, are required to make contact with hydrophobic residues of Bcl-X_L. Additionally, an arginine (Arg⁷⁶) and two aspartate residues (Asp⁸³ and Asp⁸⁴) are believed to contribute to binding.⁹ The 2-naphthylmethylene terphenyl derivative binds HDM2 over 100-fold more strongly than its isomer and the reverse is true for the Bcl proteins. The

specificity achieved for two proteins due to such a subtle difference is indicative of challenges that are faced when targeting protein-protein interactions.

Another successful molecular scaffold that inhibits protein-protein interactions is a β -peptide and various derivatives developed in the Gellman and Schepartz labs. Gellman and co-workers synthesized β -peptides and hybrid α/β -peptides that adopt a structure mimicking an α -helix. Using cyclic constrained β -amino acids to enhance helicity and water solubility, they designed an α/β -chimeric peptide with an additional α -peptide chain that bound to the Bcl-x_L protein with a K_i of 0.034 μ M.¹⁰ As seen in Figure III-3, the chimeric peptide mimicked four of the hydrophobic residues and two of the hydrophilic residues important for Bak binding.

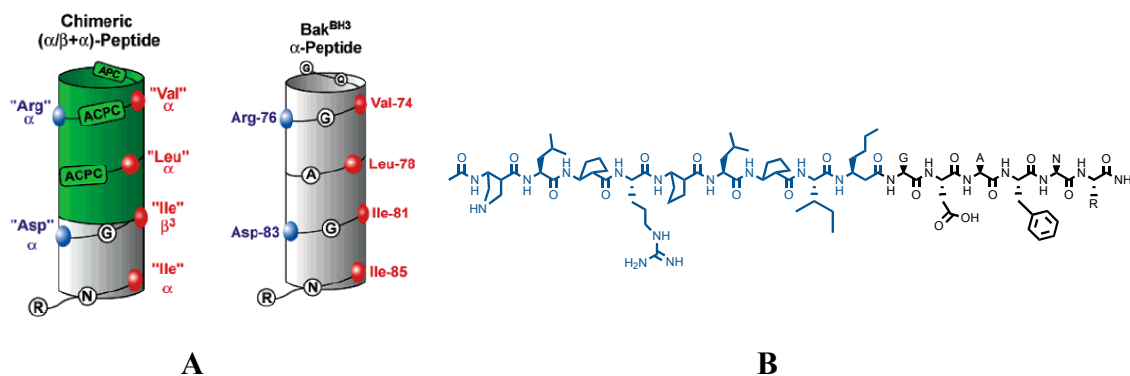


Figure III-3: A) Schematic representation of the chimeric peptide mimicking the structure of the Bak helix B) Structure of the (α/β) peptide (blue) + α peptide chain¹⁰

Schepartz and co-workers produced a β^3 -decapeptide that bound HDM2 with sub-micromolar affinity.^{11, 12} One helical face of their β^3 -decapeptide possessed residues to mimic the key p53 residues, F¹⁹, W²³, and L²⁶, required for binding, while another helical face consisted of residues to stabilize the helical structure in aqueous solution (Figure III-4).

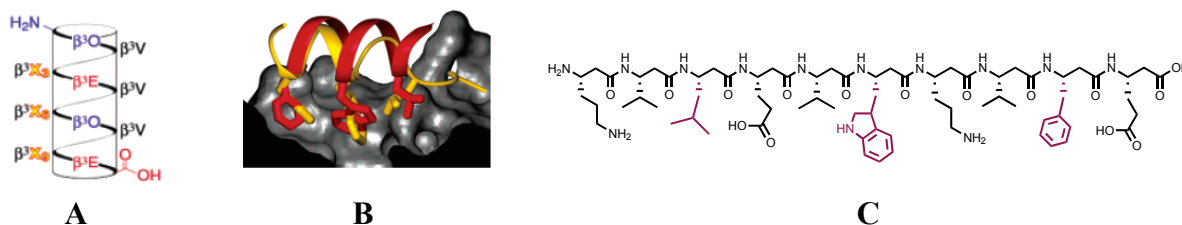


Figure III-4: A) Representation of the three faces of the β^3 -peptide helix B) Overlay of the solution structure of the p53 helix (gold) and the β^3 -peptide helix (red) C) Structure of the β^3 -peptide with the hydrophobic binding residues in red^{11, 12}

Inhibition of protein-protein interactions is not limited to the Bcl and HDM2 proteins. Various other proteins such as β -catenin,¹³ IXAP/Smac,^{14, 15} and IL-2¹⁶ have been targeted and numerous small molecules and scaffolds have been designed for this purpose.¹⁷⁻¹⁹

3.3 N-acyl polyamine design and synthesis

To design an inhibitor of protein-protein interactions, we drew inspiration from the polyamine scaffold developed in our laboratory (Figure III-5). The polyamine scaffold is ideal for a solid-phase library synthesis using a variety of amino acids and also consists of four amines that can accommodate further functionalization.

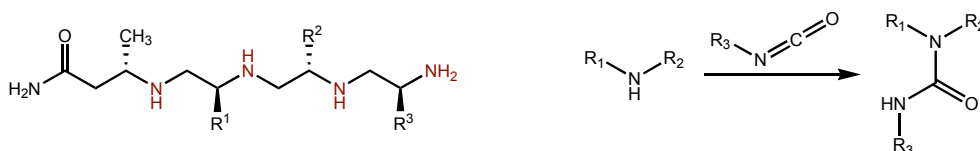
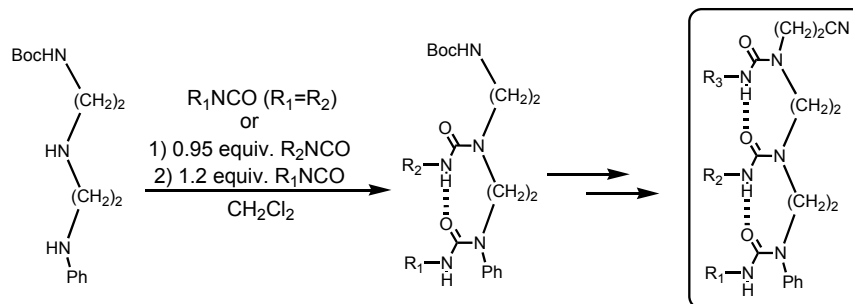


Figure III-5: Polyamine scaffold

Scheme III-1: Formation of an urea side-chain by the addition of an isocyanate to an amine

We also drew inspiration from polyamines that were derivatized with isocyanates to form urea side chains (Scheme III-1). Nowick and coworkers used this structure to create artificial β -sheet formation (Scheme III-2).^{20, 21} Rather than form urea side chains on the polyamine backbone, we pursued amide bonds (Figure III-6) .



Scheme III-2: Synthesis of triureas to create artificial β -sheets

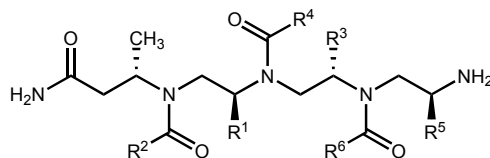


Figure III-6: Proposed N-acyl polyamine scaffold

A comparison of our scaffold design to peptides, peptoids, and the terphenyl α -helix mimetic demonstrates the dense nature of N-acylated polyamines (Figure III-7). Acylating polyamines allows for the introduction of six residues into the same amount of space as three residues on the other structures. This highly compact design should allow the inclusion of necessary side chains for protein binding, but also permit additional side chains to guide specificity or to enhance hydrophobicity or hydrophilicity.

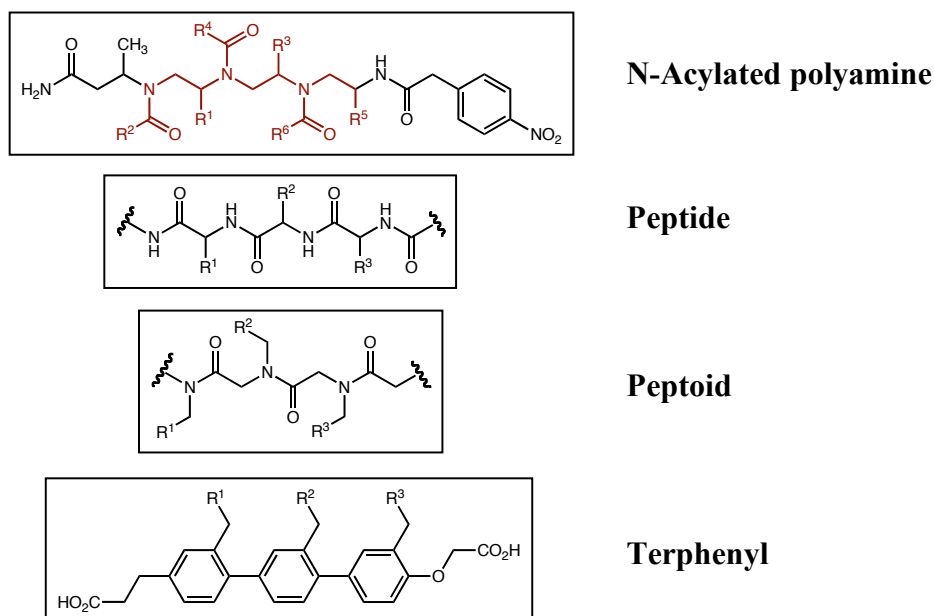
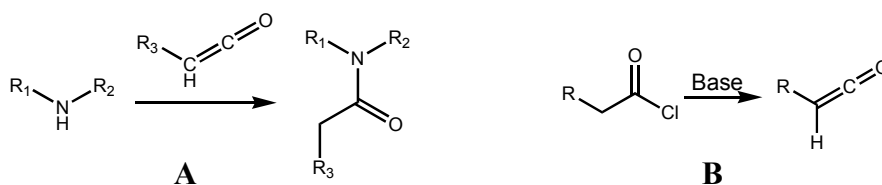


Figure III-7: Scaffold comparison – Six NAPA residues (red) are possible in the same amount of space as three residues on other scaffolds

In our experience, it is extremely difficult to synthesize amide side chains on the polyamine using standard amide bond coupling procedures. Therefore, we decided to use ketenes to acylate the secondary amines (Scheme III-3A).

Due to their high reactivity, ketenes must be synthesized immediately prior to use or *in situ*. Ketenes can be synthesized a number of ways with one of the most common methods being the addition of a base to an acid chloride (Scheme III-3B).²²⁻²⁴ We first tried to pre-form the ketene by reacting isobutyryl chloride with DIEA, which we then added for 15 minutes to a one-residue amine made from alanine on Fmoc- β -homoalanine Rink resin using our polyamine chemistry.



Scheme III-3: A) Proposed synthesis of amide side-chains with ketenes B) Synthesis of ketenes from acid chlorides

After resin cleavage with 10% TFA in dichloromethane, the products formed were analyzed by LC-MS. This initial procedure produced the desired product (Figure III-8B) as well as addition of the isobutyryl moiety to the Fmoc-protected terminal amine (Figure III-8C). When this procedure was tried by forming the ketene *in situ*, both the desired product and starting material (Figure III-8A) were found.

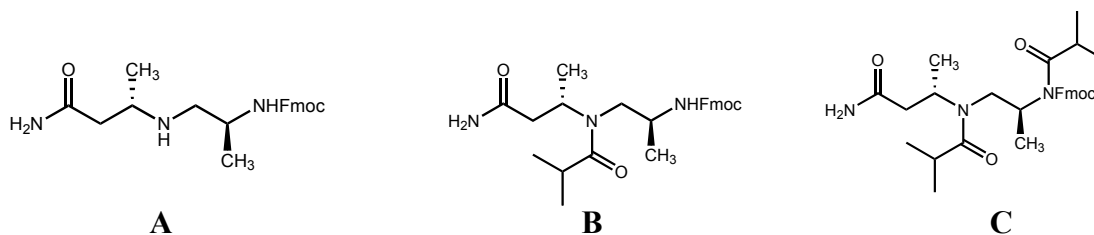
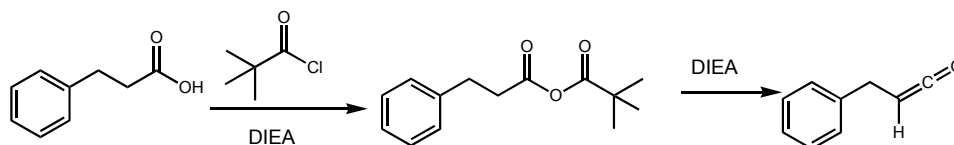


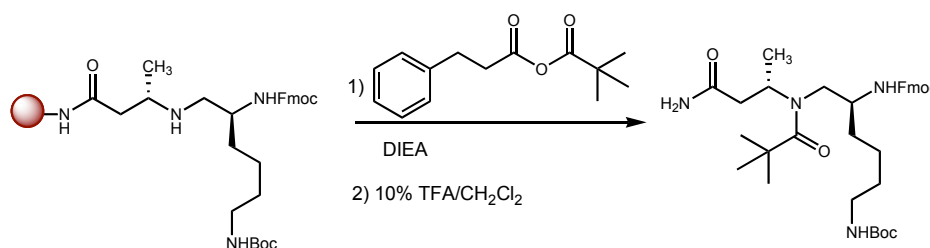
Figure III-8: Products from the addition of isobutyryl ketene to a secondary amine – A) Starting material B) Desired product C) Over-acylated product

Hoping to obtain more consistent results, we next attempted to form a ketene starting with a mixed anhydride (Scheme III-4). The mixed anhydride was synthesized with hydrocinnamic acid and pivaloyl chloride and then excess base was added to form a ketene; the pivaloyl chloride itself should not form a ketene due to the absence of a β -hydrogen. However, examination of the product after cleavage showed that the pivaloyl chloride used to make the mixed anhydride was adding to the amines and producing the major product (Scheme III-5). It became clear that the acid chloride was responsible for acylating the amine, not a ketene. Since acid chlorides were

sufficiently reactive to acylate the amines, ketene synthesis was likely not required. Hence, isobutyryl chloride, not a ketene, was probably adding to alanine in our first endeavor to acylate the amines.



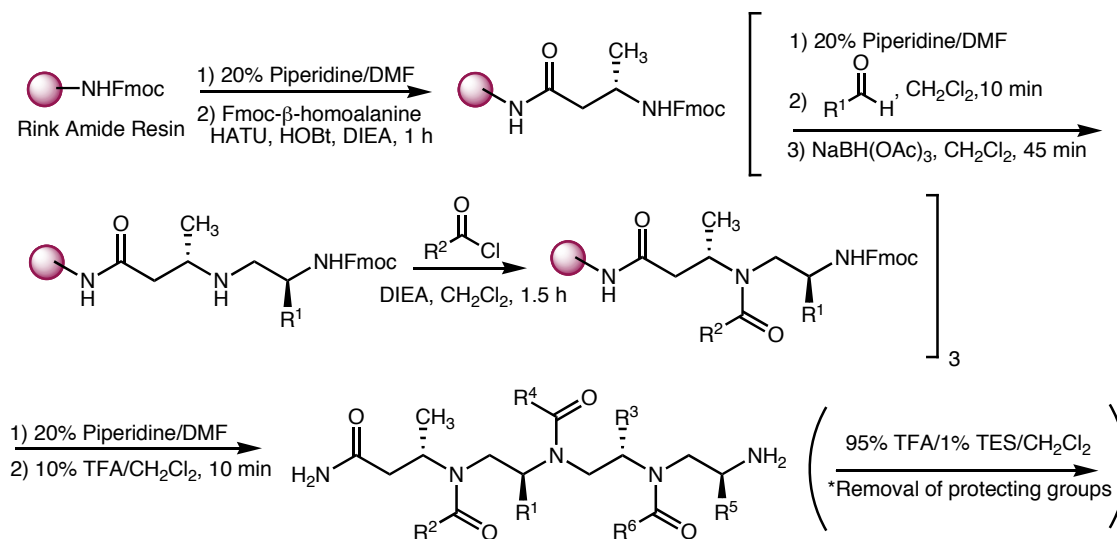
Scheme III-4: Synthesis of a ketene from a mixed anhydride



Scheme III-5: Attempted formation of hydrocinnamoyl amide side-chain; the pivaloyl chloride added to the amine in its place

After it was determined that acid chlorides could acylate the first secondary amine, longer molecules had to be synthesized to test the chemistry on the second and third amines, which are more hindered by the presence of amino acid side chains (Scheme III-6). The synthesis of these molecules involved our polyamine chemistry with the additional acylation step. First, Fmoc- β -homoalanine was coupled to Rink Amide resin using HATU, HOBT, and DIEA. The β -homoalanine was deprotected with 20% piperidine in DMF for 5 minutes followed by an additional 20 minutes. A primary amine could be detected by the presence of a red bead in a solution of 2% chloranil/DMF.²⁵ Fmoc-amino acid aldehyde was then added to the resin for 10 minutes, drained, and followed by the addition of NaBH(OAc)₃ in dichloromethane for 45 minutes. A green bead in a solution of 2% acetaldehyde/DMF and 2% chloranil/DMF indicated

a secondary amine was formed.²⁶ Once the amine was formed, an acid chloride was added to the resin in DCM with an excess of DIEA and allowed to react for 1.5 hours. Complete acylation was indicated by a colorless chloranil/acetaldehyde test. At this point in the synthesis, acyl transfer of the acid chloride between two amines became a concern and to help minimize this problem, the length of the Fmoc-deprotection step was decreased to 5 minutes and repeated three times. No acyl transfer was ever noticed by LC-MS using this procedure. The remaining steps were all repeated as necessary to form dimers and trimers and all steps were monitored using the chloranil colorimetric test. The molecules were cleaved from the resin with a solution of 10% TFA/DCM for 10 minutes. After the collected solvent was evaporated under nitrogen, the protecting groups were removed with a solution of 95% TFA/1% Triethylsilane/DCM for 1 hour. The final product was precipitated out of cold ether and analyzed via LC-MS producing one clean major product peak. With this procedure, several dimers and trimers were successfully synthesized and we proceeded to make a library of these molecules.



Scheme III-6: Solid-phase synthesis of N-acylated polyamines

3.4 1st generation library

For the library, we were faced with the possibility of having a molecule containing no chromophore for HPLC purification. Thus 4-nitrophenylacetic acid was coupled to the terminal primary amine of the molecule using standard amide bond formation (Figure III-9). This functionality would not only ensure the molecule would be visible by HPLC, but the nitro moiety should also aid in aqueous solubility.

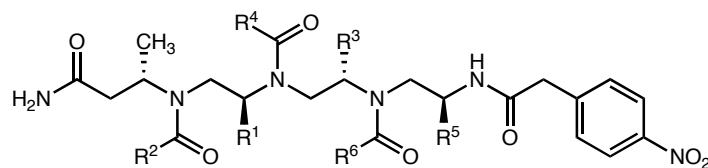


Figure III-9: NAPA scaffold with 4-nitrophenylacetic acid

3.4.1 Synthetic optimization

To synthesize the library, 96-well filter plates would be used and several test molecules were made in these plates using Rink Amide resin. We quickly realized that the current chemistry would have to be altered to synthesize a library in 96-well plates. Much of the chemistry is typically performed in dichloromethane in a sealed peptide reaction vessel. In the plates, however, the dichloromethane would only last for approximately 10 to 15 minutes as it would seep through the filter. This difficulty affected both the imine reduction and the acid chloride addition and new methods to either shorten the reaction times or change the solvent would be required.

Dichloroethane was immediately tried as a substitute for dichloromethane since it is less volatile, but the same difficulties occurred. Thus, NMP and DMF were tried for the reactions. Additionally, trimethylorthoformate (TMOF), which has been used as a solvent for reductive aminations,²⁷ and acetic acid, which will catalyze a reduction with $\text{NaBH}(\text{OAc})_3$,²⁸ were utilized as solvent conditions. The solvents and reaction times that were tried for each step, using lysine aldehyde and hydrocinnamoyl chloride, are demonstrated in Table III-1.

Synthetic Step	Conditions
<i>Aldehyde Addition</i>	Dichloroethane, 10 min NMP, 10 min DMF, 10 min; 1 h; 3 h Trimethylorthoformate (TMOF), 2.5 h DMF, TMOF (60 equiv), 2.5 h
<i>$\text{NaBH}(\text{OAc})_3$ Reduction</i>	NMP, 45 min DMF, 45 min 1% AcOH/DMF, 45 min
<i>Acid Chloride Addition</i>	NMP, 1.5 h

Table III-1: Conditions tested for filter plate synthesis optimization

The combination of TMOF (2.5 hours) for imine formation, 1% AcOH/DMF (45 minutes) for the reduction, NMP (1.5 hours) for the acid chloride addition, and the standard 20% piperidine/DMF (3 x 5 minutes) for Fmoc deprotection finally gave the desired monomer. This combination also produced the side product of 4-nitrophenylalanine coupled directly to β -homoalanine (Figure III-10). Based on the LC-MS trace, the ratio of product to by-product was approximately 2 to 1.

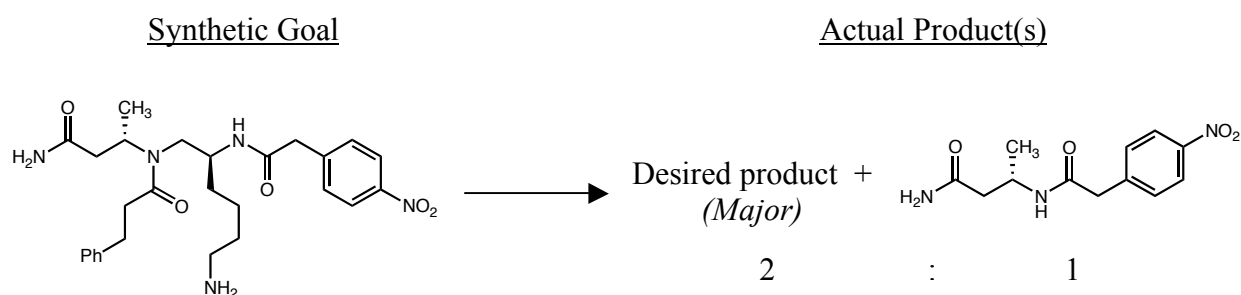


Figure III-10: Desired product achieved with TMOF (2.5 hr), 1% AcOH/DMF (45 min), and NMP (1.5 hr)

When these conditions were applied to the synthesis of a trimer made with three lysines and three hydrocinnamoyl side chains, the sole product was the monomer of one lysine, one hydrocinnamoyl amide, and the 4-nitrophenylacetic acid (Figure III-11), despite the fact that the chloranil tests indicated that every step was going to completion.

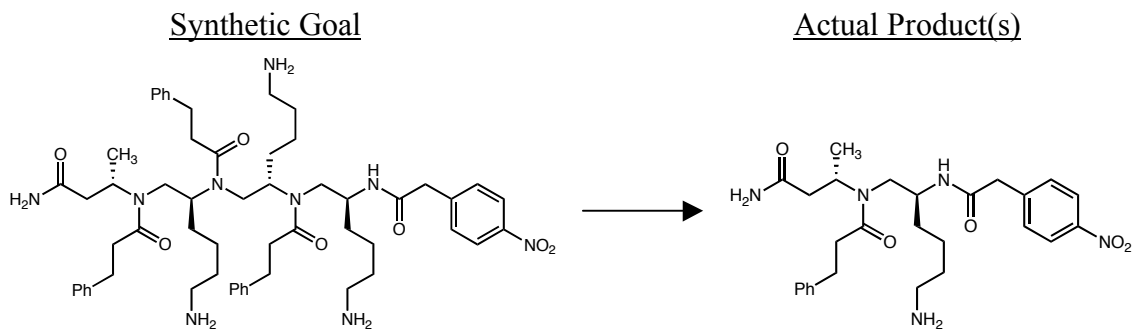


Figure III-11: Truncated product achieved with TMOF (2.5 hr), 1% AcOH/DMF (45 min), and NMP (1.5 hr)

Since the previous trimer that was attempted consisted of all the same residues, it was difficult to pinpoint where the synthesis may have gone awry. A new trimer using three different amino acids, tyrosine, histidine, and lysine, and benzoyl chloride was synthesized using these same conditions. The surprising result was three different products, all in approximately equal amounts. A monomer of each amino acid, with the benzoyl side chain and the 4-nitrophenylacetic acid was produced (Figure III-12). A minor product of tyrosine with the benzoyl amide and the terminal amine capped with benzoyl chloride was also present. These results were puzzling. If both the reduction and acylation occur much more slowly in DMF and NMP, it is probable that reversed imine formation followed by incomplete reactions led to these products. One might expect to observe more truncated molecules capped by one or two benzoyl moieties from the acid chloride. The possibility of product degradation or rearrangement also exists. Trimethylorthoformate, which is present in almost 2000-fold excess, is a potent dehydrating agent that may have led to some product break-down or rearrangement.

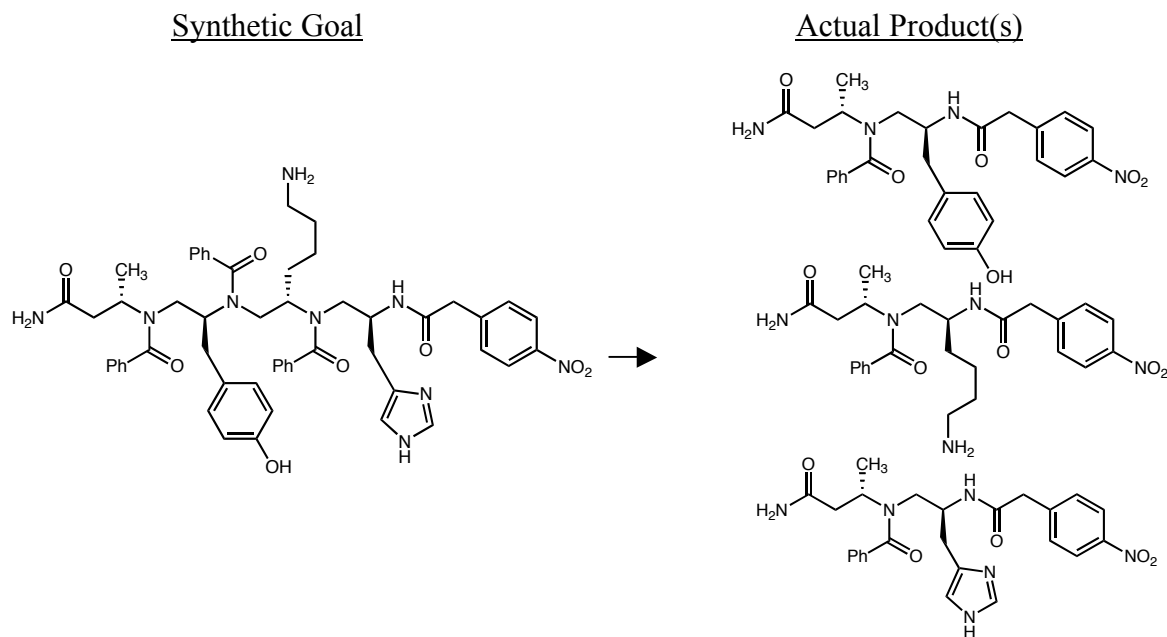
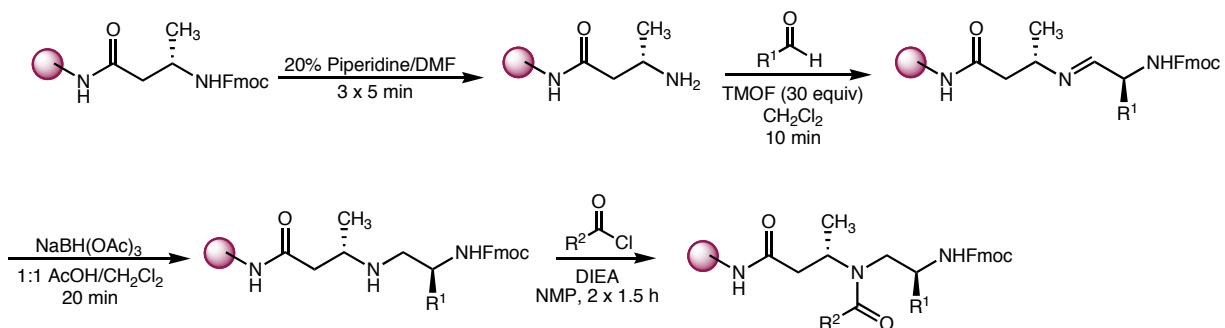


Figure III-12: Three different truncated products achieved with TMOF (2.5 hr), 1% AcOH/DMF (45 min), and NMP (1.5 hr)

At this juncture, we decided to revisit dichloromethane as a solvent; dichloromethane was usable in the plates as long as the reaction times were under 15 minutes. The amount of TMOF was reduced and used as a reagent in dichloromethane instead of being utilized as a reaction solvent. A solution of acetic acid and dichloromethane was made for the reduction to catalyze the reaction and to improve the viscosity and lower the volatility of the solvent mixture. As an added benefit, acetic acid aided in the dissolution of $\text{NaBH}(\text{OAc})_3$, which was not completely soluble in dichloromethane. We found that the amine could successfully be synthesized using an excess of TMOF in dichloromethane for 10 minutes for the imine formation and a 1:1 mixture of AcOH/DCM for 20 minutes for the reduction. The 20 minutes was still slightly too long, but additional $\text{NaBH}(\text{OAc})_3$ in this solvent mixture could be added as needed, or repeated in two 10 minute cycles. The acylation step could not be modified to a shorter time in dichloromethane, but NMP for 1.5 hours worked well and this step could be repeated until the chloranil test indicated that the reaction had gone to completion. The use of dichloromethane is not only the best solvent for the reactions, but it greatly decreased the reaction time from using either DMF or NMP. The final synthesis for the 96-well plates (Scheme III-7) thus involved 20% piperidine/DMF (3 x 5 minutes) for Fmoc-deprotection, TMOF/DCM (10 minutes) for imine formation, 1:1 AcOH/DCM (20 minutes) for the reduction, and NMP (2 x 1.5 hours) for acylation. The acid couplings of Fmoc- β -homoalanine and 4-nitrophenylacetic acid remained the same. To deprotect the molecules, a solution of 95% TFA/DCM was added to the plates and had to be added almost continuously for up to 30 minutes because it seeped through the filters readily.



Scheme III-7: Optimized NAPA synthesis for filter plates

Now that the synthesis was successfully modified for the 96-well plates and complete N-acylated polyamines could be synthesized in the wells, the library had to be constructed. Screening of the library involved keeping the molecules on the resin so a TentaGel-NH₂ macrobead was used for the library. TentaGel is not only larger and more visible, but it is not acid labile and it is able to swell in water, which is an important property since proteins in buffer would be added to the resins.

3.4.2 Library design

The selection of amino acid and acid chloride residues for the library involved the endeavor to make the molecules water-soluble. The acid chlorides had to be commercially available since an attempt to synthesize them from carboxylic acids and cyanuric chloride²⁹ was unsuccessful. This option left us mainly with hydrophobic acid chlorides (isobutyryl and hydrocinnamoyl). We then chose hydrophilic amino acids (lysine, histidine, and tyrosine) to aid water solubility. To identify the molecules in the screen, each amino acid residue was identified by their one-letter code (lysine = K, histidine = H, tyrosine = Y) and the acid chlorides were given numbers (isobutyryl chloride = 1, hydrocinnamoyl chloride = 2) (Table III-2). A NAPA consisting of three lysines and three hydrocinnamoyl moieties would therefore be referred to as

K2K2K2 (Figure III-13). With three amino acids available for each of three different positions and two acid chlorides available for the remaining three positions, $3^3 \times 2^3$, or 216 possible molecular combinations were possible. Using a computer program specially designed to output all 216 molecules (Figure III-14), the library was divided up into three plates, the *K Series*, the *H Series*, and the *Y Series*, each consisting of 72-members.

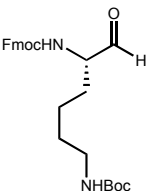
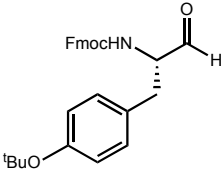
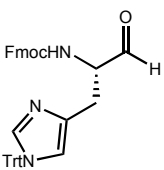
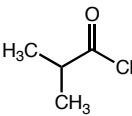
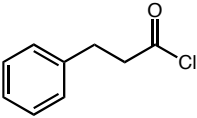
<i>Aldehyde or Acid Chloride</i>	<i>Code</i>
Lysine 	K
Tyrosine 	Y
Histidine 	H
Isobutyryl chloride 	1
Hydrocinnamoyl chloride 	2

Table III-2: 1st generation library code

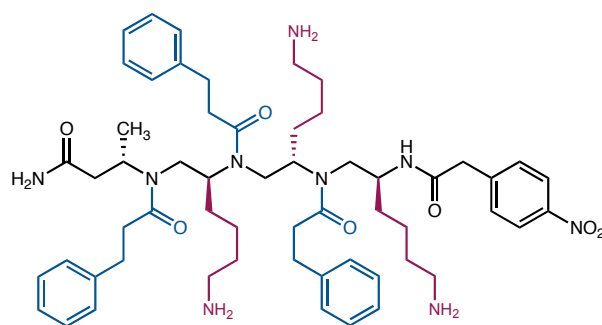


Figure III-13: Library code example – lysine or *K* residues are in red, hydrocinnamoyl or 2 residues are in blue to give *K2K2K2*

	A	B	C	D	E	F	G	H	
1	Y1Y1Y1	Y1Y1Y2	Y1Y2Y1	Y1Y2Y2	Y2Y1Y1	Y2Y1Y2	Y2Y2Y1	Y2Y2Y2	Y Series
2	Y1Y1H1	Y1Y1H2	Y1Y2H1	Y1Y2H2	Y2Y1H1	Y2Y1H2	Y2Y2H1	Y2Y2H2	
3	Y1Y1K1	Y1Y1K2	Y1Y2K1	Y1Y2K2	Y2Y1K1	Y2Y1K2	Y2Y2K1	Y2Y2K2	
4	Y1H1Y1	Y1H1Y2	Y1H2Y1	Y1H2Y2	Y2H1Y1	Y2H1Y2	Y2H2Y1	Y2H2Y2	
5	Y1H1H1	Y1H1H2	Y1H2H1	Y1H2H2	Y2H1H1	Y2H1H2	Y2H2H1	Y2H2H2	
6	Y1H1K1	Y1H1K2	Y1H2K1	Y1H2K2	Y2H1K1	Y2H1K2	Y2H2K1	Y2H2K2	
7	Y1K1Y1	Y1K1Y2	Y1K2Y1	Y1K2Y2	Y2K1Y1	Y2K1Y2	Y2K2Y1	Y2K2Y2	
8	Y1K1H1	Y1K1H2	Y1K2H1	Y1K2H2	Y2K1H1	Y2K1H2	Y2K2H1	Y2K2H2	
9	Y1K1K1	Y1K1K2	Y1K2K1	Y1K2K2	Y2K1K1	Y2K1K2	Y2K2K1	Y2K2K2	
1	H1Y1Y1	H1Y1Y2	H1Y2Y1	H1Y2Y2	H2Y1Y1	H2Y1Y2	H2Y2Y1	H2Y2Y2	H Series
2	H1Y1H1	H1Y1H2	H1Y2H1	H1Y2H2	H2Y1H1	H2Y1H2	H2Y2H1	H2Y2H2	
3	H1Y1K1	H1Y1K2	H1Y2K1	H1Y2K2	H2Y1K1	H2Y1K2	H2Y2K1	H2Y2K2	
4	H1H1Y1	H1H1Y2	H1H2Y1	H1H2Y2	H2H1Y1	H2H1Y2	H2H2Y1	H2H2Y2	
5	H1H1H1	H1H1H2	H1H2H1	H1H2H2	H2H1H1	H2H1H2	H2H2H1	H2H2H2	
6	H1H1K1	H1H1K2	H1H2K1	H1H2K2	H2H1K1	H2H1K2	H2H2K1	H2H2K2	
7	H1K1Y1	H1K1Y2	H1K2Y1	H1K2Y2	H2K1Y1	H2K1Y2	H2K2Y1	H2K2Y2	
8	H1K1H1	H1K1H2	H1K2H1	H1K2H2	H2K1H1	H2K1H2	H2K2H1	H2K2H2	
9	H1K1K1	H1K1K2	H1K2K1	H1K2K2	H2K1K1	H2K1K2	H2K2K1	H2K2K2	
1	K1Y1Y1	K1Y1Y2	K1Y2Y1	K1Y2Y2	K2Y1Y1	K2Y1Y2	K2Y2Y1	K2Y2Y2	K Series
2	K1Y1H1	K1Y1H2	K1Y2H1	K1Y2H2	K2Y1H1	K2Y1H2	K2Y2H1	K2Y2H2	
3	K1Y1K1	K1Y1K2	K1Y2K1	K1Y2K2	K2Y1K1	K2Y1K2	K2Y2K1	K2Y2K2	
4	K1H1Y1	K1H1Y2	K1H2Y1	K1H2Y2	K2H1Y1	K2H1Y2	K2H2Y1	K2H2Y2	
5	K1H1H1	K1H1H2	K1H2H1	K1H2H2	K2H1H1	K2H1H2	K2H2H1	K2H2H2	
6	K1H1K1	K1H1K2	K1H2K1	K1H2K2	K2H1K1	K2H1K2	K2H2K1	K2H2K2	
7	K1K1Y1	K1K1Y2	K1K2Y1	K1K2Y2	K2K1Y1	K2K1Y2	K2K2Y1	K2K2Y2	
8	K1K1H1	K1K1H2	K1K2H1	K1K2H2	K2K1H1	K2K1H2	K2K2H1	K2K2H2	
9	K1K1K1	K1K1K2	K1K2K1	K1K2K2	K2K1K1	K2K1K2	K2K2K1	K2K2K2	

Figure III-14: The 216 compounds of the 1st generation library divided into the *Y series*, *H series*, and *K series*

3.4.3 Library screen

Our library screen was designed to detect protein binding using a colorimetric sandwich assay (Figure III-15A). Since the ligands were immobilized on TentaGel resin, the desired protein required a biotin label that could be recognized by a streptavidin labeled-fluorescent dye. Any protein that bound to our ligands could then be visualized under a fluorescent microscope. Previous work in our lab discovered that the TentaGel resin itself has a green autofluorescence and standard fluorescent dyes, such as Texas Red, were difficult to visualize because of the background autofluorescence. This phenomenon was noted by Kodadek and co-workers and they were able to overcome this problem using streptavidin-coated quantum dots (Qdots).^{30, 31} Qdots (Invitrogen) are nanoparticle semiconductors (Figure III-15B) that exhibit a large Stokes shift and emit strongly in the red region. The result is a two-color assay where the green autofluorescence is observed in the absence of protein binding and the red fluorescence of the Qdot is observed in the presence of protein binding.

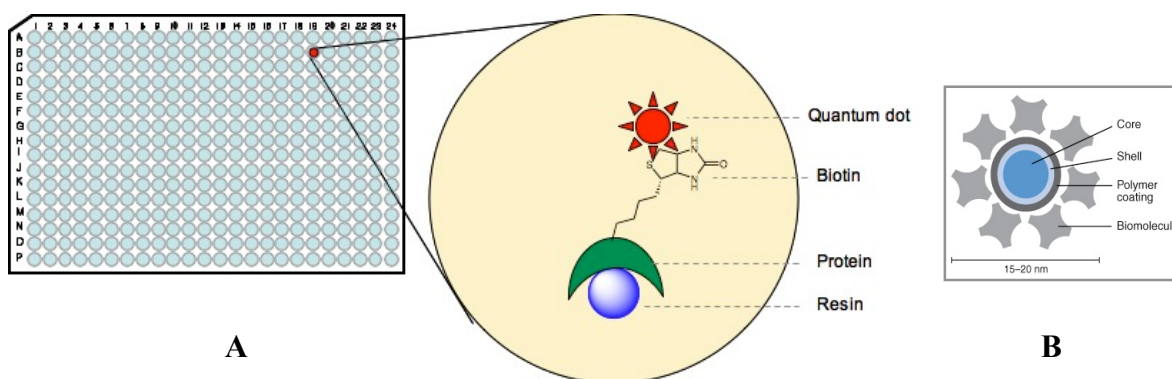


Figure III-15: A) Representation of the colorimetric sandwich assay for the library screens B) Qdot design

3.4.4 Myostatin

The first protein we screened was growth and differentiation factor-8 (GDF-8) or myostatin (25 kDa homodimer). Myostatin is a negative regulator of skeletal-muscle development and its inhibition could lead to therapeutics for muscular degenerative diseases.^{32 33} Cases also exist where the myostatin gene is absent, such as in Belgian Blue Cattle (Figure III-16), resulting in an extremely muscular animal. Currently, there is no small molecule inhibitor of myostatin. Due to a complicated cysteine-knot folding structure, myostatin could not be biotinylated, thus biotinylated antibody was used in the screen.



Figure III-16: Belgian Blue Cattle, which lacks the myostatin gene

The library was screened using a procedure similar to that of the Kodadek lab.³¹ A few beads from each well were transferred to a 384-well filter plate and blocked with 2% BSA in 1X PBS for 4 hours at 4 °C followed by 1X PBS washes. 175 nM myostatin in 4 mM HCl and 1% BSA was added to the resin and incubated for 24 hours at 4 °C then washed with 1X PBS. At this point, a 0.5 µg/mL solution of the GDF-8 PAb in 1X TBS buffer with 0.1% BSA was added and incubated for 3 hours at 4 °C. After incubation, the wells were washed with 1X TBS buffer and 50 nM streptavidin coated Qdots in 1X TBS buffer were added to the plates and incubated for 30 minutes at room temperature. Several washes with 1X TBS buffer were required to remove any excess Qdot signal and the plates were visualized under a fluorescent microscope.

Upon visualization of the plate, the majority of the beads were in fact green, but a handful of wells mainly in the *H series* plate were red. The screen was repeated a second time except

that the protein was allowed to incubate for 1 week at 4 °C. In addition, two rows of controls were run: one group contained beads, antibody and Qdots and the other group contained only beads and Qdots. Again the *H series* contained wells with red beads and three of the wells, H1H2K2, H2H2H2, and H2H1K1, were hits in both screens. The control wells were all negative except for a faint pink color on the beads from the histidine series containing only antibody and Qdots indicating some non-specific binding may be involved.

Efforts to remake the three hits on a larger scale for biological testing were met with mixed results. H2H2H2 was synthesized cleanly with little difficulty while H1H2K2 had some side product that may have been an incomplete reaction. Nonetheless, an adequate amount was synthesized for testing. H2H1K1, however, could not be reproduced in sufficient quantities. We speculate that isobutyryl chloride over-acylated the molecule creating numerous by-products. Purified H2H2H2 and H1H2K2 (Figure III-17) were sent for testing in a cellular myostatin assay by the McPherron Lab in the National Institute of Diabetes and Digestive and Kidney Diseases (NIDDK), but unfortunately did not inhibit myostatin *in vivo* (Figure III-18).

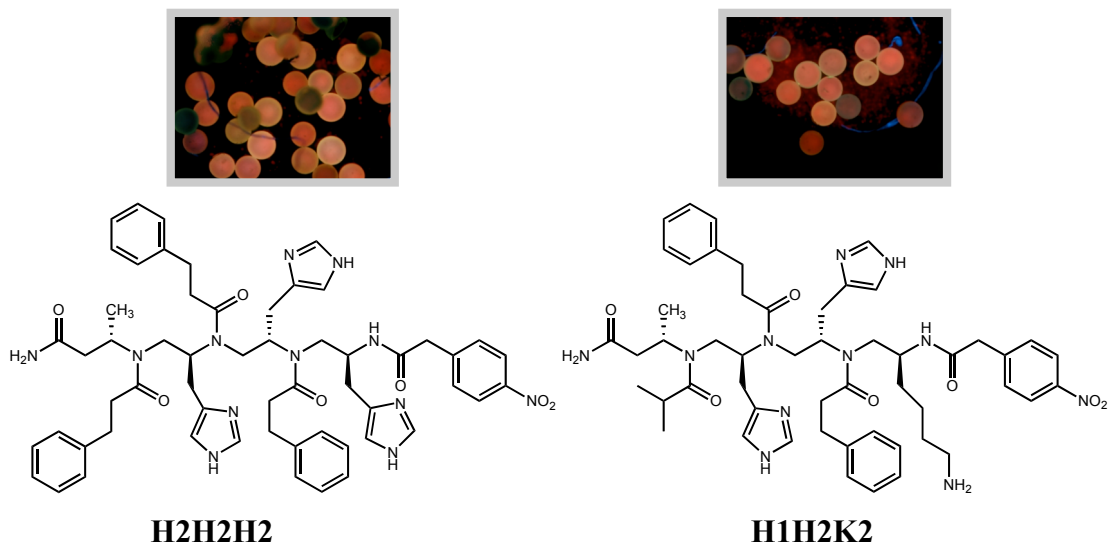


Figure III-17: Two positive hits from the myostatin screen

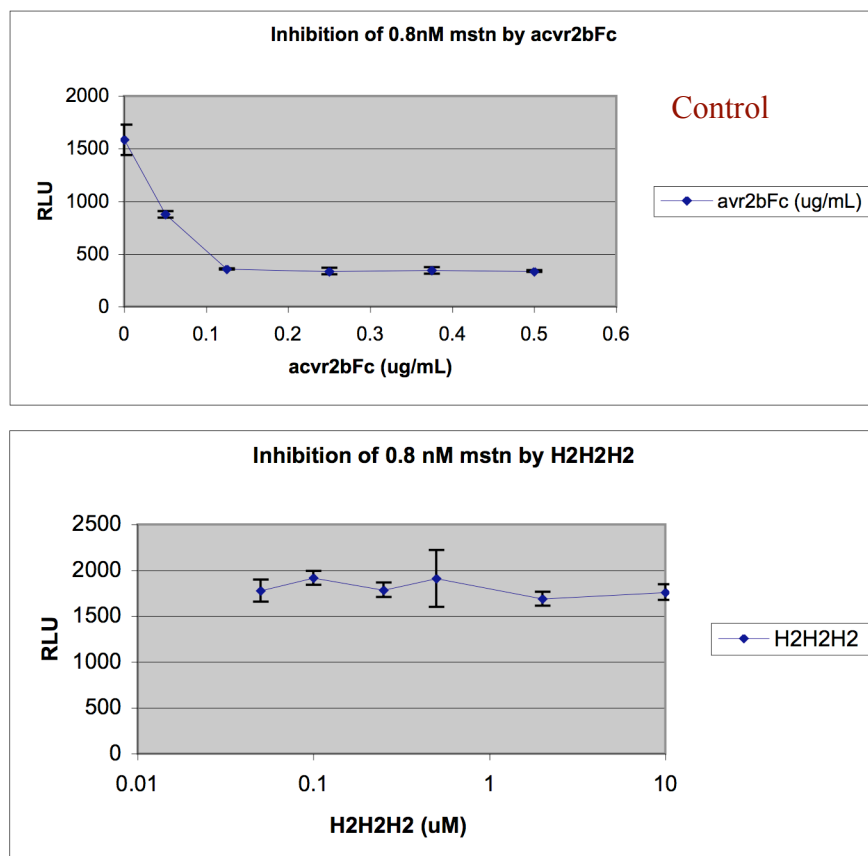


Figure III-18: Results from the myostatin cellular assay with H2H2H2; Inhibition is seen with the control but not with H2H2H2

3.4.5 Anthrax Lethal Factor

The next protein we sought to screen was the anthrax lethal factor (LF) protein. Lethal factor (90 kDa) is one of three proteins that make up the anthrax toxin (Figure III-19A). The first protein, protective antigen (PA) is responsible for binding to the host cell surface where it is cleaved and assembles a pore with six other PA molecules. This seven-membered pore is capable of binding LF and the third protein, edema factor (EF), and the cell engulfs this entire complex (Figure III-19B). The complex of LF and PA is known as lethal toxin (LTx), and the presence of LTx in the bloodstream is fatal.^{34, 35}

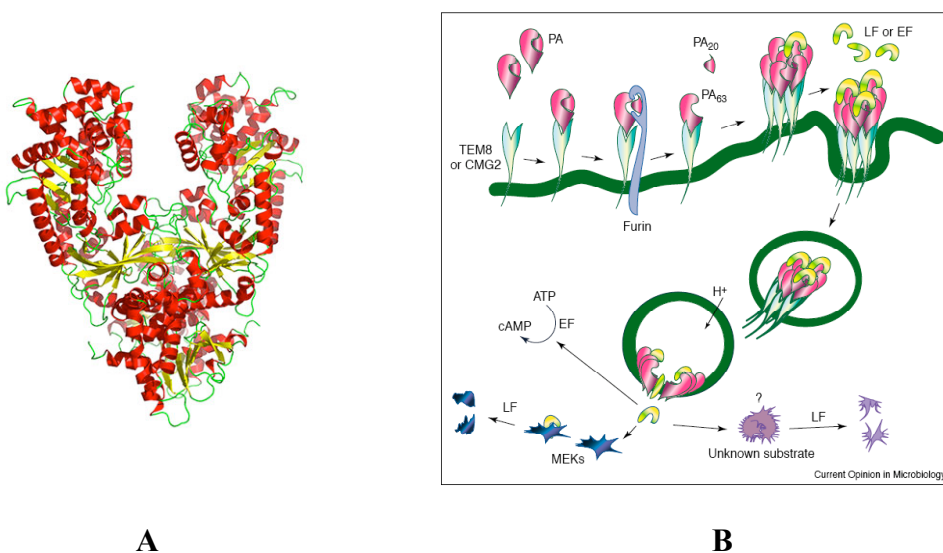


Figure III-19: A) Crystal structure of LF B) Diagram of the incorporation of the PA, LF, and EF proteins into a cell

A great deal of research has been dedicated to discovering small molecules that inhibit LF³⁶⁻³⁹ and some success has been met, but there is currently nothing for clinical use. The screen was performed in a similar manner as the myostatin screen with 175 nM biotinylated LF in 10 mM HEPES buffer. 0.1% Tween-20 was added to the protein in this screen to help reduce non-specific interactions, the protein was incubated for 3 days at 4 °C, and the antibody step was

eliminated since the protein was biotinylated directly. Controls consisting of a sample of wells from each series were run by adding only buffer when the library was incubated with the protein. One of the controls from the *H series* had a faint pink tint as did some of the wells in the H-series of the library screen. At this point we were beginning to suspect that histidine was causing some non-specific interactions and may have lead to false data in our first screen. The *Y series* contained no positive hits, but two very bright hits were found in the *K series*. K2Y1H1 and K1K2Y1 fluoresced much more brightly than any of the hits in the myostatin screen (Figure III-20).

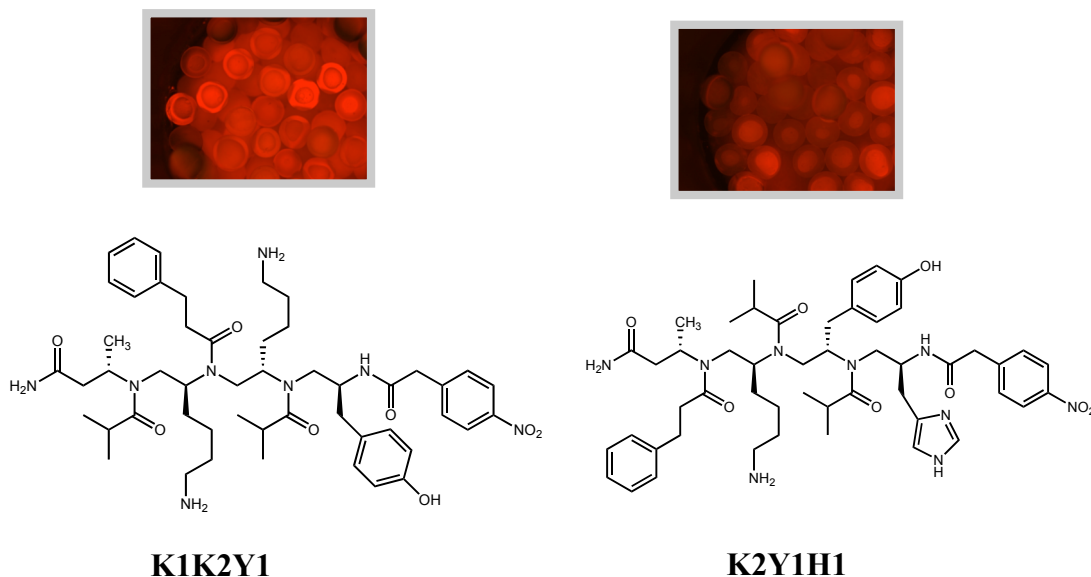


Figure III-20: Two positive hits from the LF screen

The synthesis of K1K2Y1 went cleanly and produced a significant amount of material, but the synthesis of K2Y1H1 was more difficult. Both molecules were sent for testing in the Leppa Lab in the National Institute of Allergy and Infectious Diseases (NIAID); the assay examined whether or not our molecules could protect RAW cells 264.7, a macrophage-like cell

line, from cell death when infected with the anthrax toxin. K1K2Y1 had no activity while K2Y1H1 initially looked like it protected cells from the LF toxin. With various amounts of K2Y1H1 and 1000 $\mu\text{g}/\text{mL}$ of toxin, living cells were still present (Figure III-21).

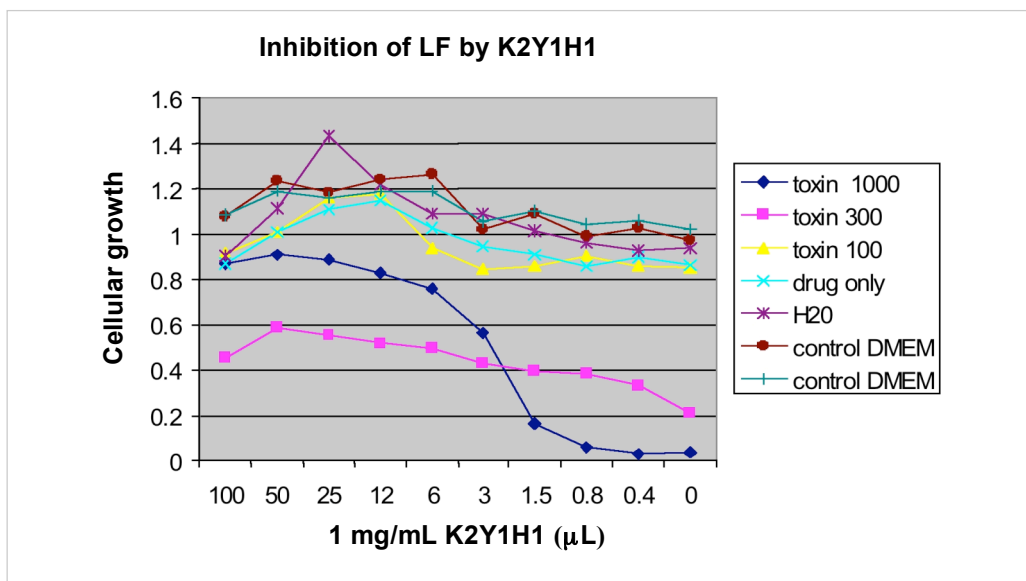


Figure III-21: Initial results from the LF cellular assay; K2Y1H1 protects the cell from the anthrax toxin

More K2Y1H1 was required for additional tests, but it could not be re-synthesized. Initial chloranil tests remained green after acylation indicating that the second isobutyryl group was not adding to the molecule. Mass spectrometry data indicated, however, that histidine was not adding and truncated versions of the molecule were being formed. The two main products had the molecule capped after the tyrosine with isobutyryl chloride (K2Y11) or capped after the tyrosine with 4-nitrophenylacetic acid (K2Y1) (Figure III-22). Concerned that one of these

molecules produced the hit in the library, they were sent for testing but did not possess cellular activity.

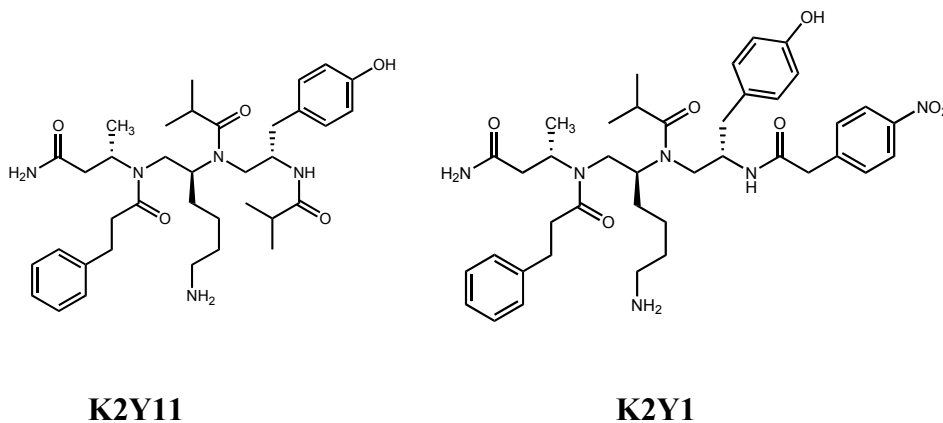


Figure III-22: Truncated forms of K2Y1H1 synthesized for testing

Finally, after various attempts at getting the histidine to add to the molecule the synthesis was successful. It is still unclear why histidine was not adding to the molecule, but the synthesis could now be repeated although it did not produce as much material as some of the more successful syntheses. Unfortunately, additional biological testing of this molecule did not reproduce the original results that had indicated activity. Upon further consideration, we believe that the large size of LF, 90 kDa, was far too large for our molecules to have any successful binding.

3.4.6 HIV Integrase

The last protein we screened with this library was HIV integrase (32 kDa). HIV integrase (IN) is an enzyme that is responsible for the integration of viral DNA into the host chromosome. Two key steps necessary for the integration of viral DNA are catalyzed by IN. The first step, occurring in the cytoplasm, involves cleaving nucleotides from the 3' end of viral DNA and

translocating the DNA to the cell nucleus. Once in the nucleus, the second step of cleaving the host DNA and covalently attaching the host DNA to the viral DNA occurs.⁴⁰ Recently, Merck developed a small molecule inhibitor of HIV integrase, MK-0518 or Raltegravir (Figure III-23),⁴¹ that was approved by the FDA in 2007 as an HIV drug.

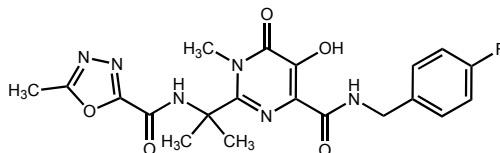
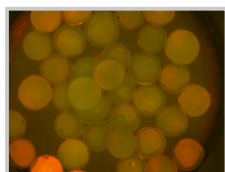
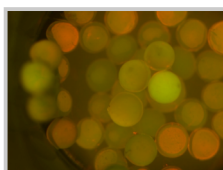


Figure III-23: Raltegravir

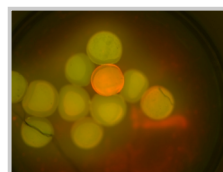
Biotinylated HIV integrase in 1X PBS buffer was incubated with the library for 3 days at 4 °C; all other steps of the screen were the same as in the previous screens. Unfortunately, in this screen no hits were observed. A control well from the *H series* as well as some wells in the H-series again exhibited a faint pink color convincing us there must be some non-specific binding. Nine wells from the *H series* were therefore selected and tested as controls by incubating them in 1X PBS only before adding the Qdots. All nine wells had a faint pink color (Figure III-24) indicating that there is indeed some non-specific binding in the histidine group that may have lead to some false positives, particularly in the myostatin screen.



H1H1H1



H1H2Y2



H2Y2K2

Figure III-24: A few wells in the H-series as controls; the faint pink color indicates non-specific interactions

3.5 2nd generation library

3.5.1 Library Design

Having learned that histidine was causing difficulties with our library both in the synthesis and in the screen, we sought to make a second larger library containing different amino acids that we hoped would not have as much non-specific interaction. To make the second library, four amino acids and two acid chlorides would be used to create 512 possible molecules. Lysine and tyrosine remained two of the amino acids, but norvaline and 4-fluorophenylalanine were used in place of histidine. Norvaline was chosen to help create some hydrophobic molecules instead of having all charged amino acid residues that may have enhanced the non-specific interactions and 4-fluorophenylalanine was chosen as an uncharged amino acid that could aid solubility. Hydrocinnamoyl chloride also remained in the library synthesis, but isobutyryl chloride was replaced with isovaleryl chloride. Isobutyryl chloride gave us some problems in the syntheses and we hoped that the extended chain of isovaleryl would relieve some of the sterics at the backbone and be easier to work with. Norvaline was given the code J since it does not have a one-letter code, 4-fluorophenylalanine was referred as F_f, and isovaleryl chloride was given the reference number 3 (Table III-3).

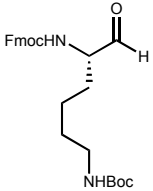
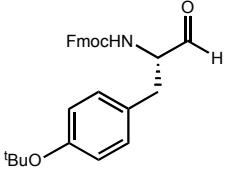
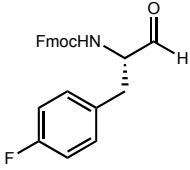
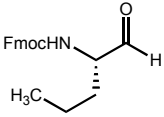
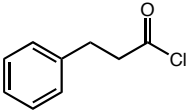
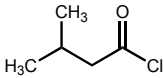
<i>Aldehyde or Acid Chloride</i>	<i>Code</i>
Lysine 	K
Tyrosine 	Y
(4-F)-Phenylalanine 	F_f
Norvaline 	J
Hydrocinnamoyl chloride 	2
Isovaleryl chloride 	3

Table III-3: 2nd generation library code

A few test molecules with the new amino acids and acid chloride were synthesized and worked with little difficulty. The only change necessary was the addition of some MeOH to help (4-F)-phenylalanine aldehyde dissolve in dichloromethane. Four aldehydes and two acid chlorides resulted in 512 possible compounds and again we used our computer program to output all 512 possible combinations (Figure III-25). The 512 member library was synthesized in six 96 well plates using the same procedure as in the first library. All random chloranil tests indicated that the syntheses had proceeded.

	A	B	C	D	E	F	G	H	I	J	K	L		
1	K2K2K2	K2K2K3	K2K2F2	K2K2F3	K2K2Y2	K2K2Y3	K2K2J2	K2K2J3	K2K3K2	K2K3K3	K2K3F2	K2K3F3	K Series	
2	K2K3Y2	K2K3Y3	K2K3J2	K2K3J3	K2F2K2	K2F2K3	K2F2F2	K2F2F3	K2F2Y2	K2F2Y3	K2F2J2	K2F2J3		
3	K2F3K2	K2F3K3	K2F3F2	K2F3F3	K2F3Y2	K2F3Y3	K2F3J2	K2F3J3	K2Y2K2	K2Y2K3	K2Y2F2	K2Y2F3		
4	K2Y2Y2	K2Y2Y3	K2Y2J2	K2Y2J3	K2Y3K2	K2Y3K3	K2Y3F2	K2Y3F3	K2Y3Y2	K2Y3Y3	K2Y3J2	K2Y3J3		
5	K2J2K2	K2J2K3	K2J2F2	K2J2F3	K2J2Y2	K2J2Y3	K2J2J2	K2J2J3	K2J3K2	K2J3K3	K2J3F2	K2J3F3		
6	K2J3Y2	K2J3Y3	K2J3J2	K2J3J3	K3K2K2	K3K2K3	K3K2F2	K3K2F3	K3K2Y2	K3K2Y3	K3K2J2	K3K2J3		
7	K3K3K2	K3K3K3	K3K3F2	K3K3F3	K3K3Y2	K3K3Y3	K3K3J2	K3K3J3	K3F2K2	K3F2K3	K3F2F2	K3F2F3		
8	K3F2Y2	K3F2Y3	K3F2J2	K3F2J3	K3F3K2	K3F3K3	K3F3F2	K3F3F3	K3F3Y2	K3F3Y3	K3F3J2	K3F3J3		
1	K3Y2K2	K3Y2K3	K3Y2F2	K3Y2F3	K3Y2Y2	K3Y2Y3	K3Y2J2	K3Y2J3	K3Y3K2	K3Y3K3	K3Y3F2	K3Y3F3	F_f Series	
2	K3Y3Y2	K3Y3Y3	K3Y3J2	K3Y3J3	K3J2K2	K3J2K3	K3J2F2	K3J2F3	K3J2Y2	K3J2Y3	K3J2J2	K3J2J3		
3	K3J3K2	K3J3K3	K3J3F2	K3J3F3	K3J3Y2	K3J3Y3	K3J3J2	K3J3J3						
4	F2K2Y2	F2K2Y3	F2K2J2	F2K2J3	F2K3K2	F2K3K3	F2K3F2	F2K3F3	F2K3Y2	F2K3Y3	F2K3J2	F2K3J3		
5	F2F2K2	F2F2K3	F2F2F2	F2F2F3	F2F2Y2	F2F2Y3	F2F2J2	F2F2J3	F2F3K2	F2F3K3	F2F3F2	F2F3F3		
6	F2F3Y2	F2F3Y3	F2F3J2	F2F3J3	F2Y2K2	F2Y2K3	F2Y2F2	F2Y2F3	F2Y2Y2	F2Y2Y3	F2Y2J2	F2Y2J3		
1	F2Y3K2	F2Y3K3	F2Y3F2	F2Y3F3	F2Y3Y2	F2Y3Y3	F2Y3J2	F2Y3J3	F2J2K2	F2J2K3	F2J2F2	F2J2F3		Y Series
2	F2J2Y2	F2J2Y3	F2J2J2	F2J2J3	F2J3K2	F2J3K3	F2J3F2	F2J3F3	F2J3Y2	F2J3Y3	F2J3J2	F2J3J3		
3	F3K2K2	F3K2K3	F3K2F2	F3K2F3	F3K2Y2	F3K2Y3	F3K2J2	F3K2J3	F3K3K2	F3K3K3	F3K3F2	F3K3F3		
4	F3K3Y2	F3K3Y3	F3K3J2	F3K3J3	F3F2K2	F3F2K3	F3F2F2	F3F2F3	F3F2Y2	F3F2Y3	F3F2J2	F3F2J3		
5	F3F3K2	F3F3K3	F3F3F2	F3F3F3	F3F3Y2	F3F3Y3	F3F3J2	F3F3J3	F3Y2K2	F3Y2K3	F3Y2F2	F3Y2F3		
6	F3Y2Y2	F3Y2Y3	F3Y2J2	F3Y2J3	F3Y3K2	F3Y3K3	F3Y3F2	F3Y3F3	F3Y3Y2	F3Y3Y3	F3Y3J2	F3Y3J3		
7	F3J2K2	F3J2K3	F3J2F2	F3J2F3	F3J2Y2	F3J2Y3	F3J2J2	F3J2J3	F3J3K2	F3J3K3	F3J3F2	F3J3F3		
8	F3J3Y2	F3J3Y3	F3J3J2	F3J3J3	F2K2K2	F2K2K3	F2K2F2	F2K2F3						
	A	B	C	D	E	F	G	H	I	J	K	L		
1	Y2K3K2	Y2K3K3	Y2K3F2	Y2K3F3	Y2K3Y2	Y2K3Y3	Y2K3J2	Y2K3J3	Y2F2K2	Y2F2K3	Y2F2F2	Y2F2F3	J Series	
2	Y2F2Y2	Y2F2Y3	Y2F2J2	Y2F2J3	Y2F3K2	Y2F3K3	Y2F3F2	Y2F3F3	Y2F3Y2	Y2F3Y3	Y2F3J2	Y2F3J3		
3	Y2Y2K2	Y2Y2K3	Y2Y2F2	Y2Y2F3	Y2Y2Y2	Y2Y2Y3	Y2Y2J2	Y2Y2J3	Y2Y3K2	Y2Y3K3	Y2Y3F2	Y2Y3F3		
4	Y2Y3Y2	Y2Y3Y3	Y2Y3J2	Y2Y3J3	Y2J2K2	Y2J2K3	Y2J2F2	Y2J2F3	Y2J2Y2	Y2J2Y3	Y2J2J2	Y2J2J3		
5	Y2J3K2	Y2J3K3	Y2J3F2	Y2J3F3	Y2J3Y2	Y2J3Y3	Y2J3J2	Y2J3J3	Y3K2K2	Y3K2K3	Y3K2F2	Y3K2F3		
6	Y3K2Y2	Y3K2Y3	Y3K2J2	Y3K2J3	Y3K3K2	Y3K3K3	Y3K3F2	Y3K3F3	Y3K3Y2	Y3K3Y3	Y3K3J2	Y3K3J3		
7	Y3F2K2	Y3F2K3	Y3F2F2	Y3F2F3	Y3F2Y2	Y3F2Y3	Y3F2J2	Y3F2J3	Y3F3K2	Y3F3K3	Y3F3F2	Y3F3F3		
8	Y3F3Y2	Y3F3Y3	Y3F3J2	Y3F3J3	Y3Y2K2	Y3Y2K3	Y3Y2F2	Y3Y2F3	Y3Y2Y2	Y3Y2Y3	Y3Y2J2	Y3Y2J3		
1	Y3Y3K2	Y3Y3K3	Y3Y3F2	Y3Y3F3	Y3Y3Y2	Y3Y3Y3	Y3Y3J2	Y3Y3J3	Y3J2K2	Y3J2K3	Y3J2F2	Y3J2F3	J Series	
2	Y3J2Y2	Y3J2Y3	Y3J2J2	Y3J2J3	Y3J3K2	Y3J3K3	Y3J3F2	Y3J3F3	Y3J3Y2	Y3J3Y3	Y3J3J2	Y3J3J3		
3	Y2K2K2	Y2K2K3	Y2K2F2	Y2K2F3	Y2K2Y2	Y2K2Y3	Y2K2J2	Y2K2J3						
4	J2K2K2	J2K2K3	J2K2F2	J2K2F3	J2K2Y2	J2K2Y3	J2K2J2	J2K2J3	J2K3K2	J2K3K3	J2K3F2	J2K3F3		
5	J2K3Y2	J2K3Y3	J2K3J2	J2K3J3	J2F2K2	J2F2K3	J2F2F2	J2F2F3	J2F2Y2	J2F2Y3	J2F2J2	J2F2J3		
6	J2F3K2	J2F3K3	J2F3F2	J2F3F3	J2F3Y2	J2F3Y3	J2F3J2	J2F3J3	J2Y2K2	J2Y2K3	J2Y2F2	J2Y2F3		
1	J2Y2Y2	J2Y2Y3	J2Y2J2	J2Y2J3	J2Y3K2	J2Y3K3	J2Y3F2	J2Y3F3	J2Y3Y2	J2Y3Y3	J2Y3J2	J2Y3J3		J Series
2	J2J2K2	J2J2K3	J2J2F2	J2J2F3	J2J2Y2	J2J2Y3	J2J2J2	J2J2J3	J2J3K2	J2J3K3	J2J3F2	J2J3F3		
3	J2J3Y2	J2J3Y3	J2J3J2	J2J3J3	J3K2K2	J3K2K3	J3K2F2	J3K2F3	J3K2Y2	J3K2Y3	J3K2J2	J3K2J3		
4	J3K3K2	J3K3K3	J3K3F2	J3K3F3	J3K3Y2	J3K3Y3	J3K3J2	J3K3J3	J3F2K2	J3F2K3	J3F2F2	J3F2F3		
5	J3F2Y2	J3F2Y3	J3F2J2	J3F2J3	J3F3K2	J3F3K3	J3F3F2	J3F3F3	J3F3Y2	J3F3Y3	J3F3J2	J3F3J3		
6	J3Y2K2	J3Y2K3	J3Y2F2	J3Y2F3	J3Y2Y2	J3Y2Y3	J3Y2J2	J3Y2J3	J3Y3K2	J3Y3K3	J3Y3F2	J3Y3F3		
7	J3Y3Y2	J3Y3Y3	J3Y3J2	J3Y3J3	J3J2K2	J3J2K3	J3J2F2	J3J2F3	J3J2Y2	J3J2Y3	J3J2J2	J3J2J3		
8	J3J3K2	J3J3K3	J3J3F2	J3J3F3	J3J3Y2	J3J3Y3	J3J3J2	J3J3J3						

Figure III-25: The 512 compounds in the 2nd generation library divided into the K Series, F_f Series, Y Series, and J Series

3.5.2 HIV Vpr-1

The first protein we screened the new library with was HIV viral protein regulator (Vpr-1). Vpr (14 kDa) is 96 amino acid protein consisting of three well defined helices connected by two loops (Figure III-26).⁴² The protein has a variety of functions including the regulation of the transcription of HIV-1 long terminal repeat, nuclear translocation of the HIV-1 preintegration complex, and inducing cell cycle arrest the G2 phase.^{43, 44} While a few small molecules have been found to inhibit some Vpr activity,⁴⁵⁻⁴⁸ there is no clinical drug that targets Vpr.

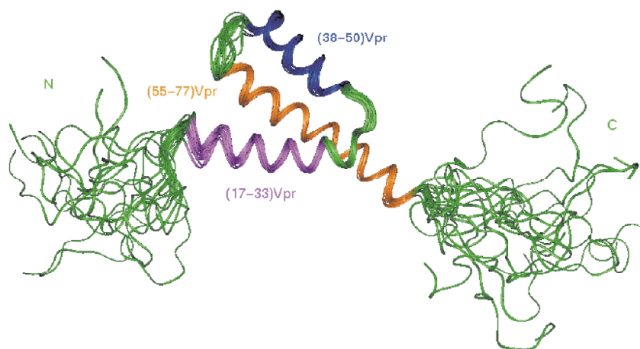


Figure III-26: Overlay of 15 NMR structures of the three α -helices

Hoping to eliminate false positives with slightly more stringent conditions, 175 nM of the protein was incubated for only 2 hours at 4 °C. Surprisingly, a large number of the wells had very bright red beads. All the control wells were green and we surmised the large number of hits may be due to the sticky nature of Vpr.⁴⁹ The brightest wells, 80 in all, were re-plated into another 384-well plate and re-screened with only 75 nM of protein for 30 minutes. This time there were far fewer hits and the controls were again green. Out of a handful of hits, the two brightest ones were chosen, K2K2Y2 and K2K3Y2, and re-synthesized. K2K2Y2 was synthesized cleanly with one major HPLC peak, but K2K3Y2 produced a large amount of a

amount of K2K2Y2 does not alter the effect of the assay and more tests are being conducted with our molecule.

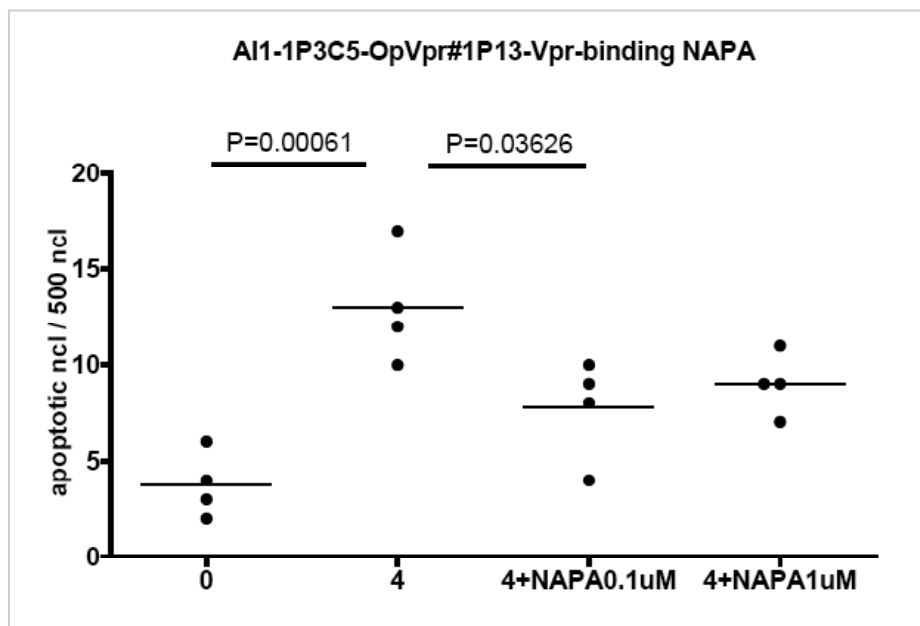


Figure III-28: Diagram showing the number of apoptotic nuclei as a result of DOX induced Vpr expression; K2K2Y2 partially reverses this effect

In this cellular assay, DOX, the transcriptional inducer RheoSwitch ligand (RSL-1) (Figure III-29),⁵⁰ and an antibiotic mixture of streptomycin and penicillin mixture were present.

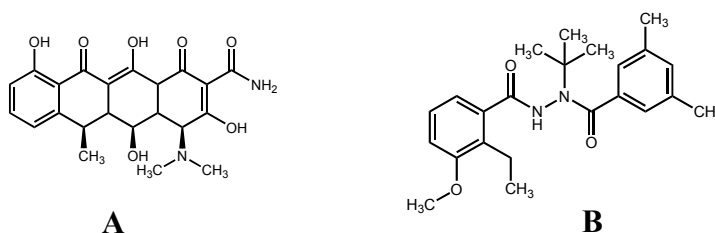


Figure III-29: A) Doxycyclin B) RSL-1

To ensure that our molecule was not reacting with these small molecules and affecting the activity, an assay was run on LC-MS to look for any interactions. A series of eight tubes (Table III-4) were set up and incubated at 37 °C for 72 hours. Every 24 hours an aliquot was run on the LC-MS to determine if any of the molecules had reacted with one another. Fortunately, there were no interactions observed. A second assay between doxycycline and a much larger concentration of K2K2Y2 was run under the same conditions to see if equimolar amounts of each would lead to reactions, but again there were no interactions observed.

Tube	Contents in 1X PBS
1	1 μ M K2K2Y2
2	10 μ M DOX
3	0.5 μ M RSL-1
4	1X Strep/Pen solution
5	1 μ M K2K2Y2 10 μ M DOX
6	1 μ M K2K2Y2 0.5 μ M RSL-1
7	1 μ M K2K2Y2 1X Strep/Pen solution
8	1 μ M K2K2Y2 10 μ M DOX 0.5 μ M RSL-1 1X Strep/Pen solution

Table III-4: Assay setup to test for interactions between chemical additives in the cell studies

In addition to the biological assays, we wanted to determine a binding constant for our molecule and Vpr. Initial data was obtained using Biacore instrumentation⁵¹ with the help of Dr. Carol Bewley's laboratory in the NIDDK. Biotin-labeled protein is plated onto a streptavidin coated gold chip and the Biacore uses surface plasmon resonance (SPR) to detect small molecule binding. Initially, the K2K2Y2 ligand was dissolved in water for the assay but a large amount of background was exhibited in addition to the binding data. Four buffers, PBS (1X), Tris (25 mM

+ 150 mM NaCl), HEPES (1X), and sodium acetate (25 mM + 150 mM NaCl), were used for the dissolution of K2K2Y2 to help remove background signal. 0.05% P-20 surfactant and 0.005% P-20 in water were also tried as solvents for K2K2Y2 to help reduce background signal. PBS buffer with 0.05% P-20 surfactant reduced the non-specific interactions the most successfully. Using these buffer conditions, a series of dilutions of K2K2Y2 was made for a kinetic binding experiment on the Biacore to estimate the binding constant. The resulting data was broader than expected, with a K_D between 15 μM and 60 μM . Regardless, we were encouraged by the data and now had a starting point. For a more accurate binding constant, we turned to isothermal titration calorimetry (ITC).^{52, 53} ITC is a very sensitive technique that measures the enthalpic change produced when a molecule binds to a protein. With the help of Dr. Lisa Jenkins in the National Cancer Institute (NCI), we ran an ITC experiment with 10 μM Vpr. Due to the difficulty of obtaining large quantities of the protein, we initially had a limited amount to work with and used this minimal concentration for an initial run. Even with this small amount of protein, ITC did show some K2K2Y2-protein binding (Figure III-30A) but a binding constant was difficult to determine. Once a greater amount of the protein was obtained, a second ITC experiment was run with 1000 μM of Vpr. A more pronounced binding curve was produced (Figure III-30B) and from this result the K_D was determined to be approximately 25 μM , which is in agreement with the range of values acquired from the Biacore.

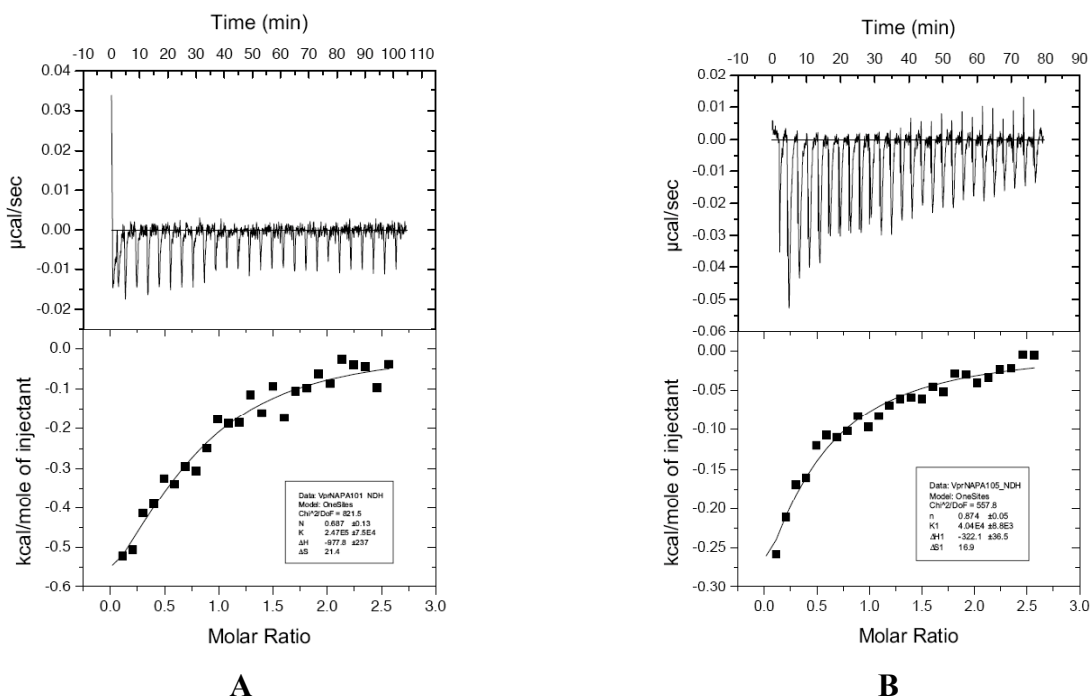


Figure III-30: ITC results for K2K2Y2 and A) 10 μM Vpr protein B) 1000 μM Vpr protein

3.5.3 MDMX

With the success of finding a lead compound for Vpr binding from our library, we screened a couple more proteins for binding. The second protein we screened was MDMX, a homolog of the MDM2 protein. MDMX is also a negative regulator of p53 and inhibits p53 transcription. Unlike MDM2, though, MDMX does not ubiquitinate p53 and its expression levels are not p53 dependent.^{54, 55} It is interesting that several of the MDM2 binders, such as the Nutlins and MI-219, do not bind to MDMX.⁶ MDMX possesses a shallower binding pocket than MDM2 (Figure III-31) thus obstructing the binding of known MDM2 inhibitors.⁵⁵

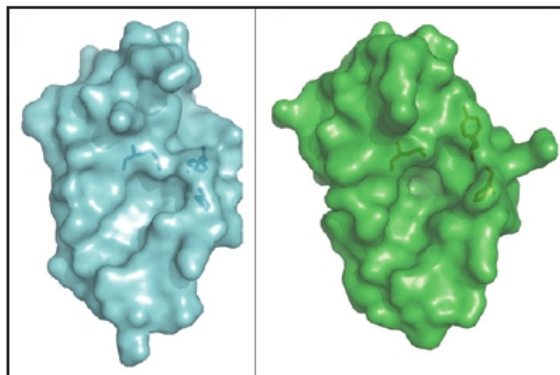
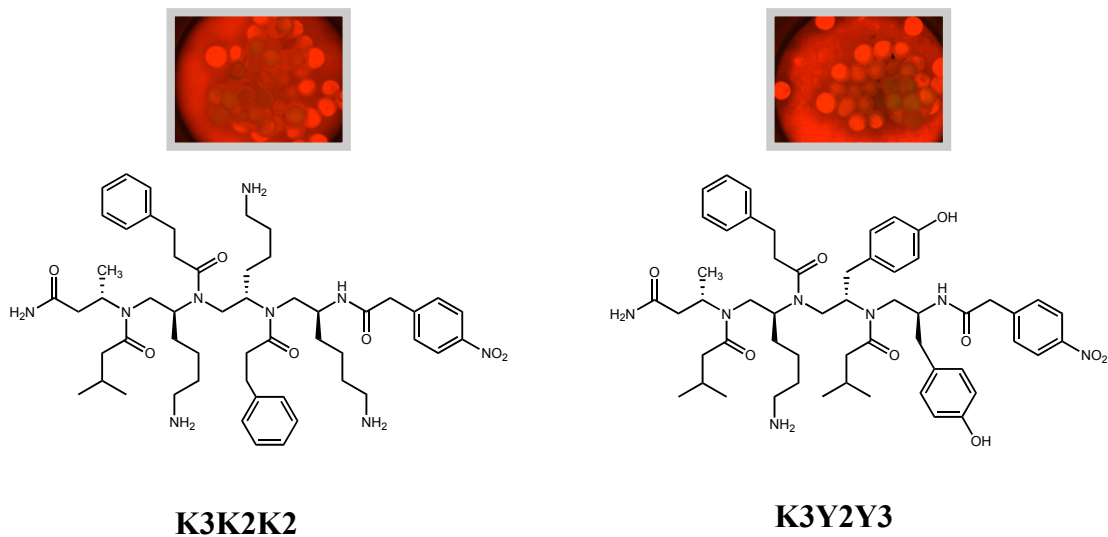


Figure III-31: Surface representations of the binding pockets of MDMX (left) and HDM2 (right)

The library was screened following the usual procedure and using 75 nM of biotinylated MDMX per well and incubating for 2 hours. Upon visualization of the libraries, several hits were found (Figure III-32). One hit, K3K2K2, was particularly bright, and two other hits, K3Y2Y3 and Y3K3Y2, were bright, but not as bright as K3K2K2 and none of the hits were as bright as the hits in the Vpr screen.



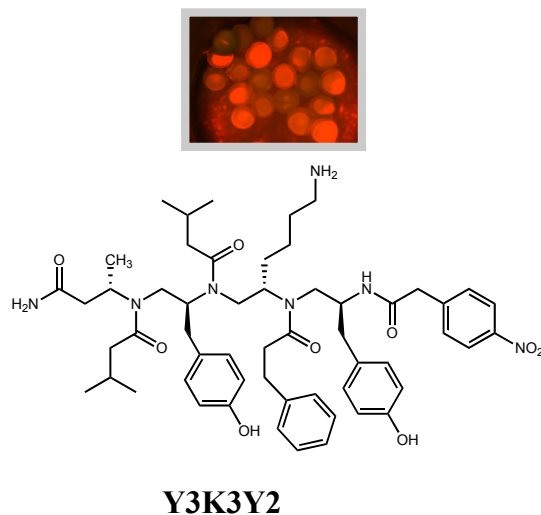


Figure III-32: Three positive hits from the MDMX screen

When the molecules were re-synthesized, there again was a large amount of the desired NAPA plus an additional isovaleryl moiety. The alkyl acid chlorides continue to over-acylate the molecules. While this by-product can easily be purified from the desired product by HPLC, this produces a couple of problems. The yield of the desired product decreases dramatically sometimes making more syntheses necessary, and it is unknown whether the hit came from the protein binding to the correct product, or this by-product that is most likely also in the library. The by-product could be purified and sent for biological testing along with the product to try and resolve this quandary, but should the by-product be the binding molecule, its structure is unknown. It is probable that the acid chloride is acylating the ϵ -amine on lysine, but presently there is no swift method for determining the structure.

Upon completion of the three NAPAs, they were submitted to Dr. Jenkins in the NCI for testing in a p53 competition assay with MDMX. Unfortunately, none of the molecules inhibited

p53 binding to MDMX. Additionally, no binding was found when ITC was run for each NAPA with MDMX.

3.5.4 FKBP52

The last protein we screened was FK506-binding protein 52 (FKBP52). FKBP52 (52 kDa) is an immunophilin that binds the immunosuppressant drug FK506. It contains peptidyl-prolyl *cis-trans* isomerase (PPIase) activity, which catalyzes the rate-limiting step of prolyl-peptide bond isomerization. FKBP52 is often found complexed with Hsp90 and it is involved in many cellular functions, most notably the regulation of steroid receptor signaling.⁵⁶

For this screen, we had a very small amount of biotinylated FKBP52 available, so the library was screened with only 50 nM of protein for 2 hours. None of the hits were exceptionally bright possibly due to the low concentration of protein, but the brightest hit, Y3K2J3 was selected and re-synthesized. The only difficulty associated with the synthesis of Y3K2J3 was the inability to precipitate the product from ether after resin cleavage, but this is not unexpected due to the number of hydrophobic residues present. The amount of over-acylated product in this synthesis was not as great as in some of the other NAPAs synthesized. One major difference with this molecule is that a hydrocinnamoyl chloride was added directly after the lysine moiety as opposed to an isovaleryl chloride. It is highly probable that the over-acylation is occurring on the lysine side chain.

Y3K2J3 was sent to the lab of Dr. Len Neckers in the NCI for biological testing, but unfortunately our molecule possessed no activity.

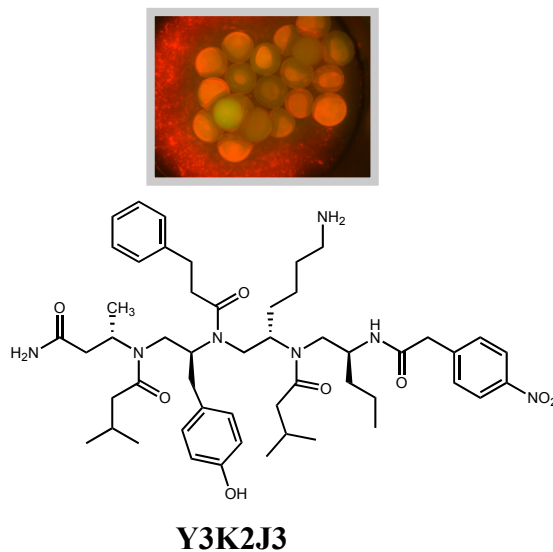


Figure III-33: Positive hit from the FKBP52 screen

3.6 Future Work

This project is still in relatively early stages and a large amount of work remains to be done. With all the difficulties encountered concerning over-acylation with the alkyl acid chlorides, the synthesis of the NAPAs needs to be optimized. Shortening the reaction times for the acylation may be sufficient to circumvent this dilemma and there is also the possibility that a double Boc-protection of the lysine side chain may be necessary. In addition to synthetic optimization, obtaining structural data would be ideal. The extent of racemization of the amino acids during the reductive amination has always been a concern. The LAH reduction of the Weinreb amides has been shown to be virtually racemization free,⁵⁷ and previous studies performed in our lab (unpublished results) have indicated that minimal epimerization occurs during solid-phase reductive amination. However, those studies were performed under acid-free conditions. Our optimized NAPA synthesis requires the use of acetic acid with $\text{NaBH}(\text{OAc})_3$,

which could influence imine-enamine tautomerization.⁵⁸ It has also been shown that the tertiary amides in peptoids undergo *cis/trans* isomerization⁵⁹ and NAPAs also contain tertiary amides that may experience the same phenomena. In many instances during the purification of synthesized NAPAs, the desired molecule was noticed to have two to three HPLC peaks that were usually impossible to separate, but all consisted of the exact same mass. It is unknown whether or not a variety of isomers contributed to this characteristic of the molecules and information on racemization and isomerization could clarify this problem.

The library synthesis and screen also requires optimization. Currently the library is synthesized manually, which is a long and laborious task; automation of the synthesis would greatly increase the rate of progress of this project and the size of libraries possible. Typically when libraries are screened for biological hits, the library consists of thousands of compound. Our libraries of hundreds of compounds are exceedingly small in comparison. Lastly, our screening method seems to produce either very weak binders, or false positives, as many of our hits had no activity in the biological assays. There is no obvious reason for this, although similar results were noticed with a polyamine-amide RNA screening project performed in our lab. The Qdots may be somewhat promiscuous, binding to more than just biotin. This predicament will also need to be addressed in the future.

3.7 Summary

In an attempt to inhibit protein-protein interactions, we designed and synthesized a N-acylated polyamine scaffold that consisted of six possible residues in a fairly compact space. We surmised that some of these residues would be specific for binding to a protein, while the others would aid selectivity or solubility. After much synthetic optimization, we synthesized a 216-member library that we screened for binding to myostatin, anthrax lethal factor, and HIV-1

integrase. Positive hits were identified for the myostatin and lethal factor screens, but unfortunately did not display any *in vivo* activity. After introducing new residues a second library of 512 compounds was synthesized and screened for binding to HIV-1 Vpr, MDMX, and FKBP52. While we got positive hits in most of the screens, only the NAPA we produced for HIV Vpr binding produced results in the biological assays. This NAPA, K2K2Y2, was found to bind to Vpr with a K_D of approximately 25 μM , which we found encouraging as to the validity of our assay. As additional residues are added to the library, the number of possible NAPAs increases exponentially allowing for the synthesis of much larger libraries. The larger libraries will provide many more options for protein screens in the future.

3.8 Experimental Procedures

General Methods

Proton nuclear magnetic resonances (^1H NMR) were recorded in deuterated solvents on a Gemini 300 (300 MHz) relative to tetramethylsilane (δ 0.00). Proton-decoupled carbon (^{13}C -NMR) spectra were recorded on a Gemini 300 (75 MHz) and are reported in ppm using the solvent as an internal standard (CDCl_3 , δ 77.23; DMSO , δ 39.52). Electrospray mass spectra (ESI-MS) were obtained using an Agilent 6100 series LC-MS. Tetrahydrofuran (THF) was purified by passing solvent through a column of activated alumina on a Glass Countour Solvent Purification System. Nitrogen was bubbled through dimethylformamide (DMF) for 16 hours prior to use. All solution phase reactions were performed in oven dry glassware under a positive pressure of nitrogen. Silanization of glassware was performed using Sigmacote, in accordance with the manufacturer's instructions. All protected amino acids, Rink resin, and HOBt hydrate were purchased from Advanced ChemTech. HATU was purchased from Applied Biosystems. TentaGel-NH₂ macrobeads were purchased from Peptides International. Fmoc- β -homoalanine

was purchased from Fluka. Streptavidin Qdots were purchased from Invitrogen. Myostatin and PAb were purchased from R&D Systems, while all other proteins were obtained from research labs within the NIH. All other chemicals were purchased from Sigma-Aldrich. All HPLC purification was done via reverse phase on an Agilent 1100 series semi-prep system with UV detection at 254 nm. A Vydac C18 semi-prep column was utilized. The column was kept at room temperature. Solution A was 0.05% TFA in water and solution B was 0.05% TFA in acetonitrile. A typical elution was a gradient of 100% A to 100% B over 40 minutes at a flow rate of 5.0 mL/min.

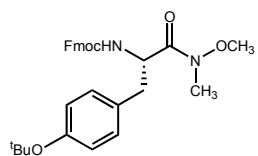
Abbreviations

(Fmoc), *N*-(9-fluorenylmethoxycarbonyl); (DIEA), *N*-diisopropylethylamine; (HATU), *O*-(7-Azabenzotriazol-1-yl)-*N,N,N',N'*-tetramethyluronium hexafluorophosphate); (HOBt), 1-hydroxybenzotriazole; (EDC), 1-Ethyl-3-(3-dimethylaminopropyl)carbodiimide hydrochloride; (Boc), *t*-butoxycarbonyl); (DMF), dimethylformamide; (THF), tetrahydrofuran; (DCM), dichloromethane; (NMP), *N*-methylpyrrolidinone; (TFA), trifluoroacetic acid; (TES), triethylsilane.

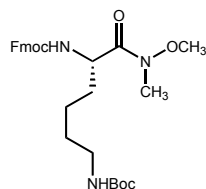
3.8.1 General Synthesis of Fmoc-Weinreb Amides

A Fmoc-L-amino acid (10.9 mmol) was dissolved in DCM with DIEA (1.9 mL, 10.9 mmol) and the reaction was allowed to cool to 0 °C. Once cool, HOBt hydrate (1.98 g, 13.1 mmol) and EDC (2.5 g, 13.1 mmol) were added to the reaction, which was allowed to stir for 10 minutes at 0 °C. *N,O*-dimethylamine hydrochloride (1.3 g, 13.1 mmol) and second portion of DIEA (2.3 mL, 13.1 mmol) were added to the flask. The mixture was allowed to stir for an hour

at 0 °C and then warmed to room temperature and allowed to stir overnight. Upon completion, the reaction was transferred to a separatory funnel with DCM and washed with 1 M HCl (3 x 40 mL), sat. NaHCO₃ (2 x 40 mL), and sat. NaCl (2 x 40 mL). The organic layer was dried over anhydrous Na₂SO₄ and concentrated under vacuum to yield the Weinreb amide as a white crystalline solid. In the case of norvaline, the product was a colorless oil. Weinreb amides could be stored at 4 °C or -20 °C and there did not appear to be any degradation after months of storage.

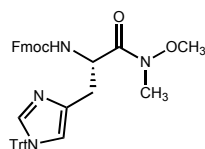


Fmoc-Tyr(tBu)-Weinreb Yield: 94% ¹H-NMR (CDCl₃, 300 MHz): δ 7.73 (d, *J* = 7.41 Hz, 2H, Fmoc aromatic CH), 7.56 (t, *J* = 6.85 Hz, 2H, Fmoc aromatic CH), 7.37 (t, *J* = 7.41 Hz, 2H, Fmoc aromatic CH), 7.28 (t, *J* = 7.41 Hz, 2H, Fmoc aromatic CH), 7.08 (d, *J* = 8.17 Hz, 2H, Tyr aromatic CH), 6.89 (d, *J* = 8.24 Hz, 2H, Tyr aromatic CH), 5.72 (d, *J* = 8.88 Hz, 1H, carbamate NH), 4.99 (m, 1H, CH), 4.29 (m, 2H, Fmoc CH₂), 4.16 (t, *J* = 7.12, 1H, Fmoc CH), 3.60 (s, 3H, -OCH₃), 3.14 (s, 3H, -NCH₃), 3.00 (m, 2H, CH₂), 1.28 (s, 9H, C(CH₃)₃); ¹³C-NMR (CDCl₃, 75 MHz): δ 172.2, 155.9, 154.3, 144.0, 143.9, 141.3, 131.4, 130.0, 127.8, 127.1, 125.3, 124.2, 120.0, 78.5, 67.1, 61.6, 52.2, 47.2, 38.3, 32.1, 29.1, 28.9; **ESI-MS** *m/z* = 502.6

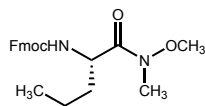


Fmoc-Lys(Boc)-Weinreb Yield: 95% ¹H-NMR (CDCl₃, 300 MHz): δ 7.75 (d, *J* = 7.49 Hz, 2H, Fmoc aromatic CH), 7.60 (t, *J* = 6.85 Hz, 2H, Fmoc aromatic CH), 7.38 (t, *J* = 7.47 Hz, 3H, Fmoc aromatic CH), 7.32 (t, *J* = 7.41 Hz, 3H, Fmoc aromatic CH), 5.66 (d, *J* = 8.86 Hz, 1H, carbamate NH), 4.74 (m, 1H, carbamate NH), 4.65 (m, 1H, CH), 4.36 (d, *J* = 7.13 Hz, 2H, Fmoc CH₂), 4.21 (t, *J* = 6.97 Hz, 1H, Fmoc

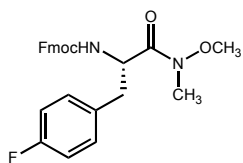
CH), 3.76 (s, 3H, -OCH₃), 3.21 (s, 3H, -NCH₃), 3.11 (d, $J = 5.74$ Hz, 2H, CHCH₂), 1.75 (m, 2H, CH₂), 1.63 (m, 2H, CH₂), 1.49 (m, 2H, CH₂), 1.43 (s, 9H, C(CH₃)₃); ¹³C-NMR (CDCl₃, 75 MHz): δ 172.8, 156.3, 156.1, 144.0, 143.9, 141.3, 127.7, 127.1, 125.2, 120.0, 79.1, 67.0, 61.7, 50.8, 47.2, 40.3, 32.4, 32.1, 29.6, 28.5, 22.5; **ESI-MS** $m/z = 511.6$



Fmoc-His(Trt)-Weinreb Yield: 98% ¹H-NMR (CDCl₃, 300 MHz): δ 7.85 (d, $J = 7.85$ Hz, 2H, Fmoc aromatic CH), 7.72 (d, $J = 7.72$ Hz, 2H, Fmoc aromatic CH), 7.42 (m, 14H, Fmoc aromatic CH, Trityl CH, Imidazole CH), 7.25 (dd, $J = 2.88$ Hz, 6.68 Hz, 6H, Trityl CH), 6.74 (s, 1H, Imidazole CH), 6.41 (d, $J = 8.45$ Hz, 1H, carbamate NH), 5.14 (m, 1H, CH), 4.42 (dd, $J = 3.74$ Hz, 7.33 Hz, 2H, Fmoc CH₂), 4.33 (m, 1H, Fmoc CH), 3.87 (s, 3H, -OCH₃), 3.25 (s, 3H, -NCH₃), 3.14 (m, 2H, CH₂); ¹³C-NMR (CDCl₃, 75 MHz): δ 156.25, 156.2, 142.5, 142.4, 141.3, 141.2, 138.6, 136.4, 128.8, 128.0, 127.4, 125.3, 120.7, 119.9, 75.3, 75.2, 67.0, 61.6, 53.5, 52.4, 51.7, 47.2; **ESI-MS** $m/z = 662.8$



Fmoc-Nva-Weinreb Yield: 94% ¹H-NMR (CDCl₃, 300 MHz): δ 7.74 (d, $J = 7.74$ Hz, 2H, Fmoc aromatic CH), 7.60 (t, $J = 6.85$ Hz, 2H, Fmoc aromatic C-H), 7.38 (t, $J = 7.27$, 2H, Fmoc aromatic CH), 7.29 (t, $J = 7.35$ Hz, 2H, Fmoc aromatic CH), 5.57 (s, 1H, carbamate NH), 4.78 (m, 1H, CH), 4.34 (m, 2H, Fmoc CH₂), 4.21 (t, $J = 7.00$, 1H, Fmoc CH), 3.76 (s, 3H, -OCH₃), 3.21 (s, 3H, -NCH₃), 1.68 (m, 1H, H-CH), 1.65 (m, 1H, HC-H), 1.40 (m, 2H, CH₂), 0.94 (t, $J = 7.27$ Hz, 3H, CH₃); ¹³C-NMR (CDCl₃, 75 MHz): δ 156.4, 144.1, 144.0, 141.3, 127.7, 127.1, 125.3, 120.0, 67.0, 61.6, 50.8, 47.3, 34.9, 32.1, 18.8, 13.9; **ESI-MS** $m/z = 382.4$



Fmoc-(4-F)Phe-Weinreb Yield: 91% $^1\text{H-NMR}$ (CDCl_3 , 300 MHz): δ

7.88 (d, $J = 7.41$ Hz, 2H, Fmoc aromatic CH), 7.68 (t, $J = 7.15$ Hz, 2H,

Fmoc aromatic CH), 7.51 (t, $J = 7.47$ Hz, 2H, Fmoc aromatic CH), 7.42 (t,

$J = 7.41$ Hz, 2H, Fmoc aromatic CH), 7.25 (m, 2H, aromatic CH), 7.09 (t, $J = 8.60$ Hz, 2H,

aromatic CH), 5.84 (d, $J = 8.75$ Hz, 1H, carbamate NH), 5.12 (m, 1H, CH), 4.51 (m, 1H, Fmoc

H-CH), 4.42 (m, 1H, Fmoc HC-H), 4.30 (t, $J = 7.03$ Hz, 1H, Fmoc CH), 3.81 (s, 3H, $-\text{OCH}_3$),

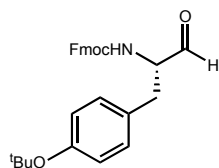
3.30 (s, 3H, $-\text{NCH}_3$), 3.20 (dd, $J = 5.64, 14.11$ Hz, 1H, H-CH), 3.05 (dd, $J = 7.07, 13.58$ Hz, 1H,

HC-H); $^{13}\text{C-NMR}$ (CDCl_3 , 75 MHz): δ 171.9, 163.6, 160.4, 155.9, 143.9, 141.4, 132.2, 131.0,

127.8, 127.1, 124.5, 120.06, 115.2, 100.32, 67.0, 61.7, 47.2, 32.2; **ESI-MS** $m/z = 448.5$

8.8.2 General Synthesis of Aldehydes

A Fmoc-Weinreb amide (4.5 mmol) was dissolved in dry THF and cooled to 0 °C. Lithium aluminum hydride (212 mg, 5.6 mmol) was added slowly to the reaction. The mixture was allowed to stir for 1 hour at 0 °C. The reaction was quenched with 0.1 M NaHSO_4 (2.6 g, 18.9mmol), which was added dropwise. The mixture was allowed to stir an additional 10 minutes at 0 °C before being transferred to a separatory funnel with EtOAc and sat. NaCl. The aqueous layer was extracted with EtOAc and combined organic layers were washed with 1 M HCl (3 x 40 mL), sat. NaHCO_3 (2 x 40 mL), and sat. NaCl (2 x 40 mL). The organic layer was dried over anhydrous Na_2SO_4 and concentrated under vacuum to yield an oil. Re-dissolving the product in ether and removing the solvent under vacuum produced the aldehyde as a solid. The aldehydes were found to be stable for at least 1 month if stored at -20 °C.



Fmoc-Tyr(tBu)-Aldehyde Yield: 82% $^1\text{H-NMR}$ (CDCl_3 , 300 MHz): δ 9.59

(s, 1H, CHO), 7.75 (d, $J = 7.47$ Hz, 2H, Fmoc aromatic CH), 7.55 (d, $J = 7.10$,

2H, Fmoc aromatic CH), 7.39 (t, $J = 7.44$, 2H, Fmoc aromatic CH), 7.30 (t, $J =$

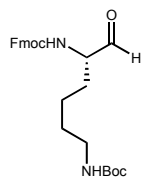
7.38 Hz, 2H Fmoc aromatic CH), 7.00 (d, $J = 8.03$ Hz, 2H, Tyr aromatic CH), 6.89 (d, $J = 8.30$

Hz, 2H, Tyr aromatic CH), 5.36 (d, $J = 6.88$ Hz, 1H, carbamate NH), 4.42 (m, 3H, CH , Fmoc

CH_2), 4.19 (t, $J = 6.68$, 1H, Fmoc CH), 3.07 (d, $J = 6.47$, 2H, CH_2), 1.32 (s, 9H, $\text{C}(\text{CH}_3)_3$); $^{13}\text{C-}$

NMR (CDCl_3 , 75 MHz): δ 198.97, 155.94, 154.60, 143.78, 141.42, 127.85, 127.00, 125.10,

124.41, 124.09, 120.10, 119.92, 100.33, 67.03, 61.24, 47.28, 34.80, 28.92; **ESI-MS** $m/z = 443.5$



Fmoc-Lys(Boc)-Aldehyde Yield: 89% $^1\text{H-NMR}$ (CDCl_3 , 300 MHz): δ 9.49 (s,

1H, CHO), 7.72 (d, $J = 7.41$ Hz, 2H, Fmoc aromatic CH), 7.57 (d, $J = 7.25$ Hz, 2H,

Fmoc aromatic CH), 7.36 (t, $J = 7.18$ Hz, 2H, Fmoc aromatic CH), 7.26 (m, 2H,

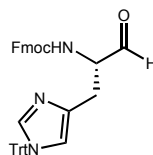
Fmoc aromatic CH), 5.79 (d, $J = 5.95$ Hz, 1H, carbamate NH), 4.76 (m, 1H, CH), 4.39 (d, $J =$

7.25 Hz, 2H, Fmoc CH , carbamate NH), 4.18 (m, 2H, Fmoc CH_2), 3.06 (m, 2H, CH_2), 1.83 (m,

2H, CH_2), 1.51 (m, 2H, CH_2), 1.41 (s, 9H, $\text{C}(\text{CH}_3)_3$), 1.33 (m, 2H, CH_2); $^{13}\text{C-NMR}$ (CDCl_3 , 75

MHz): δ 199.8, 156.4, 143.8, 141.4, 127.8, 127.0, 125.2, 124.1, 120.0, 79.3, 67.0, 60.1, 47.3,

39.9, 29.8, 28.5, 22.3, 18.3; **ESI-MS** $m/z = 452.5$



Fmoc-His(Trt)-Aldehyde Yield: 72% $^1\text{H-NMR}$ (CDCl_3 , 300 MHz): δ 9.80 (s, 1H,

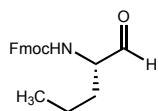
CHO), 7.88 (d, $J = 7.31$ Hz, 2H, Fmoc aromatic CH), 7.73 (d, $J = 7.46$ Hz, 2H,

Fmoc aromatic CH), 7.64 (m, 1H, imidazole CH), 7.46 (m, 14H, Fmoc aromatic

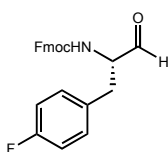
CH , trityl CH), 7.23 (m, 5H, trityl CH), 6.76 (s, 1H, imidazole CH), 6.62 (d, $J = 6.84$ Hz, 1H,

NH), 4.57 (m, 1H, CH), 4.49 (m, 2H, Fmoc CH_2), 4.36 (m, 1H, Fmoc CH), 3.21 (m, 2H, CH_2);

$^{13}\text{C-NMR}$ (CDCl_3 , 75 MHz): δ 200.4, 156.4, 143.9, 142.3, 141.3, 138.8, 135.9, 130.8, 128.1, 127.7, 127.1, 126.9, 125.2, 120.0, 75.4, 60.4, 59.9, 47.2, 21.1, 14.2; **ESI-MS** m/z = 603.7



Fmoc-Nva-Aldehyde Yield: 84% $^1\text{H-NMR}$ (CDCl_3 , 300 MHz): δ 9.66 (s, 1H, CHO), 7.89 (d, J = 7.48 Hz, 2H, Fmoc aromatic CH), 7.74 (d, J = 7.43 Hz, 2H, Fmoc aromatic CH), 7.53 (t, J = 7.18 Hz, 2H, Fmoc aromatic CH), 7.45 (t, J = 7.45 Hz, 2H, Fmoc aromatic CH), 5.66 (d, J = 7.18 Hz, 1H, CH), 4.57 (d, J = 6.81 Hz, 1H, Fmoc CH), 4.38 (m, 3H, Fmoc CH_2 , carbamate NH), 1.97 (m, 1H, H-CH), 1.67 (m, 1H, HC-H), 1.50 (m, 2H, CH_2), 1.08 (t, J = 7.15 Hz, 3H, CH_3); $^{13}\text{C-NMR}$ (CDCl_3 , 75 MHz): δ 199.7, 156.3, 143.9, 141.4, 127.9, 127.1, 125.2, 120.1, 67.0, 60.1, 47.7, 47.3, 31.2, 18.6, 13.9; **ESI-MS** m/z = 323.4



Fmoc-(4-F)Phe-Aldehyde Yield: 89% $^1\text{H-NMR}$ (CDCl_3 , 300 MHz): δ 9.57 (s, 1H, CHO), 7.87 (m, 2H, Fmoc aromatic CH), 7.66 (d, J = 7.39 Hz, 2H, Fmoc aromatic CH), 7.41 (t, J = 7.38 Hz, 2H, Fmoc aromatic CH), 7.29 (m, 4H, phenyl aromatic CH), 7.08 (t, J = 8.90 Hz, 2H, Fmoc aromatic CH), 5.92 (dd, J = 6.03, 16.13 Hz, 1H, NH), 4.86 (m, 1H, CH), 4.36 (m, 2H, Fmoc CH_2), 4.22 (m, 1H, Fmoc CH), 3.10 (m, 1H, H-CH), 2.72 (m, 1H, HC-H); $^{13}\text{C-NMR}$ (CDCl_3 , 75 MHz): δ 200.9, 156.4, 144.0, 141.0, 134.1, 131.3, 131.2, 127.8, 127.2, 125.3, 124.3, 115.0, 65.7, 61.3, 46.9, 32.7; **ESI-MS** m/z = 389.

3.8.3 Solid-phase synthesis of N-acylated polyamines

Preparation of resin: Rink amide resin (1.0 g, 0.75 mmol) was swelled in a silanized filter vessel with DMF. The Fmoc protecting group was cleaved with 20% piperidine in DMF (5 min., DMF wash, 20 min.). The resin was washed with DMF (3x) and DCM (3x). A red chloranil test

indicated the presence of a primary amine. Fmoc- β -homoalanine (793 mg, 2.25 mmol) was dissolved in DMF and added to the resin. HATU (843 mg, 2.25 mmol), HOBt (340 mg, 2.25 mmol), and DIEA (888 μ L, 5.1 mmol) were dissolved in DMF and added to the resin. The mixture was shaken for 1.5 hours. The reagents were drained and the resin was washed with MeOH, DMF, and DCM. A negative chloranil test indicated the absence of free amine. The resin was dried under vacuum and transferred to a silanized vial for storage.

NAPA synthesis: Fmoc- β -homoalanine rink resin (200 mg, 0.15 mmol) was swelled in a silanized filter vessel with DMF. The Fmoc group was deprotected with 20% piperidine in DMF (3 x 5 min) and the resin was washed with DMF (3x) and DCM (3x). This method was used for all subsequent Fmoc deprotections. A red chloranil test indicated the presence of a primary amine. A Fmoc-amino aldehyde (0.75 mmol) and TMOF (410 μ L, 3.75 mmol) in DCM were added to the resin and allowed to shake for 10 minutes. The resin was drained and rinsed with DCM (1x). NaBH(OAc)₃ (95 mg, 0.45 mmol) was added to the resin in 1:1 AcOH/DCM, shaken for 20 minutes, and the resin was washed with MeOH (1x), DMF (3x), and DCM (3x). A green chloranil/acetaldehyde test indicated the presence of a secondary amine. The acid chloride (0.60 mmol) and DIEA (261 μ L, 1.5 mmol) were added to the resin in DCM and shaken for 1.5 hours. The resin was washed with MeOH (1x), DMF (3x), and DCM (3x). A colorless chloranil/acetaldehyde test indicated the absence of free amine. The Fmoc-deprotection, reductive amination, and acid chloride addition sequence is repeated two more times, followed by a final Fmoc- deprotection. 4-Nitrophenylacetic acid (272 mg, 1.5 mmol) in DMF is added to the resin along with HATU (562 mg, 1.5 mmol), HOBt (227 mg, 1.5 mmol) and DIEA (600 μ L, 3.45 mmol) in DMF and shaken for 2 hours. The resin is washed with MeOH (1x), DMF (3x), and DCM (3x).

Resin cleavage: A solution of 10% TFA in DCM is added to resin and shaken for 10-15 minutes. The resin is drained into a clean flask and washed with DCM (3x). The resulting solution is evaporated under nitrogen and redissolved in a solution of 95% TFA/1% TES/DCM for 1 hour to deprotect all amino acid residues. The solvent is evaporated under nitrogen to produce an oil, which is divided among several eppendorf tubes (a minimal amount of DCM may be used to transfer the oil). Ether is added to each eppendorf to precipitate out product and the tubes are placed in dry ice for at least 10 minutes. The tubes are centrifuged and the ether layer is removed from the remaining pellets. The pellets are re-dissolved in a minimal amount of DCM and TFA and precipitated out of ether a second time. The combined ether layers are concentrated under nitrogen and re-dissolved in a minimal amount of DCM and TFA and any remaining product is precipitated out of ether. The pellets are all dissolved in water, combined, and purified via HPLC. In some instances, the N-acylated polyamines are hydrophobic and do not precipitate out of ether. The organic layers are then concentrated and dissolved in CH₃CN and purified via HPLC.

NAPA	Calculated Mass	Observed Mass
H2H2H2	1031.2	1031.2
H1H2K2	960.2	960.2
K1K2Y1	915.2	915.2
K2Y1H1	924.1	924.1
K2Y11	637.8	637.8
K2Y1	730.9	730.9
K2K2Y2	1039.3	1039.3
K3K2K2	956.3	956.3
K3Y2Y3	978.2	978.2
Y3K3Y2	978.2	978.2
Y3K2J3	914.2	914.2

3.8.4 Library synthesis (Note: All quantities given are the quantities per well. Each amount was scaled up for the appropriate number of wells in each plate.)

Resin preparation: TentGel NH₂ macrobeads (0.3 mmol/g loading) were divided into 96-well filter plates (300 μ L well capacity) with approximately 5 mg of resin per well and swelled in DMF (Note: It was necessary to blot the bottom of the plate on a paper towel after filtering solvent to prevent the following solvent from seeping straight through the filters). Fmoc- β -

homoalanine (0.0045 mmol) in DMF (125 μ L) was added to each well along with HATU (0.0045 mmol), HOBt (0.0045 mmol), and DIEA (0.01 mmol) in DMF (125 μ L). The plate was shaken for 3 hours. This process was repeated if necessary as indicated by the chloranil test. The wells were washed with MeOH (3x), DMF (3x), and DCM (3x) and kept in a dessicator until needed.

Plate Synthesis: Fmoc- β -homoalanine TentaGel resin was swelled in DMF. The Fmoc-protecting group was removed with 20% piperidine/DMF (200 μ L, 3 x 5 min.) and washed with DMF (3x) and DCM (3x). A red chloranil test from a random well indicated the presence of the primary amine. The first aldehyde (0.009 mmol) and TMOF (0.0375 mmol) were dissolved in DCM (200 μ L), added to the resin and shaken for 10 minutes. After draining the resin, NaBH(OAc)₃ (0.0075 mmol) in 1:1 AcOH/DCM (200 μ L) was added and shaken for 20 minutes. Additional NaBH(OAc)₃ in AcOH/DCM was added if the reagent drained before the completion of the reaction. The resin was washed with MeOH (3x), DMF (3x), and DCM (3x). A chloranil/acetaldehyde test from a random well indicated the presence of a secondary amine. The acid chloride (0.012 mmol) and DIEA (0.0225 mmol) in NMP (200 μ L) were added to the resin and shaken for 3 hours. This step was performed two times. The resin was washed with MeOH (3x), DMF (3x) and DCM (3x). A colorless chloranil/acetaldehyde test from a random well indicated the absence of free amine. The Fmoc-deprotection, reductive amination, and acid chloride addition sequence of procedures were repeated two more times as described, except with 0.015 mmol of aldehyde, followed with a final Fmoc-deprotection. 4-Nitrophenylacetic acid (0.015 mmol) in DMF (125 μ L) was added to the resin with HATU (0.015 mmol), HOBt (0.015 mmol), and DIEA (0.0345 mmol) in DMF (125 μ L) and shaken for 3 hours. The resin was washed with MeOH (3x), DMF (3x), and DCM (3x).

Resin deprotection: The plate was placed on a stack of paper towels and a solution of 95% TFA/DCM was added to the resin. This solution proceeded to seep directly through the wells and had to be added continuously to empty wells for up to 30 minutes. The resin was washed thoroughly with DCM (10x), allowed to dry, and stored in a dessicator.

3.8.5 Library screen

A few beads from each well were transferred to a 384-well filter plate and swelled in 1X PBS.

Blocking: 2% BSA in 1X PBS (50 μ L) was added to each well and incubated at 4 °C for 4 hours. The resin was drained and washed with 1X PBS (3 x 50 μ L) followed by a wash with the protein buffer (water, 1X PBS, or 1X TBS).

Protein addition: (Note: Protein concentrations and incubation times varied depending on the protein. Listed here is the standard procedure.) Biotinylated-protein in the appropriate buffer (water, 1X PBS, or 1X TBS) + 0.1% Tween-20 (25 μ L) was added to each well and incubated at room temp. with shaking for 2 hours. The resin was washed with the protein buffer (3 x 50 μ L) followed by a wash with 1X TBS (50 μ L). Buffer only + 0.1% Tween-20 (25 μ L) was added to the controls in place of protein.

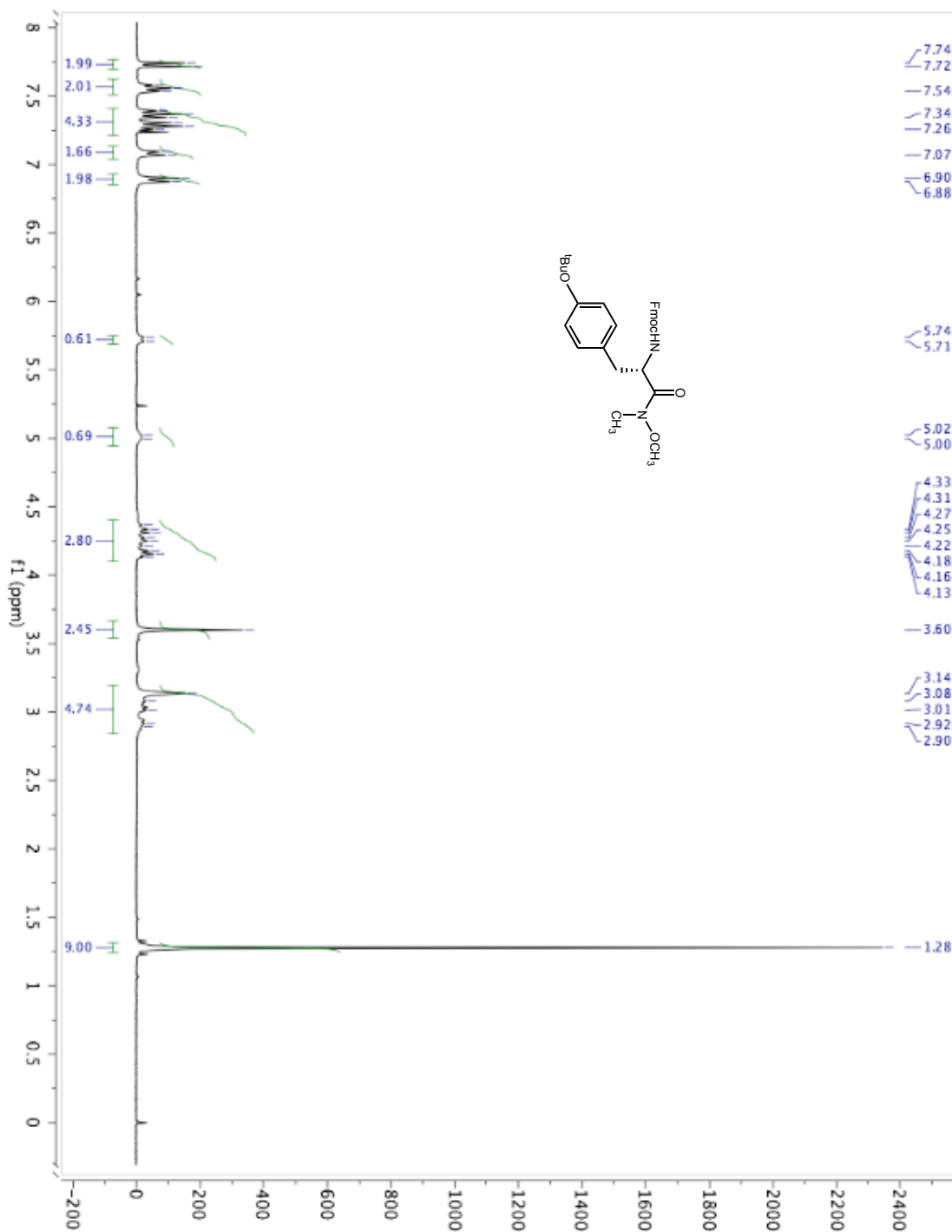
Qdots: 50 nM of streptavidin-Qdot605 in 1X TBS (20 μ L) were added to each well and incubated at room temp. with shaking for 30 minutes. The resin was washed thoroughly with 1X TBS (7-10 x 50 μ L). The library was then visualized using a fluorescent microscope equipped with a triple bandpass filter. Beads that appeared red or orange under the microscope were selected for synthetic scale-up while those that were green were disregarded.

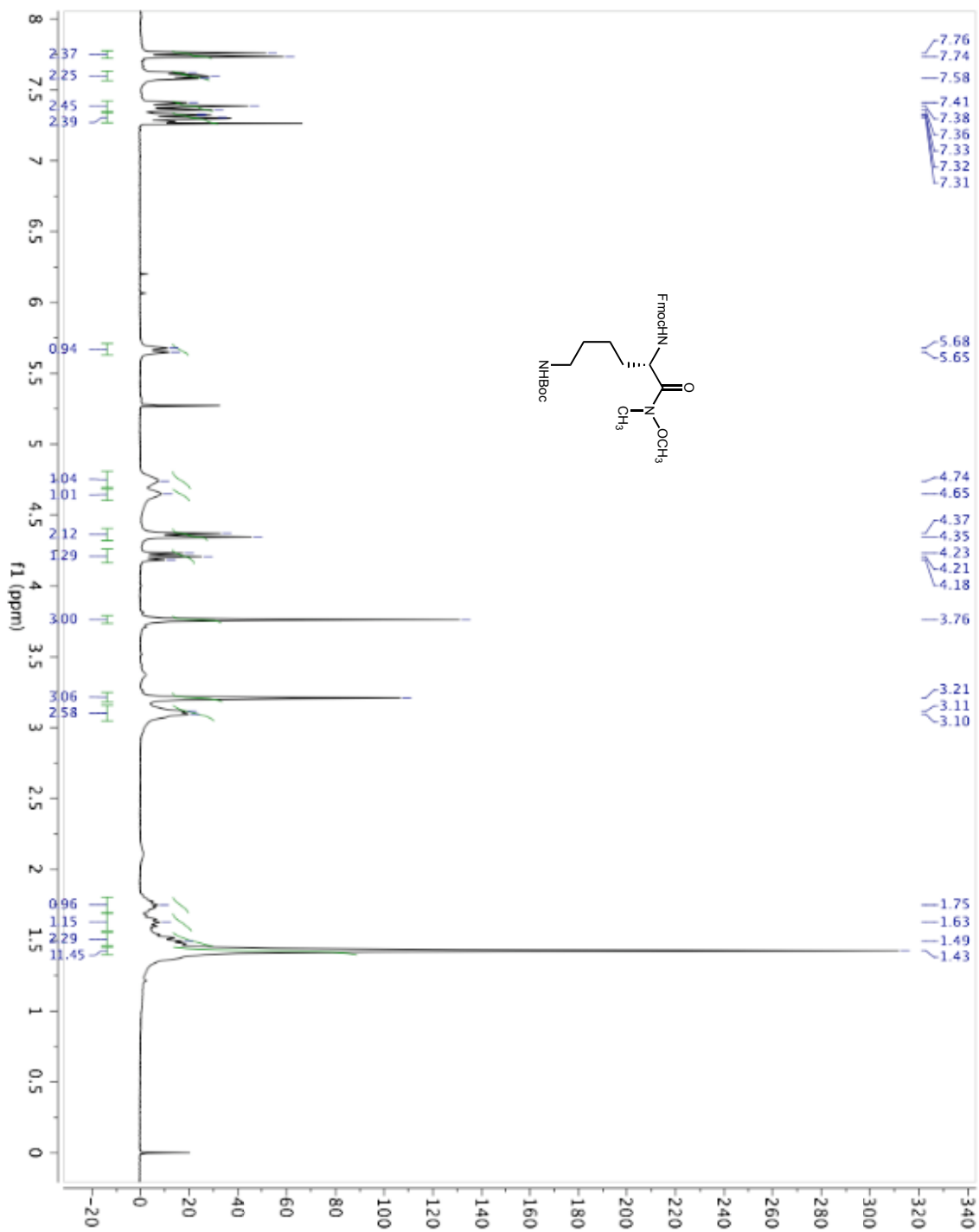
3.8.6 Biacore binding assay

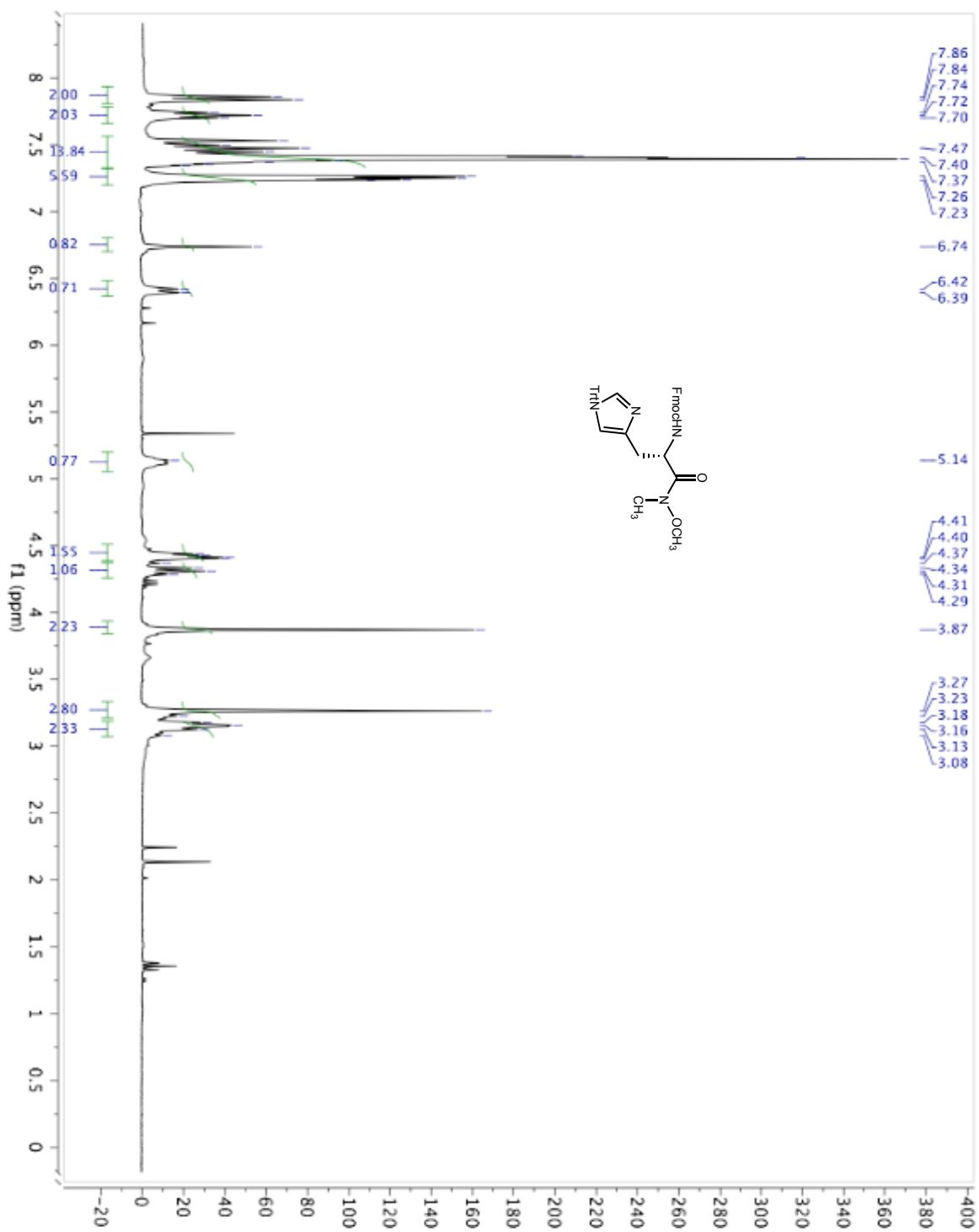
300 μL of biotinylated Vpr (1 μM in water) were plated onto a streptavidin coated gold sensor chip. 200 μL of K2K2Y2 (100 μM) in water was used for initial binding studies. To eliminate non-specific interactions, solutions of 50 μM K2K2Y2 were made with the following buffers: 1X PBS + 0.05% P-20, 1X HEPES + 0.05% P-20, 25 mM Tris + 150 mM NaCl + 0.05 % P-20, and 25 mM NaOAc + 150 mM NaCl + 0.05% P-20. Additional binding studies were done with 50 μM of K2K2Y2 in water and either 0.05% P-20 or 0.005% P-20. After determining K2K2Y2 in 1X PBS + 0.05% P-20 eliminated most non-specific interactions, a kinetics experiment was run using K2K2Y2 in 1X PBS + 0.05% P-20 at the following dilutions: 100 μM , 50 μM , 25 μM , 6.25 μM , 13.13 μM , 1.56 μM , 0.78 μM , 0.39 μM , and 0 μM . The K_D was found to be between 15 and 60 μM .

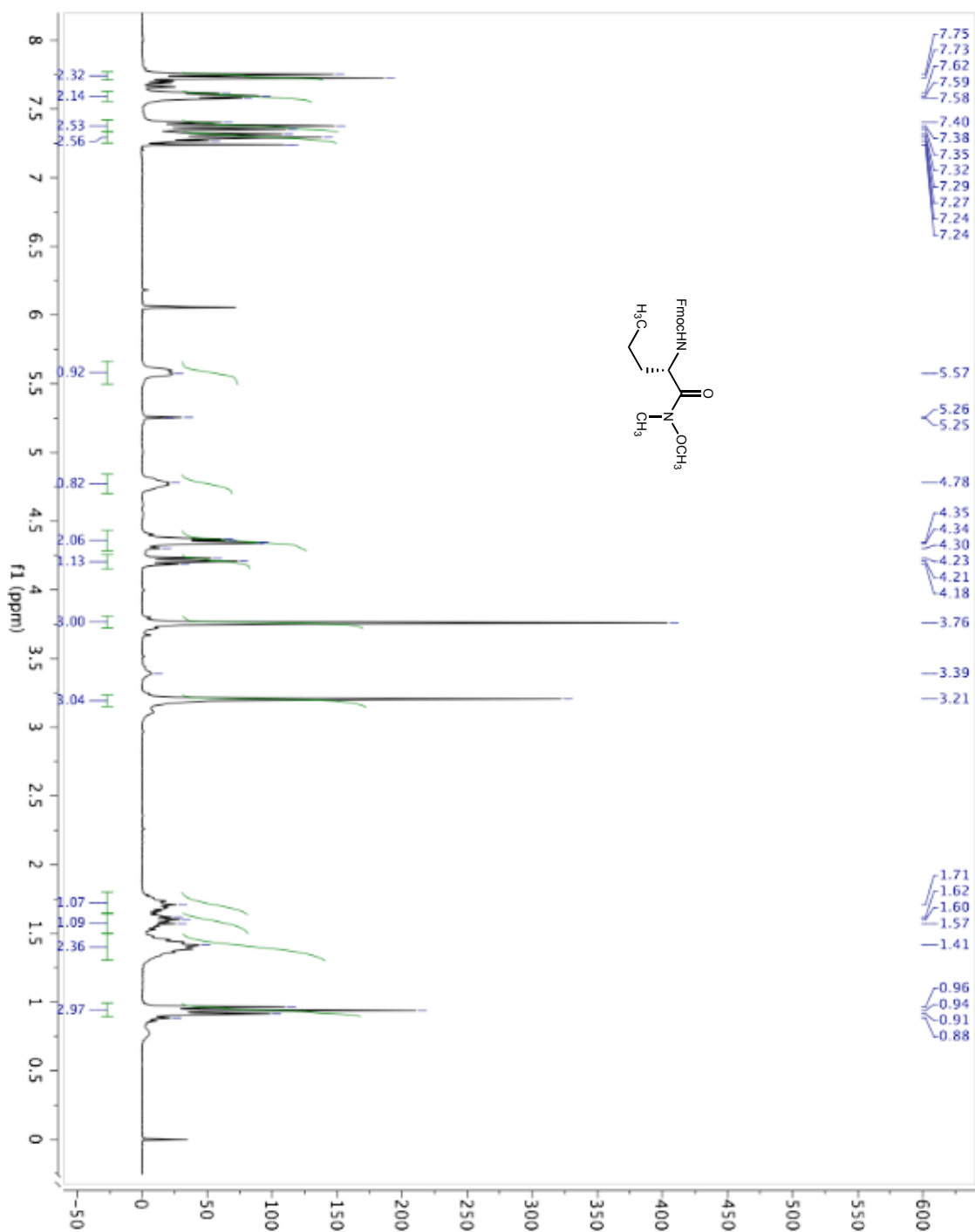
3.8.7 Isothermal Titration Calorimetry

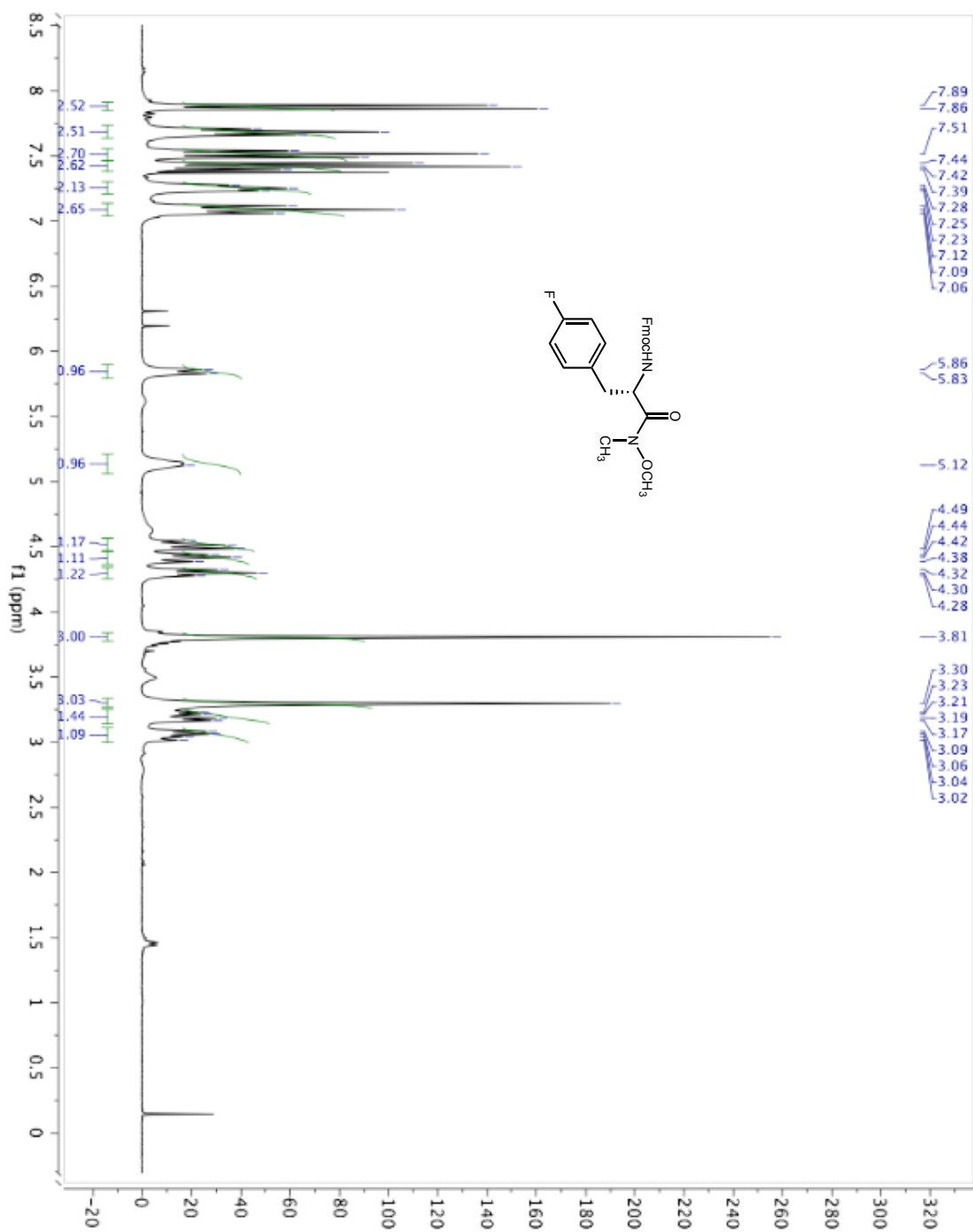
A 10 μM solution of Vpr in 10 mM Tris buffer (pH 7.4) and a 100 μM solution of K2K2Y2 in 10 mM Tris buffer (pH 7.4) were prepared. ITC was performed with 26 injections of 10 μL of ligand at 25 $^\circ\text{C}$ with 240 seconds between injections. Very small peaks were observed to indicate some binding, but an accurate binding constant could not be determined. The experiment was repeated a second time with 1000 μM Vpr following the same procedure. More pronounced peaks were observed and binding constant of approximately 25 μM was determined.

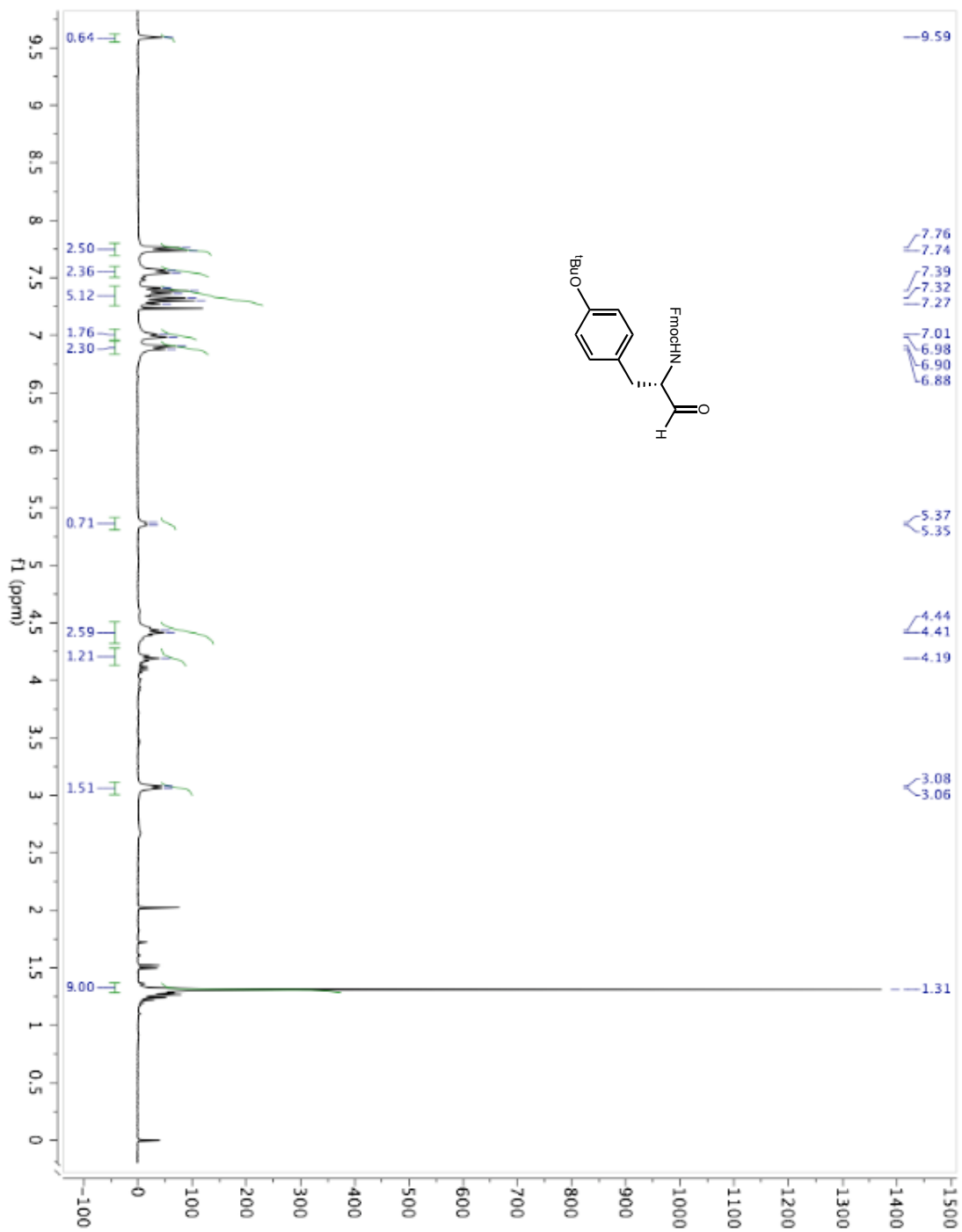
3.8.8 $^1\text{H-NMRs}$ 

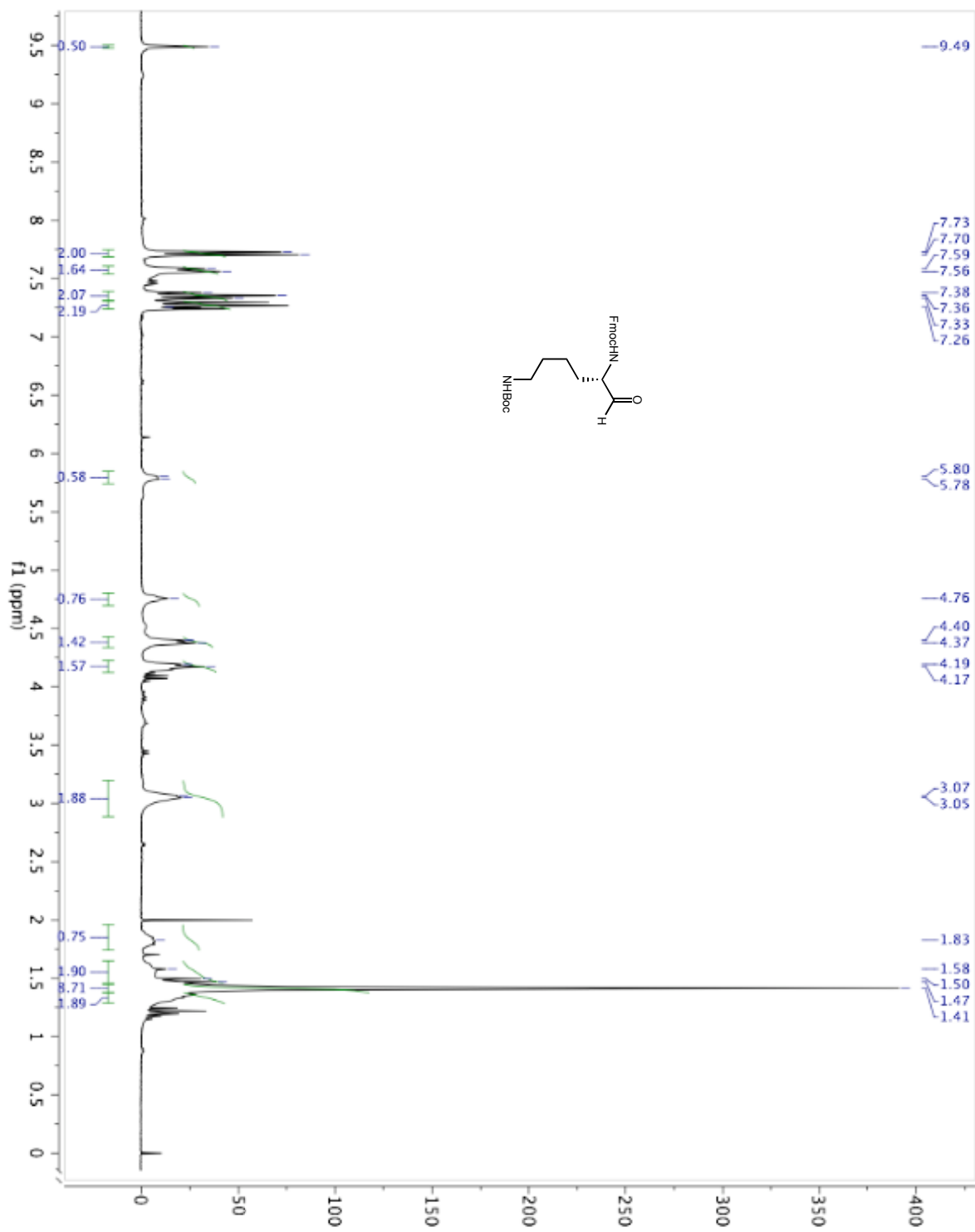


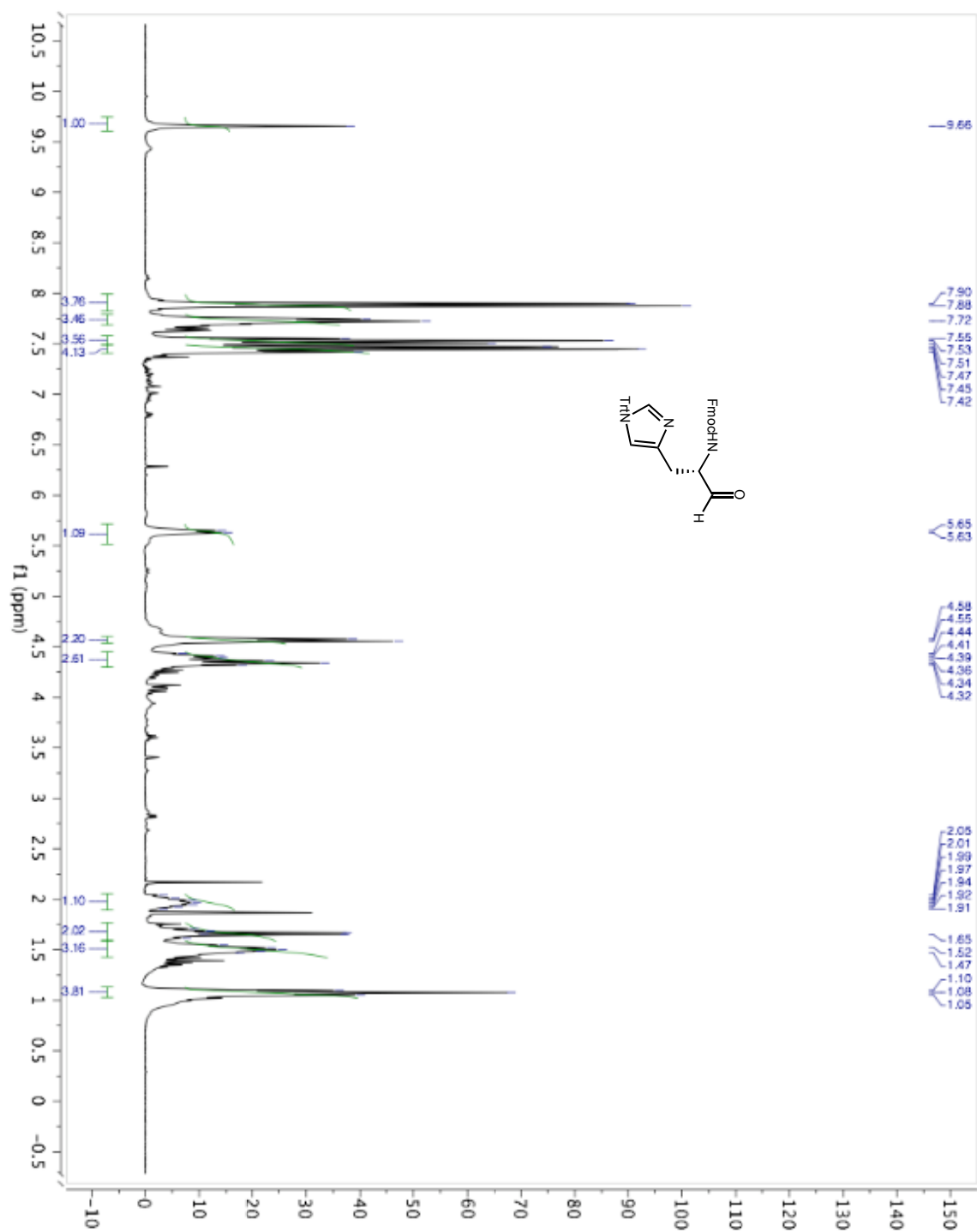


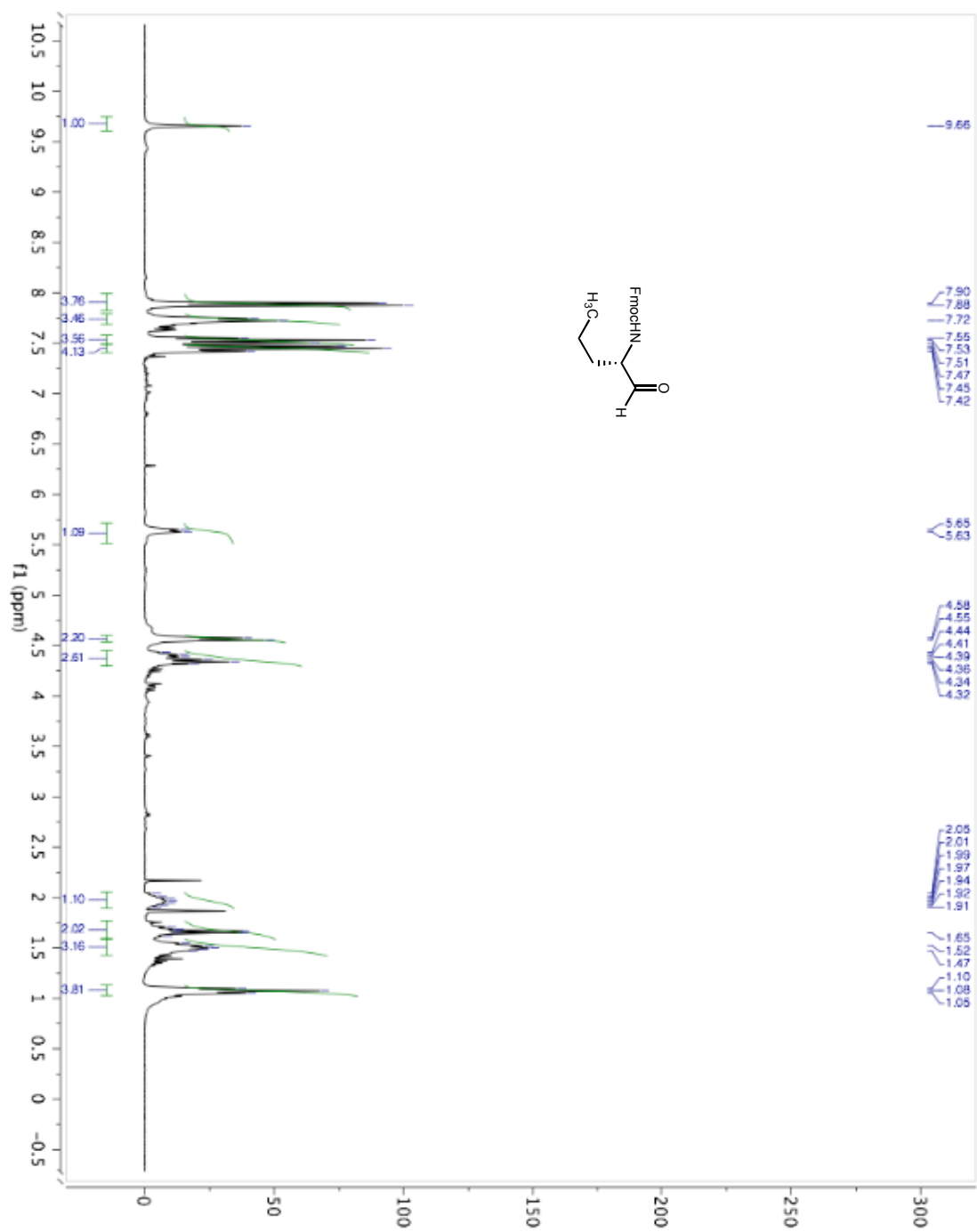


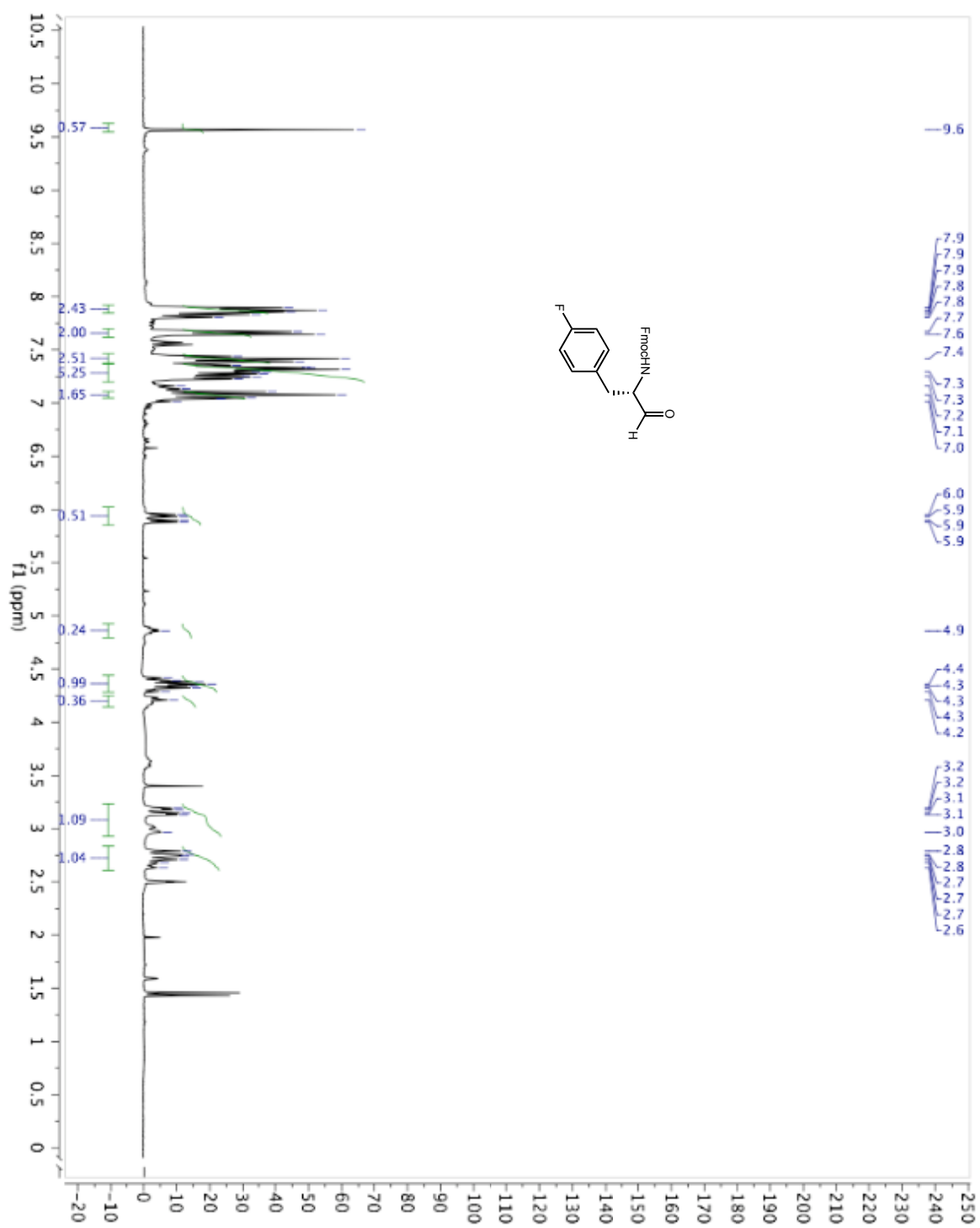












Chapter 1 References

1. DeLeo, A. B.; Jay, G.; Appella, E.; Dubois, G. C.; Law, L. W.; Old, L. J., Detection of a transformation-related antigen in chemically induced sarcomas and other transformed cells of the mouse. *Proc. Natl. Acad. Sci. U. S. A.* **1979**, 76, (5), 2420-4.
2. Lane, D. P.; Crawford, L. V., T antigen is bound to a host protein in SV40-transformed cells. *Nature* **1979**, 278, (5701), 261-3.
3. Linzer, D. I.; Levine, A. J., Characterization of a 54K dalton cellular SV40 tumor antigen present in SV40-transformed cells and uninfected embryonal carcinoma cells. *Cell* **1979**, 17, (1), 43-52.
4. Polyak, K.; Xia, Y.; Zweier, J. L.; Kinzler, K. W.; Vogelstein, B., A model for p53-induced apoptosis. *Nature* **1997**, 389, (6648), 300-5.
5. Vogelstein, B.; Lane, D.; Levine, A. J., Surfing the p53 network. *Nature* **2000**, 408, (6810), 307-10.
6. Zhao, R.; Gish, K.; Murphy, M.; Yin, Y.; Notterman, D.; Hoffman, W. H.; Tom, E.; Mack, D. H.; Levine, A. J., Analysis of p53-regulated gene expression patterns using oligonucleotide arrays. *Genes Dev.* **2000**, 14, (8), 981-93.
7. Lane, D. P., Cancer. p53, guardian of the genome. *Nature* **1992**, 358, (6381), 15-6.
8. Kubbutat, M. H.; Jones, S. N.; Vousden, K. H., Regulation of p53 stability by Mdm2. *Nature* **1997**, 387, (6630), 299-303.
9. Haupt, Y.; Maya, R.; Kazaz, A.; Oren, M., Mdm2 promotes the rapid degradation of p53. *Nature* **1997**, 387, (6630), 296-9.
10. de Rozières, S.; Maya, R.; Oren, M.; Lozano, G., The loss of mdm2 induces p53-mediated apoptosis. *Oncogene* **2000**, 19, (13), 1691-7.
11. Garcia-Echeverria, C.; Chene, P.; Blommers, M. J.; Furet, P., Discovery of potent antagonists of the interaction between human double minute 2 and tumor suppressor p53. *J. Med. Chem.* **2000**, 43, (17), 3205-8.

12. Duncan, S. J.; Gruschow, S.; Williams, D. H.; McNicholas, C.; Purewal, R.; Hajek, M.; Gerlitz, M.; Martin, S.; Wrigley, S. K.; Moore, M., Isolation and structure elucidation of Chlorofusin, a novel p53-MDM2 antagonist from a *Fusarium* sp. *J. Am. Chem. Soc.* **2001**, 123, (4), 554-60.
13. Yin, H.; Lee, G. I.; Park, H. S.; Payne, G. A.; Rodriguez, J. M.; Sebti, S. M.; Hamilton, A. D., Terphenyl-based helical mimetics that disrupt the p53/HDM2 interaction. *Angew. Chem. Int. Ed. Engl.* **2005**, 44, (18), 2704-7.
14. Vassilev, L. T.; Vu, B. T.; Graves, B.; Carvajal, D.; Podlaski, F.; Filipovic, Z.; Kong, N.; Kammlott, U.; Lukacs, C.; Klein, C.; Fotouhi, N.; Liu, E. A., In vivo activation of the p53 pathway by small-molecule antagonists of MDM2. *Science* **2004**, 303, (5659), 844-8.
15. Hara, T.; Durell, S. R.; Myers, M. C.; Appella, D. H., Probing the structural requirements of peptoids that inhibit HDM2-p53 interactions. *J. Am. Chem. Soc.* **2006**, 128, (6), 1995-2004.
16. Dudkina, A. S.; Lindsley, C. W., Small molecule protein-protein inhibitors for the p53-MDM2 interaction. *Curr. Top. Med. Chem.* **2007**, 7, (10), 952-60.
17. Hollstein, M.; Sidransky, D.; Vogelstein, B.; Harris, C. C., p53 mutations in human cancers. *Science* **1991**, 253, (5015), 49-53.
18. Cho, Y.; Gorina, S.; Jeffrey, P. D.; Pavletich, N. P., Crystal structure of a p53 tumor suppressor-DNA complex: understanding tumorigenic mutations. *Science* **1994**, 265, (5170), 346-55.
19. Clore, G. M.; Omichinski, J. G.; Sakaguchi, K.; Zambrano, N.; Sakamoto, H.; Appella, E.; Gronenborn, A. M., High-resolution structure of the oligomerization domain of p53 by multidimensional NMR. *Science* **1994**, 265, (5170), 386-91.
20. Okorokov, A. L.; Sherman, M. B.; Plisson, C.; Grinkevich, V.; Sigmundsson, K.; Selivanova, G.; Milner, J.; Orlova, E. V., The structure of p53 tumour suppressor protein reveals the basis for its functional plasticity. *Embo. J.* **2006**, 25, (21), 5191-200.
21. el-Deiry, W. S.; Kern, S. E.; Pietenpol, J. A.; Kinzler, K. W.; Vogelstein, B., Definition of a consensus binding site for p53. *Nat. Genet.* **1992**, 1, (1), 45-9.

22. Bullock, A. N.; Fersht, A. R., Rescuing the function of mutant p53. *Nat. Rev. Cancer* **2001**, 1, (1), 68-76.
23. Romer, L.; Klein, C.; Dehner, A.; Kessler, H.; Buchner, J., p53 - A natural cancer killer: Structural insights and therapeutic concepts. *Angew. Chem. Int. Ed. Engl.* **2006**, 45, (39), 6440-60.
24. Orgad, S.; Goldfinger, N.; Cohen, G.; Rotter, V.; Solomon, B., Single chain antibody against the common epitope of mutant p53 restores wild-type activity to mutant p53 protein. *FEBS Lett.* **2005**, 579, (25), 5609-15.
25. Selivanova, G.; Ryabchenko, L.; Jansson, E.; Iotsova, V.; Wiman, K. G., Reactivation of mutant p53 through interaction of a C-terminal peptide with the core domain. *Mol. Cell. Biol.* **1999**, 19, (5), 3395-402.
26. Foster, B. A.; Coffey, H. A.; Morin, M. J.; Rastinejad, F., Pharmacological rescue of mutant p53 conformation and function. *Science* **1999**, 286, (5449), 2507-10.
27. Rippin, T. M.; Bykov, V. J.; Freund, S. M.; Selivanova, G.; Wiman, K. G.; Fersht, A. R., Characterization of the p53-rescue drug CP-31398 in vitro and in living cells. *Oncogene* **2002**, 21, (14), 2119-29.
28. Bykov, V. J.; Issaeva, N.; Shilov, A.; Hultcrantz, M.; Pugacheva, E.; Chumakov, P.; Bergman, J.; Wiman, K. G.; Selivanova, G., Restoration of the tumor suppressor function to mutant p53 by a low-molecular-weight compound. *Nat. Med.* **2002**, 8, (3), 282-8.
29. Bykov, V. J.; Issaeva, N.; Zache, N.; Shilov, A.; Hultcrantz, M.; Bergman, J.; Selivanova, G.; Wiman, K. G., Reactivation of mutant p53 and induction of apoptosis in human tumor cells by maleimide analogs. *J. Biol. Chem.* **2005**, 280, (34), 30384-91.
30. Myers, M. C.; Wang, J.; Iera, J. A.; Bang, J. K.; Hara, T.; Saito, S.; Zambetti, G. P.; Appella, D. H., A new family of small molecules to probe the reactivation of mutant p53. *J. Am. Chem. Soc.* **2005**, 127, (17), 6152-3.
31. Peng, Y.; Li, C.; Chen, L.; Sebt, S.; Chen, J., Rescue of mutant p53 transcription function by ellipticine. *Oncogene* **2003**, 22, (29), 4478-87.

32. Wang, P. L.; Sait, F.; Winter, G., The 'wildtype' conformation of p53: epitope mapping using hybrid proteins. *Oncogene* **2001**, 20, (18), 2318-24.
33. Joerger, A. C.; Fersht, A. R., Structure-function-rescue: the diverse nature of common p53 cancer mutants. *Oncogene* **2007**, 26, (15), 2226-42.
34. Englund, E. A.; Gopi, H. N.; Appella, D. H., An efficient synthesis of a probe for protein function: 2,3-diaminopropionic acid with orthogonal protecting groups. *Org. Lett.* **2004**, 6, (2), 213-5.
35. Spino, C.; Joly, M. A.; Godbout, C.; Arbour, M., Ti-catalyzed reactions of hindered isocyanates with alcohols. *J. Org. Chem.* **2005**, 70, (15), 6118-21.

Chapter 2 References

1. Hermann, T.; Tor, Y., RNA as a target for small-molecule therapeutics. *Expert Opin. Ther. Patents* **2005**, 15, (1), 49-62.
2. Tor, Y., RNA and the small molecule world. *Angew. Chem. Int. Ed. Engl.* **1999**, 38, (11), 1579-82.
3. Batey, R. T.; Rambo, R. P.; Doudna, J. A., Tertiary Motifs in RNA Structure and Folding. *Angew. Chem. Int. Ed. Engl.* **1999**, 38, 2326-43.
4. Berkhout, B.; Jeang, K. T., trans activation of human immunodeficiency virus type 1 is sequence specific for both the single-stranded bulge and loop of the trans-acting-responsive hairpin: a quantitative analysis. *J. Virol.* **1989**, 63, (12), 5501-4.
5. Berkhout, B.; Silverman, R. H.; Jeang, K. T., Tat trans-activates the human immunodeficiency virus through a nascent RNA target. *Cell* **1989**, 59, (2), 273-82.
6. Bannwarth, S.; Gatignol, A., HIV-1 TAR RNA: the target of molecular interactions between the virus and its host. *Curr. HIV Res.* **2005**, 3, (1), 61-71.
7. Sharp, P. A.; Marciniak, R. A., HIV TAR: an RNA enhancer? *Cell* **1989**, 59, (2), 229-30.
8. Rana, T. M.; Jeang, K. T., Biochemical and functional interactions between HIV-1 Tat protein and TAR RNA. *Arch. Biochem. Biophys.* **1999**, 365, (2), 175-85.
9. Fulcher, A. J.; Jans, D. A., The HIV-1 Tat transactivator protein: a therapeutic target? *IUBMB Life* **2003**, 55, (12), 669-80.
10. Hwang, S.; Tamilarasu, N.; Kibler, K.; Cao, H.; Ali, A.; Ping, Y. H.; Jeang, K. T.; Rana, T. M., Discovery of a small molecule Tat-trans-activation-responsive RNA antagonist that potently inhibits human immunodeficiency virus-1 replication. *J. Biol. Chem.* **2003**, 278, (40), 39092-103.
11. Emerman, M.; Malim, M. H., HIV-1 Regulatory/Accessory Genes: Keys to Unraveling Viral and Host Cell Biology. *Science* **1998**, 280, 1880-4.

12. Richter, S. N.; Palu, G., Inhibitors of HIV-1 Tat-mediated transactivation. *Curr. Med. Chem.* **2006**, 13, (11), 1305-15.
13. Ptak, R. G., HIV-1 regulatory proteins: targets for novel drug development. *Expert Opin. Investig. Drugs.* **2002**, 11, (8), 1099-115.
14. Wang, D.; de la Fuente, C.; Deng, L.; Wang, L.; Zilberman, I.; Eadie, C.; Healey, M.; Stein, D.; Denny, T.; Harrison, L. E.; Meijer, L.; Kashanchi, F., Inhibition of human immunodeficiency virus type 1 transcription by chemical cyclin-dependent kinase inhibitors. *J. Virol.* **2001**, 75, (16), 7266-79.
15. Baba, M.; Okamoto, M.; Makino, M.; Kimura, Y.; Ikeuchi, T.; Sakaguchi, T.; Okamoto, T., Potent and selective inhibition of human immunodeficiency virus type 1 transcription by piperazinyloxoquinoline derivatives. *Antimicrob. Agents Chemother.* **1997**, 41, (6), 1250-5.
16. Baba, M.; Okamoto, M.; Kawamura, M.; Makino, M.; Higashida, T.; Takashi, T.; Kimura, Y.; Ikeuchi, T.; Tetsuka, T.; Okamoto, T., Inhibition of human immunodeficiency virus type 1 replication and cytokine production by fluoroquinoline derivatives. *Mol. Pharmacol.* **1998**, 53, (6), 1097-103.
17. Hsu, M. C.; Dhingra, U.; Earley, J. V.; Holly, M.; Keith, D.; Nalin, C. M.; Richou, A. R.; Schutt, A. D.; Tam, S. Y.; Potash, M. J.; et al., Inhibition of type 1 human immunodeficiency virus replication by a tat antagonist to which the virus remains sensitive after prolonged exposure in vitro. *Proc. Natl. Acad. Sci. U. S. A.* **1993**, 90, (14), 6395-9.
18. Haubrich, R. H.; Flexner, C.; Lederman, M. M.; Hirsch, M.; Pettinelli, C. P.; Ginsberg, R.; Lietman, P.; Hamzeh, F. M.; Spector, S. A.; Richman, D. D.; The AIDS Clinical Trials Group 213 Team, A randomized trial of the activity and safety of Ro 24-7429 (Tat antagonist) versus nucleoside for human immunodeficiency virus infection. *J. Infect. Dis.* **1995**, 172, (5), 1246-52.
19. Krebs, A.; Ludwig, V.; Boden, O.; Gobel, M. W., Targeting the HIV trans-activation responsive region--approaches towards RNA-binding drugs. *ChemBiochem* **2003**, 4, (10), 972-8.
20. Yang, M., Discoveries of Tat-TAR interaction inhibitors for HIV-1. *Curr. Drug. Targets Infect. Disord.* **2005**, 5, (4), 433-44.
21. Calnan, B. J.; Tidor, B.; Biancalana, S.; Hudson, D.; Frankel, A. D., Arginine-mediated RNA recognition: the arginine fork. *Science* **1991**, 252, (5010), 1167-71.

22. Hamy, F.; Felder, E. R.; Heizmann, G.; Lazdins, J.; Aboul-ela, F.; Varani, G.; Karn, J.; Klimkait, T., An inhibitor of the Tat/TAR RNA interaction that effectively suppresses HIV-1 replication. *Proc. Natl. Acad. Sci. U. S. A.* **1997**, *94*, (8), 3548-53.
23. Hwang, S.; Tamilarasu, N.; Ryan, K.; Huq, I.; Richter, S.; Still, W. C.; Rana, T. M., Inhibition of gene expression in human cells through small molecule-RNA interactions. *Proc. Natl. Acad. Sci. U. S. A.* **1999**, *96*, (23), 12997-3002.
24. Tamilarasu, N.; Huq, I.; Rana, T. M., Design, synthesis, and biological activity of a cyclic peptide: An inhibitor of HIV-1 Tat-TAR interactions in human cells. *Bioorg. Med. Chem. Lett.* **2000**, *10*, (9), 971-974.
25. Peytou, V.; Condom, R.; Patino, N.; Guedj, R.; Aubertin, A. M.; Gelus, N.; Bailly, C.; Terreux, R.; Cabrol-Bass, D., Synthesis and antiviral activity of ethidium-arginine conjugates directed against the TAR RNA of HIV-1. *J. Med. Chem.* **1999**, *42*, (20), 4042-53.
26. Yu, X.; Lin, W.; Li, J.; Yang, M., Synthesis and biological evaluation of novel beta-carboline derivatives as Tat-TAR interaction inhibitors. *Bioorg. Med. Chem. Lett.* **2004**, *14*, (12), 3127-30.
27. Litovchick, A.; Lapidot, A.; Eisenstein, M.; Kalinkovich, A.; Borkow, G., Neomycin B-arginine conjugate, a novel HIV-1 Tat antagonist: synthesis and anti-HIV activities. *Biochemistry* **2001**, *40*, (51), 15612-23.
28. Cecchetti, V.; Parolin, C.; Moro, S.; Pecere, T.; Filipponi, E.; Calistri, A.; Tabarrini, O.; Gatto, B.; Palumbo, M.; Fravolini, A.; Palu, G., 6-Aminoquinolones as new potential anti-HIV agents. *J. Med. Chem.* **2000**, *43*, (20), 3799-802.
29. Parolin, C.; Gatto, B.; Del Vecchio, C.; Pecere, T.; Tramontano, E.; Cecchetti, V.; Fravolini, A.; Masiero, S.; Palumbo, M.; Palu, G., New Anti-Human Immunodeficiency Virus Type 1 6-Aminoquinolones: Mechanism of Action. *Antimicrob. Agents Chemother.* **2003**, *47*, (3), 889-96.
30. MEI, H. Y.; Galan, A. A.; Halim, N. S.; Mack, D. P.; Moreland, D. W.; Sanders, K. B.; Truong, H. N.; Czarnik, A. W., Inhibition of an Hiv-1 Tat-Derived Peptide Binding to Tar Rna by Aminoglycoside Antibiotics. *Bioorg. Med. Chem. Lett.* **1995**, *5*, (22), 2755-60.

31. Hendrix, M.; Priestly, E. S.; Joyce, G. F.; Wong, C.-H., Direct Observation of Aminoglycoside-RNA Interactions by Surface Plasmon Resonance. *J. Am. Chem. Soc.* **1997**, *119*, 3641-8.
32. Alper, P. B.; Hendrix, M.; Sears, P.; Wong, C.-H., Probing the Specificity of Aminoglycoside-Ribosomal RNA Interactions with Designed Synthetic Analogs. *J. Am. Chem. Soc.* **1998**, *120*, 1965-78.
33. Riguet, E.; Tripathi, S.; Chaubey, B.; Desire, J.; Pandey, V. N.; Decout, J. L., A peptide nucleic acid-neamine conjugate that targets and cleaves HIV-1 TAR RNA inhibits viral replication. *J. Med. Chem.* **2004**, *47*, (20), 4806-9.
34. Riguet, E.; Desire, J.; Boden, O.; Ludwig, V.; Gobel, M.; Bailly, C.; Decout, J. L., Neamine dimers targeting the HIV-1 TAR RNA. *Bioorg. Med. Chem. Lett.* **2005**, *15*, (21), 4651-4655.
35. Ludwig, V.; Krebs, A.; Stoll, M.; Dietrich, U.; Ferner, J.; Schwalbe, H.; Scheffer, U.; Durner, G.; Gobel, M. W., Tripeptides from synthetic amino acids block the Tat-TAR association and slow down HIV spread in cell cultures. *Chembiochem* **2007**, *8*, (15), 1850-6.
36. Lee, Y.; Hyun, S.; Kim, H. J.; Yu, J., Amphiphilic helical peptides containing two acridine moieties display picomolar affinity toward HIV-1 RRE and TAR. *Angew. Chem. Int. Ed. Engl.* **2008**, *47*, (1), 134-7.
37. Lawton, G. R.; Appella, D. H., Nonionic side chains modulate the affinity and specificity of binding between functionalized polyamines and structured RNA. *J. Am. Chem. Soc.* **2004**, *126*, (40), 12762-3.
38. Wen, J. J.; Crews, C. M., Synthesis of 9-fluorenylmethoxycarbonyl-protected amino aldehydes. *Tetrahedron-Asymmetry* **1998**, *9*, (11), 1855-8.
39. Wang, G.; Mahesh, U.; Chen, G. Y. J.; Yao, S. Q., Solid-phase synthesis of peptide vinyl sulfones as potential inhibitors and activity-based probes of cysteine proteases. *Org. Lett.* **2003**, *5*, (5), 737-40.
40. Baxter, E. W.; Reitz, A. G., Reductive aminations of carbonyl compounds with borohydride and borane reducing agents. In *Organic Reactions*, Overman, L. E., Ed. John Wiley and Sons: 2002; Vol. 59.

41. Gribble, G. W.; Lord, P. D.; Skotnick, J.; Dietz, S. E.; Eaton, J. T.; Johnson, J. L., Reactions of Sodium-Borohydride in Acidic Media .1. Reduction of Indoles and Alkylation of Aromatic-Amines with Carboxylic-Acids. *J. Am. Chem. Soc.* **1974**, *96*, (25), 7812-4.
42. Gribble, G. W., A reduction powerhouse. *Chemtech* **1996**, *26*, (12), 26-31.
43. AbdelMagid, A. F.; Carson, K. G.; Harris, B. D.; Maryanoff, C. A.; Shah, R. D., Reductive amination of aldehydes and ketones with sodium triacetoxyborohydride. Studies on direct and indirect reductive amination procedures. *J. Org. Chem.* **1996**, *61*, (11), 3849-62.
44. Varani, G.; Calnan, B. J.; Leroy, J. L., Opening Mechanism of G·T/U Pairs in DNA and RNA Duplexes: A Combined Study of Imino Proton Exchange and Molecular Dynamics Simulation. *J. Am. Chem. Soc.* **2004**, *126*, 14659-67.
45. Fillon, Y. A.; Anderson, J. P.; Chmielewski, J., Cell penetrating agents based on a polyproline helix scaffold. *J. Am. Chem. Soc.* **2005**, *127*, (33), 11798-803.
46. Li, L.; Kracht, J.; Peng, S.; Bernhardt, G.; Elz, S.; Buschauer, A., Synthesis and pharmacological activity of fluorescent histamine H2 receptor antagonists related to potentidine. *Bioorg. Med. Chem. Lett.* **2003**, *13*, (10), 1717-20.
47. Pauwels, R.; De Clercq, E.; Desmyter, J.; Balzarini, J.; Goubau, P.; Herdewijn, P.; Vanderhaeghe, H.; Vandeputte, M., Sensitive and rapid assay on MT-4 cells for detection of antiviral compounds against the AIDS virus. *J. Virol. Methods* **1987**, *16*, (3), 171-85.
48. Pauwels, R.; Balzarini, J.; Baba, M.; Snoeck, R.; Schols, D.; Herdewijn, P.; Desmyter, J.; De Clercq, E., Rapid and automated tetrazolium-based colorimetric assay for the detection of anti-HIV compounds. *J. Virol. Methods* **1988**, *20*, (4), 309-21.
49. Hertogs, K.; de Bethune, M. P.; Miller, V.; Ivens, T.; Schel, P.; Van Cauwenberge, A.; Van Den Eynde, C.; Van Gerwen, V.; Azijn, H.; Van Houtte, M.; Peeters, F.; Staszewski, S.; Conant, M.; Bloor, S.; Kemp, S.; Larder, B.; Pauwels, R., A rapid method for simultaneous detection of phenotypic resistance to inhibitors of protease and reverse transcriptase in recombinant human immunodeficiency virus type 1 isolates from patients treated with antiretroviral drugs. *Antimicrob. Agents Chemother.* **1998**, *42*, (2), 269-76.
50. Pauwels, R., Aspects of successful drug discovery and development. *Antiviral. Res.* **2006**, *71*, (2-3), 77-89.

51. Jeeninga, R. E.; Hoogenkamp, M.; Armand-Ugon, M.; de Baar, M.; Verhoef, K.; Berkhout, B., Functional differences between the long terminal repeat transcriptional promoters of human immunodeficiency virus type 1 subtypes A through G. *J. Virol.* **2000**, 74, (8), 3740-51.

Chapter 3 References

1. Yin, H.; Hamilton, A. D., Strategies for targeting protein-protein interactions with synthetic agents. *Angew. Chem. Int. Ed. Engl.* **2005**, *44*, (27), 4130-63.
2. Fry, D. C.; Vassilev, L. T., Targeting protein-protein interactions for cancer therapy. *J. Mol. Med.* **2005**, *83*, (12), 955-63.
3. Haupt, Y.; Maya, R.; Kazaz, A.; Oren, M., Mdm2 promotes the rapid degradation of p53. *Nature* **1997**, *387*, (6630), 296-9.
4. Kussie, P. H.; Gorina, S.; Marechal, V.; Elenbaas, B.; Moreau, J.; Levine, A. J.; Pavletich, N. P., Structure of the MDM2 oncoprotein bound to the p53 tumor suppressor transactivation domain. *Science* **1996**, *274*, (5289), 948-53.
5. Vassilev, L. T.; Vu, B. T.; Graves, B.; Carvajal, D.; Podlaski, F.; Filipovic, Z.; Kong, N.; Kammlott, U.; Lukacs, C.; Klein, C.; Fotouhi, N.; Liu, E. A., In vivo activation of the p53 pathway by small-molecule antagonists of MDM2. *Science* **2004**, *303*, (5659), 844-8.
6. Shangary, S.; Qin, D.; McEachern, D.; Liu, M.; Miller, R. S.; Qiu, S.; Nikolovska-Coleska, Z.; Ding, K.; Wang, G.; Chen, J.; Bernard, D.; Zhang, J.; Lu, Y.; Gu, Q.; Shah, R. B.; Pienta, K. J.; Ling, X.; Kang, S.; Guo, M.; Sun, Y.; Yang, D.; Wang, S., Temporal activation of p53 by a specific MDM2 inhibitor is selectively toxic to tumors and leads to complete tumor growth inhibition. *Proc. Natl. Acad. Sci. U. S. A.* **2008**, *105*, (10), 3933-8.
7. Yin, H.; Lee, G. I.; Park, H. S.; Payne, G. A.; Rodriguez, J. M.; Sebti, S. M.; Hamilton, A. D., Terphenyl-based helical mimetics that disrupt the p53/HDM2 interaction. *Angew. Chem. Int. Ed. Engl.* **2005**, *44*, (18), 2704-7.
8. Yin, H.; Lee, G. I.; Sedey, K. A.; Kutzki, O.; Park, H. S.; Orner, B. P.; Ernst, J. T.; Wang, H. G.; Sebti, S. M.; Hamilton, A. D., Terphenyl-Based Bak BH3 alpha-helical proteomimetics as low-molecular-weight antagonists of Bcl-xL. *J. Am. Chem. Soc.* **2005**, *127*, (29), 10191-6.
9. Petros, A. M.; Olejniczak, E. T.; Fesik, S. W., Structural biology of the Bcl-2 family of proteins. *Biochim. Biophys. Acta.* **2004**, *1644*, (2-3), 83-94.
10. Sadowsky, J. D.; Fairlie, W. D.; Hadley, E. B.; Lee, H. S.; Umezawa, N.; Nikolovska-Coleska, Z.; Wang, S.; Huang, D. C.; Tomita, Y.; Gellman, S. H., (alpha/beta+alpha)-peptide

antagonists of BH3 domain/Bcl-x(L) recognition: toward general strategies for foldamer-based inhibition of protein-protein interactions. *J. Am. Chem. Soc.* **2007**, 129, (1), 139-54.

11. Kritzer, J. A.; Lear, J. D.; Hodsdon, M. E.; Schepartz, A., Helical beta-peptide inhibitors of the p53-hDM2 interaction. *J. Am. Chem. Soc.* **2004**, 126, (31), 9468-9.

12. Kritzer, J. A.; Hodsdon, M. E.; Schepartz, A., Solution structure of a beta-peptide ligand for hDM2. *J. Am. Chem. Soc.* **2005**, 127, (12), 4118-9.

13. Lepourcelet, M.; Chen, Y. N.; France, D. S.; Wang, H.; Crews, P.; Petersen, F.; Bruseo, C.; Wood, A. W.; Shivdasani, R. A., Small-molecule antagonists of the oncogenic Tcf/beta-catenin protein complex. *Cancer Cell* **2004**, 5, (1), 91-102.

14. Li, L.; Thomas, R. M.; Suzuki, H.; De Brabander, J. K.; Wang, X.; Harran, P. G., A small molecule Smac mimic potentiates TRAIL- and TNFalpha-mediated cell death. *Science* **2004**, 305, (5689), 1471-4.

15. Sun, H.; Nikolovska-Coleska, Z.; Yang, C. Y.; Xu, L.; Tomita, Y.; Krajewski, K.; Roller, P. P.; Wang, S., Structure-based design, synthesis, and evaluation of conformationally constrained mimetics of the second mitochondria-derived activator of caspase that target the X-linked inhibitor of apoptosis protein/caspase-9 interaction site. *J. Med. Chem.* **2004**, 47, (17), 4147-50.

16. Braisted, A. C.; Oslob, J. D.; Delano, W. L.; Hyde, J.; McDowell, R. S.; Waal, N.; Yu, C.; Arkin, M. R.; Raimundo, B. C., Discovery of a potent small molecule IL-2 inhibitor through fragment assembly. *J. Am. Chem. Soc.* **2003**, 125, (13), 3714-5.

17. Arkin, M., Protein-protein interactions and cancer: small molecules going in for the kill. *Curr. Opin. Chem. Biol.* **2005**, 9, (3), 317-24.

18. Arkin, M. R.; Wells, J. A., Small-molecule inhibitors of protein-protein interactions: progressing towards the dream. *Nat. Rev. Drug Discov.* **2004**, 3, (4), 301-17.

19. Hershberger, S. J.; Lee, S. G.; Chmielewski, J., Scaffolds for blocking protein-protein interactions. *Curr. Top. Med. Chem.* **2007**, 7, (10), 928-42.

20. Nowick, J. S.; Powell, N. A.; Martinez, E. J.; Smith, E. M.; Noronha, G., Molecular Scaffolds .1. Intramolecular Hydrogen-Bonding in a Family of Diureas and Triureas. *J. Org. Chem.* **1992**, 57, (14), 3763-5.
21. Nowick, J. S.; Mahrus, S.; Smith, E. M.; Ziller, J. W., Triurea derivatives of diethylenetriamine as potential templates for the formation of artificial beta-sheets. *J. Am. Chem. Soc.* **1996**, 118, (5), 1066-72.
22. Tidwell, T. T., Ketene Chemistry - the 2nd Golden-Age. *Acc. Chem. Res.* **1990**, 23, (9), 273-9.
23. Tidwell, T. T., The first century of ketenes (1905-2005): the birth of a versatile family of reactive intermediates. *Angew. Chem. Int. Ed. Engl.* **2005**, 44, (36), 5778-85.
24. Tidwell, T. T., Ketene chemistry after 100 years: Ready for a new century. *Eur. J. Org. Chem.* **2006**, (3), 563-76.
25. Vazquez, J.; Qushair, G.; Albericio, F., Qualitative colorimetric tests for solid phase synthesis. *Methods Enzymol.* **2003**, 369, 21-35.
26. Vojtkovsky, T., Detection of secondary amines on solid phase. *Pept. Res.* **1995**, 8, (4), 236-7.
27. Look, G. C.; Murphy, M. M.; Campbell, D. A.; Gallop, M. A., Trimethylorthoformate: A mild and effective dehydrating reagent for solution and solid phase imine formation. *Tetrahedron Lett.* **1995**, 36, (17), 2937-40.
28. Abdel-Magid, A. F.; Carson, K. G.; Harris, B. D.; Maryanoff, C. A.; Shah, R. D., Reductive Amination of Aldehydes and Ketones with Sodium Triacetoxyborohydride. Studies on Direct and Indirect Reductive Amination Procedures(1). *J. Org. Chem.* **1996**, 61, (11), 3849-62.
29. Venkataraman, K.; Wagle, D. R., Cyanuric Chloride - Useful Reagent for Converting Carboxylic-Acids into Chlorides, Esters, Amides and Peptides. *Tetrahedron Lett.* **1979**, (32), 3037-40.
30. Olivos, H. J.; Bachhawat-Sikder, K.; Kodadek, T., Quantum dots as a visual aid for screening bead-bound combinatorial libraries. *Chembiochem* **2003**, 4, (11), 1242-5.

31. Kodadek, T.; Bachhawat-Sikder, K., Optimized protocols for the isolation of specific protein-binding peptides or peptoids from combinatorial libraries displayed on beads. *Mol. Biosyst.* **2006**, *2*, (1), 25-35.

32. McPherron, A. C.; Lawler, A. M.; Lee, S. J., Regulation of skeletal muscle mass in mice by a new TGF-beta superfamily member. *Nature* **1997**, *387*, (6628), 83-90.

33. Whittemore, L. A.; Song, K.; Li, X.; Aghajanian, J.; Davies, M.; Girgenrath, S.; Hill, J. J.; Jalenak, M.; Kelley, P.; Knight, A.; Maylor, R.; O'Hara, D.; Pearson, A.; Quazi, A.; Ryerson, S.; Tan, X. Y.; Tomkinson, K. N.; Veldman, G. M.; Widom, A.; Wright, J. F.; Wudyka, S.; Zhao, L.; Wolfman, N. M., Inhibition of myostatin in adult mice increases skeletal muscle mass and strength. *Biochem. Biophys. Res. Commun.* **2003**, *300*, (4), 965-71.

34. Moayeri, M.; Leppla, S. H., The roles of anthrax toxin in pathogenesis. *Curr. Opin. Microbiol.* **2004**, *7*, (1), 19-24.

35. Abrami, L.; Reig, N.; van der Goot, F. G., Anthrax toxin: the long and winding road that leads to the kill. *Trends Microbiol.* **2005**, *13*, (2), 72-8.

36. Panchal, R. G.; Hermone, A. R.; Nguyen, T. L.; Wong, T. Y.; Schwarzenbacher, R.; Schmidt, J.; Lane, D.; McGrath, C.; Turk, B. E.; Burnett, J.; Aman, M. J.; Little, S.; Sausville, E. A.; Zaharevitz, D. W.; Cantley, L. C.; Liddington, R. C.; Gussio, R.; Bavari, S., Identification of small molecule inhibitors of anthrax lethal factor. *Nat. Struct. Mol. Biol.* **2004**, *11*, (1), 67-72.

37. Forino, M.; Johnson, S.; Wong, T. Y.; Rozanov, D. V.; Savinov, A. Y.; Li, W.; Fattorusso, R.; Becattini, B.; Orry, A. J.; Jung, D.; Abagyan, R. A.; Smith, J. W.; Alibek, K.; Liddington, R. C.; Strongin, A. Y.; Pellecchia, M., Efficient synthetic inhibitors of anthrax lethal factor. *Proc. Natl. Acad. Sci. U. S. A.* **2005**, *102*, (27), 9499-504.

38. Numa, M. M.; Lee, L. V.; Hsu, C. C.; Bower, K. E.; Wong, C. H., Identification of novel anthrax lethal factor inhibitors generated by combinatorial Pictet-Spengler reaction followed by screening in situ. *Chembiochem* **2005**, *6*, (6), 1002-6.

39. Schepetkin, I. A.; Khlebnikov, A. I.; Kirpotina, L. N.; Quinn, M. T., Novel small-molecule inhibitors of anthrax lethal factor identified by high-throughput screening. *J. Med. Chem.* **2006**, *49*, (17), 5232-44.

40. Anthony, N. J., HIV-1 integrase: a target for new AIDS chemotherapeutics. *Curr. Top. Med. Chem.* **2004**, *4*, (9), 979-90.

41. Markowitz, M.; Morales-Ramirez, J. O.; Nguyen, B. Y.; Kovacs, C. M.; Steigbigel, R. T.; Cooper, D. A.; Liporace, R.; Schwartz, R.; Isaacs, R.; Gilde, L. R.; Wenning, L.; Zhao, J.; Tepler, H., Antiretroviral activity, pharmacokinetics, and tolerability of MK-0518, a novel inhibitor of HIV-1 integrase, dosed as monotherapy for 10 days in treatment-naive HIV-1-infected individuals. *J. Acquir. Immune. Defic. Syndr.* **2006**, 43, (5), 509-15.
42. Morellet, N.; Bouaziz, S.; Petitjean, P.; Roques, B. P., NMR structure of the HIV-1 regulatory protein VPR. *J. Mol. Biol.* **2003**, 327, (1), 215-27.
43. Bukrinsky, M.; Adzhubei, A., Viral protein R of HIV-1. *Rev. Med. Virol.* **1999**, 9, (1), 39-49.
44. Andersen, J. L.; Planelles, V., The role of Vpr in HIV-1 pathogenesis. *Curr. HIV Res.* **2005**, 3, (1), 43-51.
45. Watanabe, N.; Nishihara, Y.; Yamaguchi, T.; Koito, A.; Miyoshi, H.; Takeya, H.; Osada, H., Fumagillin suppresses HIV-1 infection of macrophages through the inhibition of Vpr activity. *FEBS Lett.* **2006**, 580, (11), 2598-602.
46. Shimura, M.; Zhou, Y.; Asada, Y.; Yoshikawa, T.; Hatake, K.; Takaku, F.; Ishizaka, Y., Inhibition of Vpr-induced cell cycle abnormality by quercetin: a novel strategy for searching compounds targeting Vpr. *Biochem. Biophys. Res. Commun.* **1999**, 261, (2), 308-16.
47. Kamata, M.; Wu, R. P.; An, D. S.; Saxe, J. P.; Damoiseaux, R.; Phelps, M. E.; Huang, J.; Chen, I. S., Cell-based chemical genetic screen identifies damnacanthal as an inhibitor of HIV-1 Vpr induced cell death. *Biochem. Biophys. Res. Commun.* **2006**, 348, (3), 1101-6.
48. Schafer, E. A.; Venkatachari, N. J.; Ayyavoo, V., Antiviral effects of mifepristone on human immunodeficiency virus type-1 (HIV-1): targeting Vpr and its cellular partner, the glucocorticoid receptor (GR). *Antiviral Res.* **2006**, 72, (3), 224-32.
49. Kino, T.; Pavlakis, G. N., Partner molecules of accessory protein Vpr of the human immunodeficiency virus type 1. *DNA Cell Biol.* **2004**, 23, (4), 193-205.
50. New England BioLabs Inc. <http://www.neb.com> (Mar 2008).
51. Princeton University Department of Chemical Engineering, Facilities: Biacore SPR - technical documentation. http://chemeng.princeton.edu/facilities/spr_tech.shtml (Feb 2008).

52. Ladbury, J. E.; Chowdhry, B. Z., Sensing the heat: the application of isothermal titration calorimetry to thermodynamic studies of biomolecular interactions. *Chem. Biol.* **1996**, 3, (10), 791-801.
53. Perozzo, R.; Folkers, G.; Scapozza, L., Thermodynamics of protein-ligand interactions: history, presence, and future aspects. *J. Recept. Signal. Transduct. Res.* **2004**, 24, (1-2), 1-52.
54. Shvarts, A.; Steegenga, W. T.; Riteco, N.; van Laar, T.; Dekker, P.; Bazuine, M.; van Ham, R. C.; van der Houven van Oordt, W.; Hateboer, G.; van der Eb, A. J.; Jochemsen, A. G., MDMX: a novel p53-binding protein with some functional properties of MDM2. *Embo. J.* **1996**, 15, (19), 5349-57.
55. Popowicz, G. M.; Czarna, A.; Rothweiler, U.; Szwagierczak, A.; Krajewski, M.; Weber, L.; Holak, T. A., Molecular Basis for the Inhibition of p53 by Mdmx. *Cell Cycle* **2007**, 6, (19), 2386-92.
56. Davies, T. H.; Sanchez, E. R., Fkbp52. *Int. J. Biochem. Cell. Biol.* **2005**, 37, (1), 42-7.
57. Coy, D. H.; Hocart, S. J.; Sasaki, Y., Solid-phase reductive alkylation techniques in analog peptide-bond and side-chain modification. *Tetrahedron* **1988**, 44, (3), 835-41.
58. Ho, P. T.; Chang, D.; Zhong, J. W.; Musso, G. F., An improved low racemization solid-phase method for the synthesis of reduced dipeptide (psi CH₂NH) bond isosteres. *Pept. Res.* **1993**, 6, (1), 10-2.
59. Sui, Q.; Borchardt, D.; Rabenstein, D. L., Kinetics and equilibria of cis/trans isomerization of backbone amide bonds in peptoids. *J. Am. Chem. Soc.* **2007**, 129, (39), 12042-8.